ep and eA physics at LHeC

DIS in the TeV range

Anna Staśto
Penn State

http://www.cern.ch/lhec

CNU Newport News, October 21, 2013

Conceptual Design Report

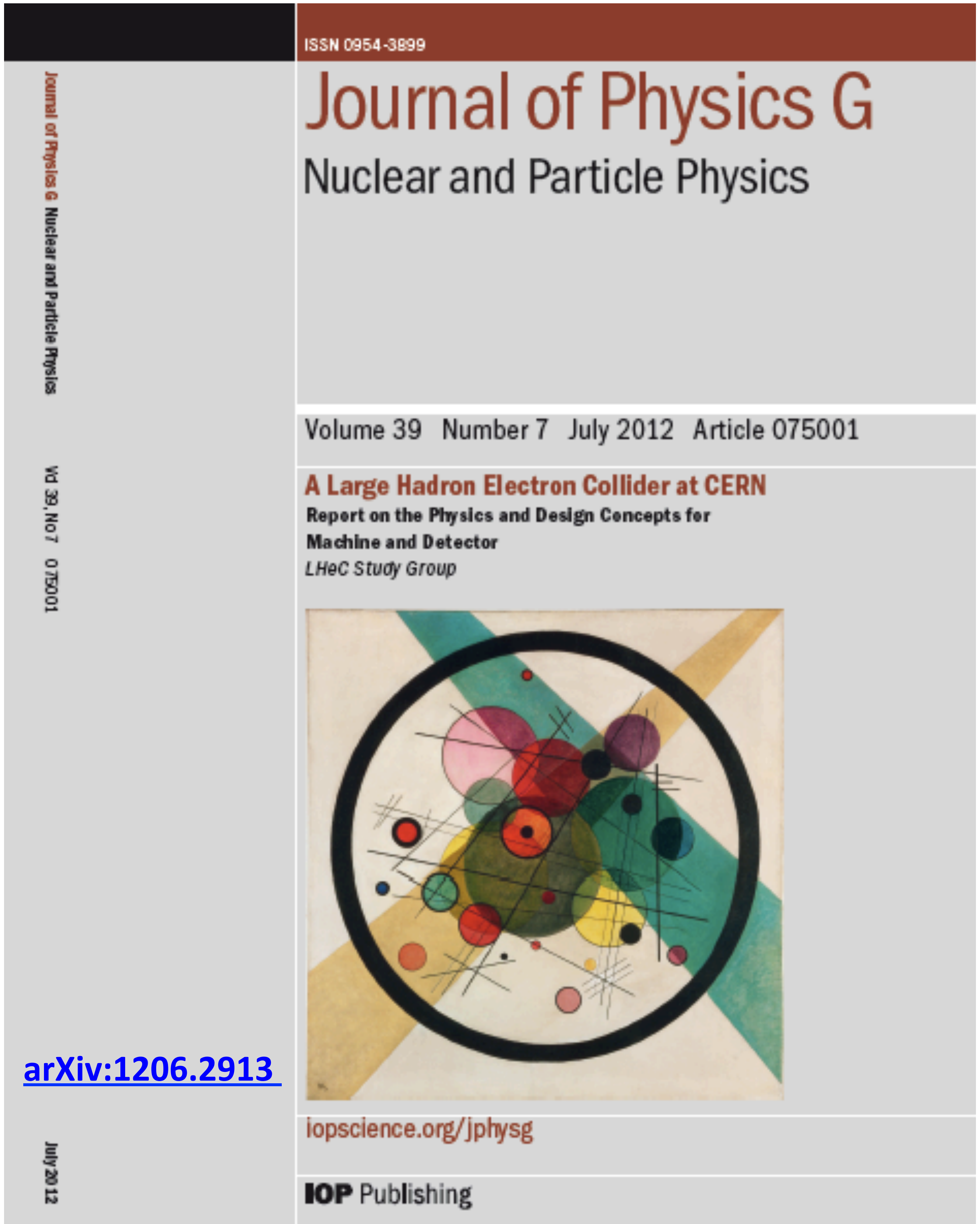

arXiv:1206.2913

193 authors
631 pages
947 references
5 chapters
14 sections

Further publications:

O. Bruening, M. Klein,
Mod. Phys. Lett. A28 (2013) 16, 133001

LHeC Study Group
arXiv:1211.5101

LHeC Study Group
arXiv:1211.4831

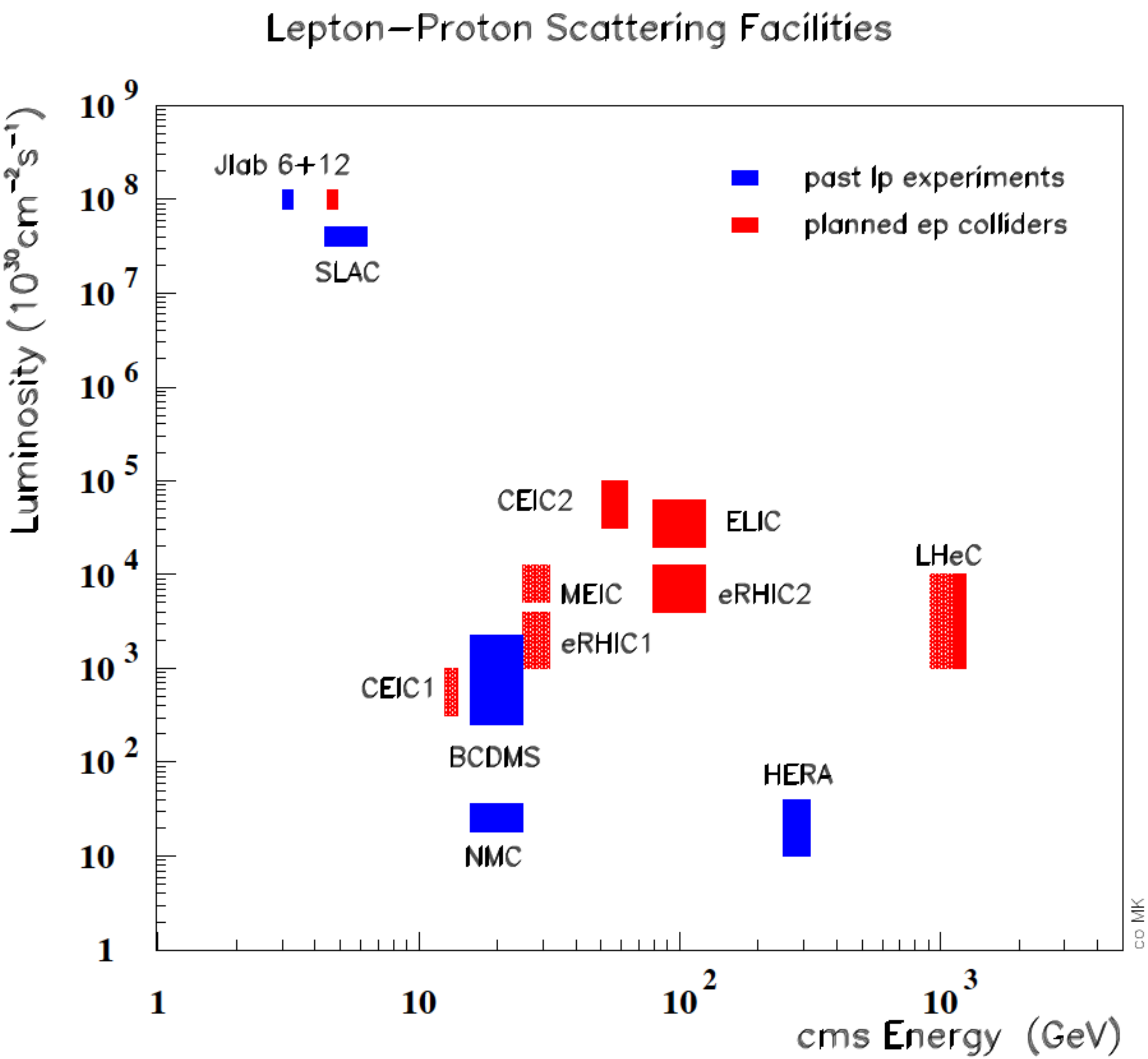

New estimate for the LHeC luminosity:

$$\mathcal{L} = 10^{34} \frac{1}{\mathrm{cm}^2\,\mathrm{s}}$$

Energy frontier deep inelastic scattering - following HERA with the LHC
LHeC: A new laboratory for particle physics, a 5th large LHC experiment

Energy Recovery Linac (3 pass)

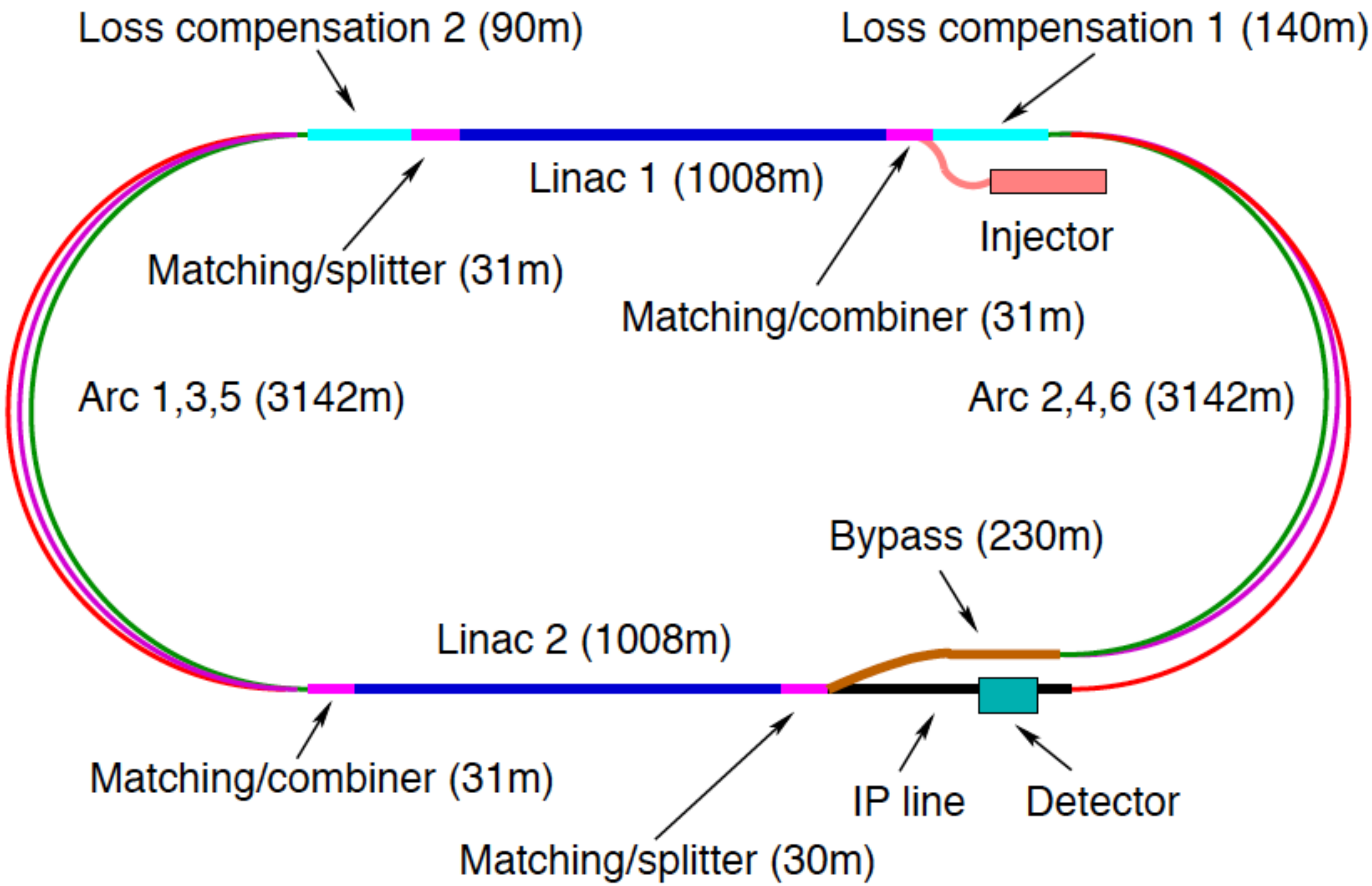

Figure 1: Schematic view on the LHeC racetrack configuration. Each linac accelerates the beam to 10 GeV, which leads to a 60 GeV electron energy at the collision point with three passes through the opposite linear structures of 60 cavity-cryo modules each. The arc radius is about 1 km, mainly determined by the synchrotron radiation loss of the 60 GeV beam which is returned from the IP and decelerated for recovering the beam power. Comprehensive design studies of the lattice, optics, beam (beam) dynamics, dump, IR and return arc magnets, as well as auxiliary systems such as RF, cryogenics or spin rotators are contained in the CDR [1], which as for physics and detector had been reviewed by 24 referees appointed by CERN.

Ring-Ring option as fall back;

Detector design

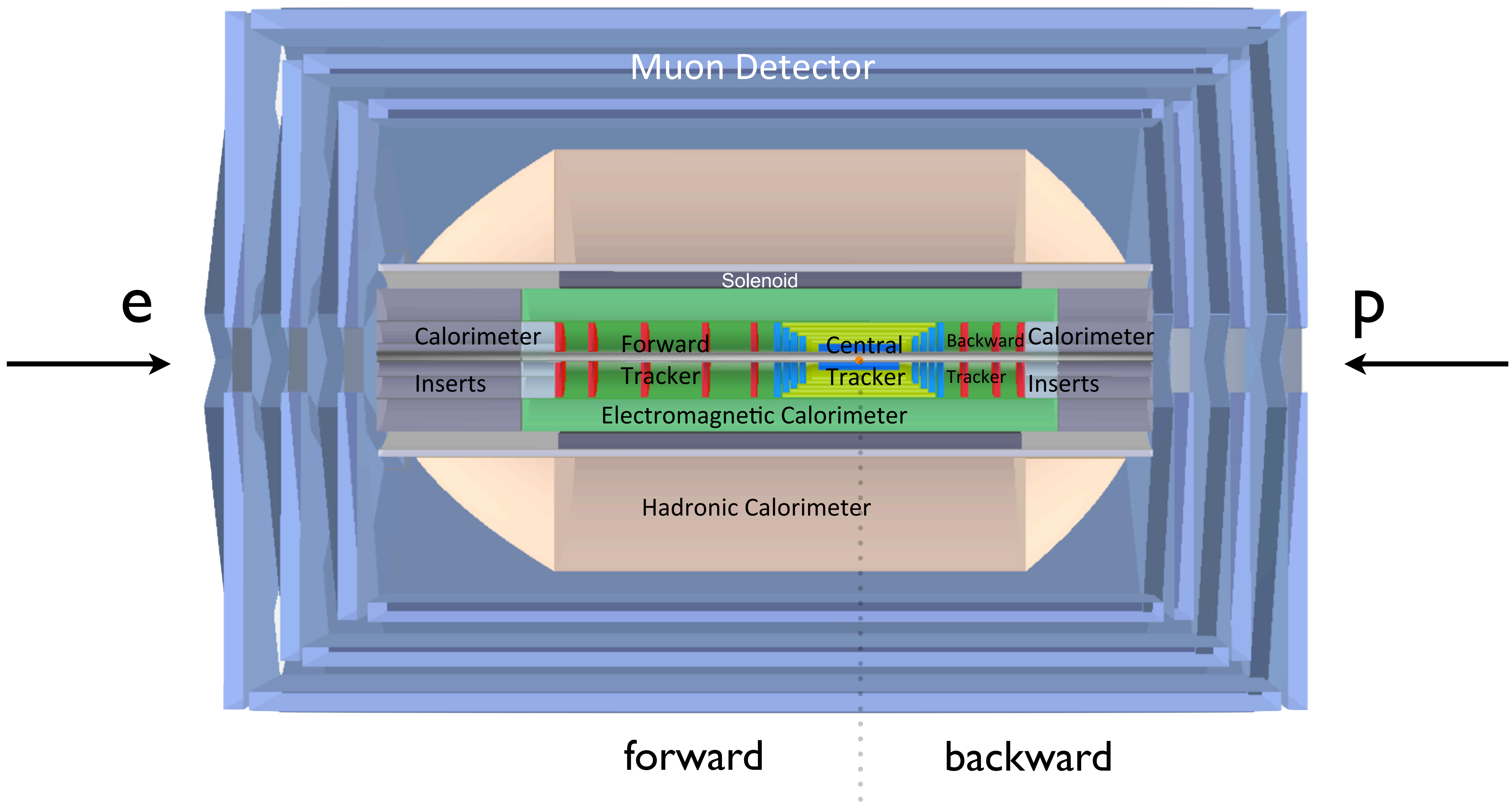

Forward/backward asymmetry in energy deposited and thus in geometry and technology
Present dimensions: LxD =14x9m² [CMS 21 x 15m², ATLAS 45 x 25 m²]
Taggers at -62m (e),100m (γ,LR), -22.4m (γ,RR), +100m (n), +420m (p)

LHeC kinematics

ep/ea collisions

$$E_p = 7 \text{ TeV}$$
$$E_A = 2.75 \text{ TeV/nucleon}$$
$$E_e = 60(50) - 140 \text{ GeV}$$
$$\sqrt{s} \simeq 1 - 2 \text{ TeV}$$

- Requirements:

* Luminosity~10^{33} $cm^{-2}s^{-1}$. eA: L_{en}~10^{32} $cm^{-2}s^{-1}$
* Acceptance: 1-179 degrees (low-x ep/eA).
* Tracking to 1 mrad.
* EMCAL calibration to 0.1 %.
* HCAL calibration to 0.5 %.
* Luminosity determination to 1 %.
* Compatible with LHC operation.

New estimate

$$\mathcal{L}^{ep} = 10^{34} \frac{1}{\mathrm{cm}^2\,\mathrm{s}}$$

ep

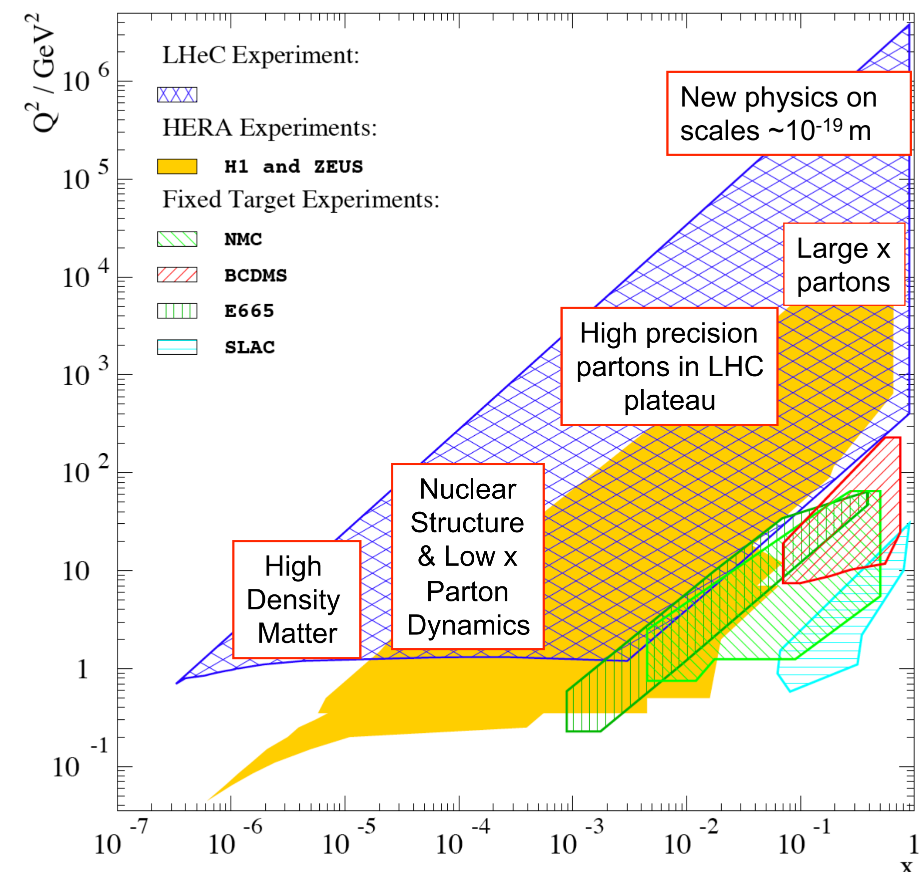

eA

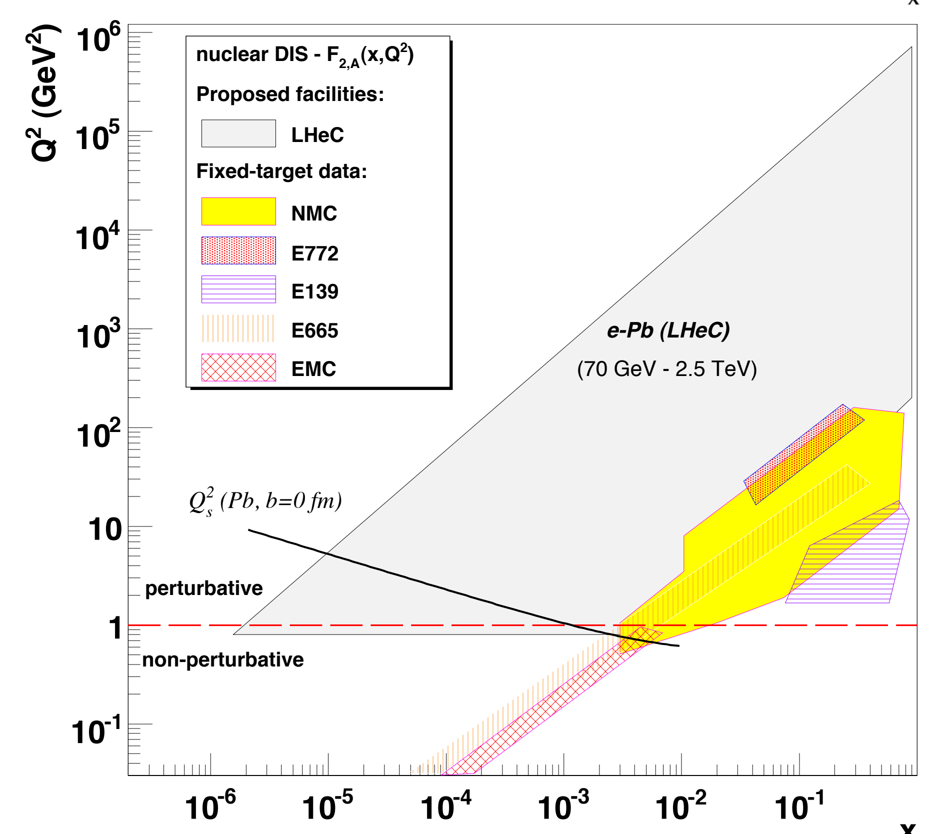

LHeC kinematics: acceptance

Kinematics in ep mode

$$Q^2_{min}(x, \theta_e^{max}) \simeq [2E_e \cot(\theta_e^{max}/2)]^2.$$

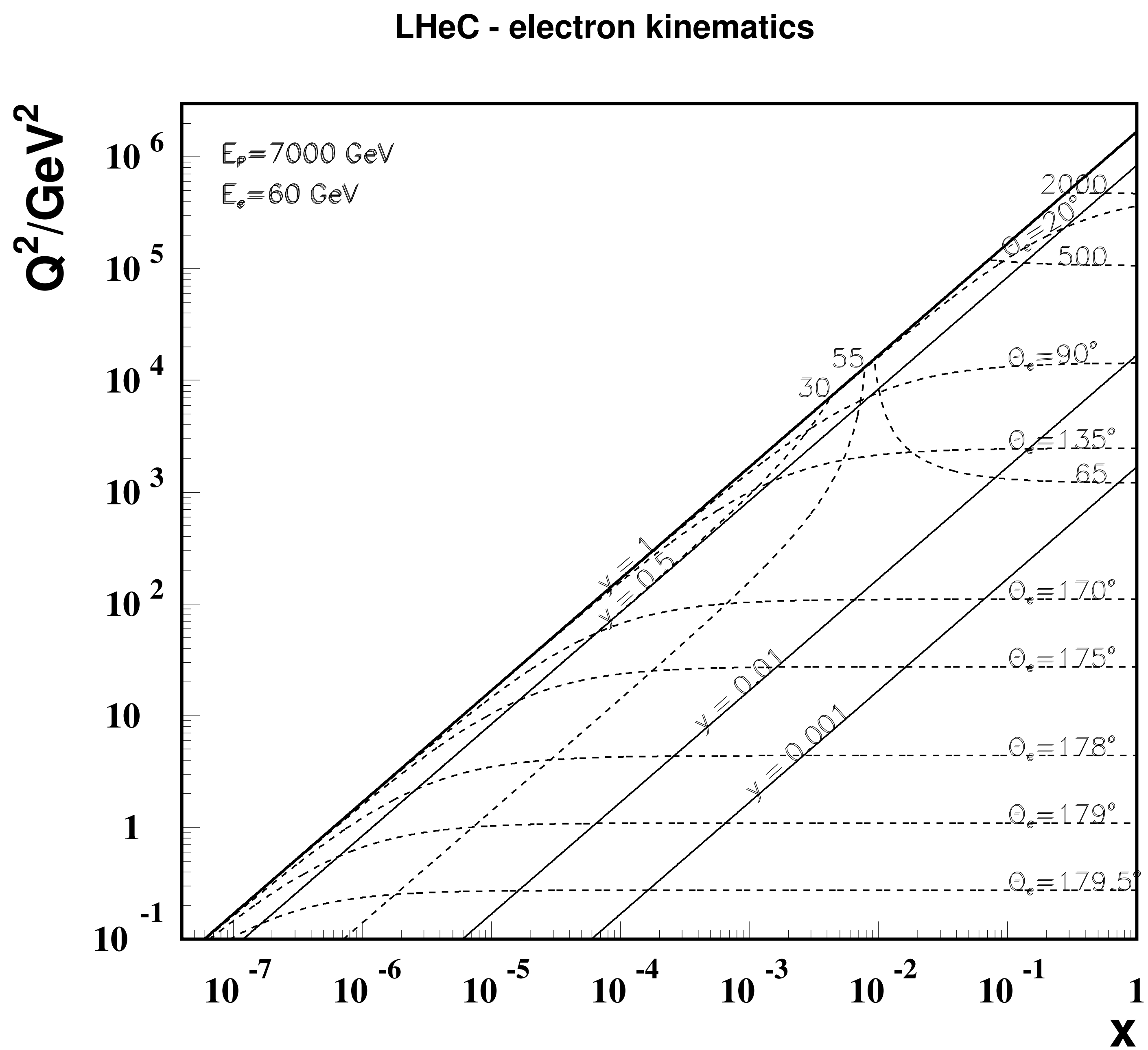

Access to low x and low Q requires electron acceptance down to 179 degrees.

$Q^2_{\rm min} = 0.03\ \mathrm{GeV}^2$ for $E_e = 10\ \mathrm{GeV}$

$Q^2_{\rm min} = 1\ \mathrm{GeV}^2$ for $E_e = 60\ \mathrm{GeV}$

$Q^2_{\rm min} = 6\ \mathrm{GeV}^2$ for $E_e = 140\ \mathrm{GeV}$

Physics motivation for ep/eA in TeV range

- Details of parton structure of the nucleon (from ep,ed/eA), full unfolding of PDFs (strange, charm, beauty). Measurement of GPDs and unintegrated PDFs.
- Mapping the gluon field down to very low x. Saturation physics.
- Heavy quarks, factorization, diffraction, electroweak processes.
- Properties of Higgs. Very good sensitivity to: H to bbar, H to WW coupling in the 125 GeV mass range.
- Very precise measurement of the coupling constant.
- Deep inelastic scattering off nuclei. Nuclear parton distributions. Pinning down the initial state for heavy ion collisions.

LHeC Project Status

2012: CDR published
arXiv:1206.2913
2013: Higgs with ep: 10^{34} Luminosity
arXiv:1211.5102, 1305.2090
ERL testfacility design, 801.58MHz →
2014: January 20/21. next workshop

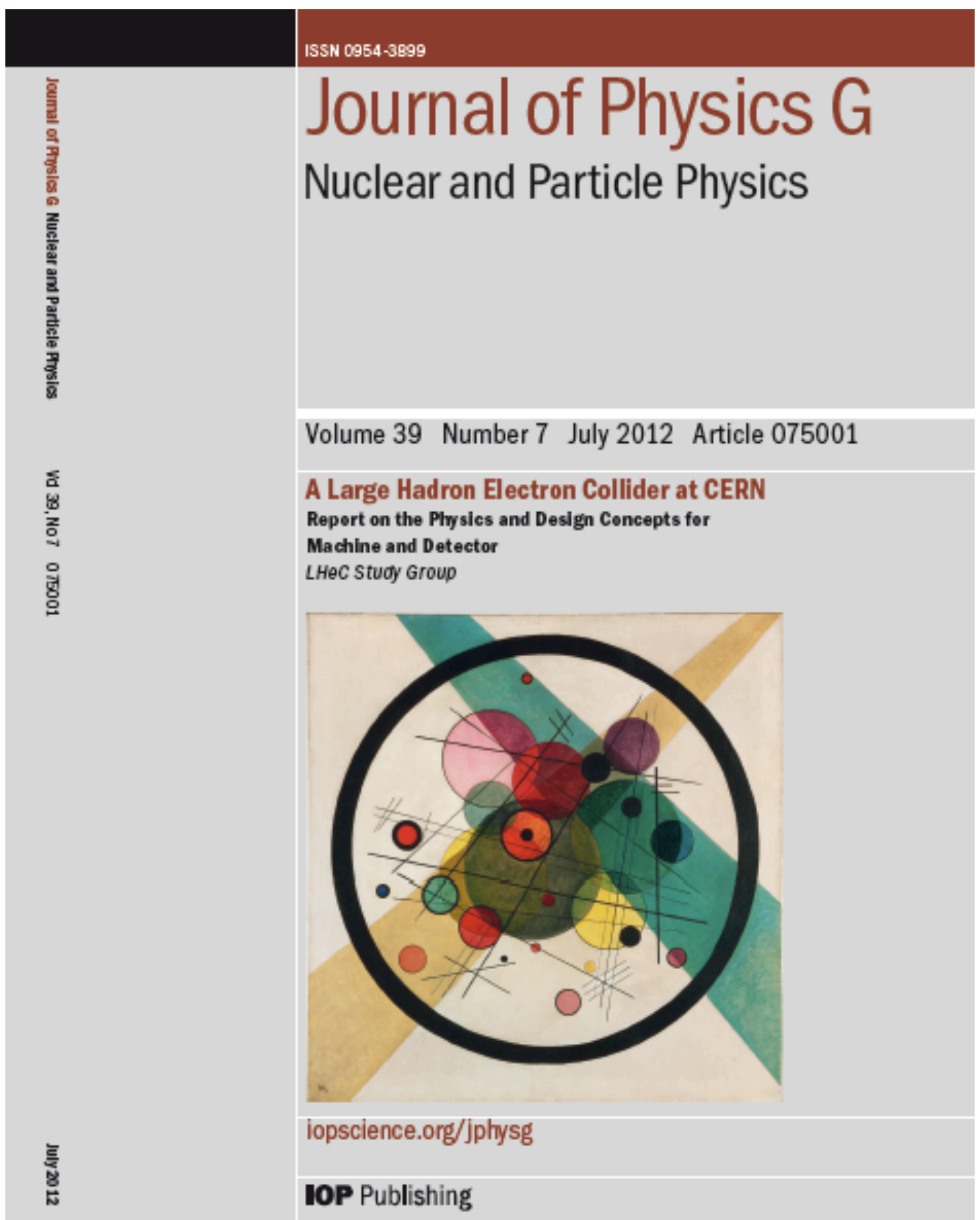

1 GeV, 3pass, ERL Testfacility - under design at CERN

Parameter	Value
Frequency	801.58 MHz
Q_0	2×10^{10}
Injection energy	5 MeV
Beam current	10 mA
Bunch population	$3\ 10^9$
Bunch spacing	50 ns
Synchrotron radiation loss at 900 MeV	55 keV
Emittance growth at 900 MeV	0.08 μm [Δε_arc] 0.11 μm [Δε_t]
Maximum beam energy	900 MeV
Distance between linacs	> 5 m
Length of each linac	~13 m
Number of dipole magnets	2 x 4 [45°] and 2 x 8 [22.5°] =24

Tentative parameters of the CERN Energy Recovery Testfacility (10.10.2013)

A. Valloni, R. Calaga, O. Brüning, E. Jensen, M. Klein, R. Tomas, F. Zimmermann, "Strawman Optics Design for the LHeC ERL Test Facility" IPAC13, Shanghai, May 2013, http://accelconf.web.cern.ch/AccelConf/IPAC2013/papers/tupme055.pdf

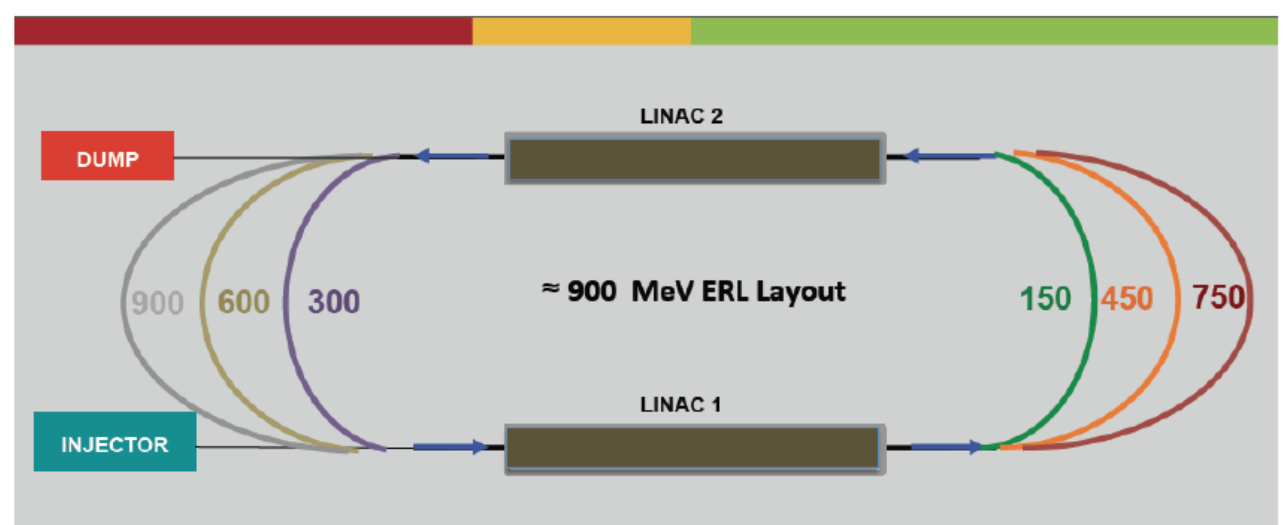

Strong international collaboration and interest:
AsTEC, Beijing, BNL, BINP, Cornell, DESY, JLab, Mainz U..

Higgs production at LHeC

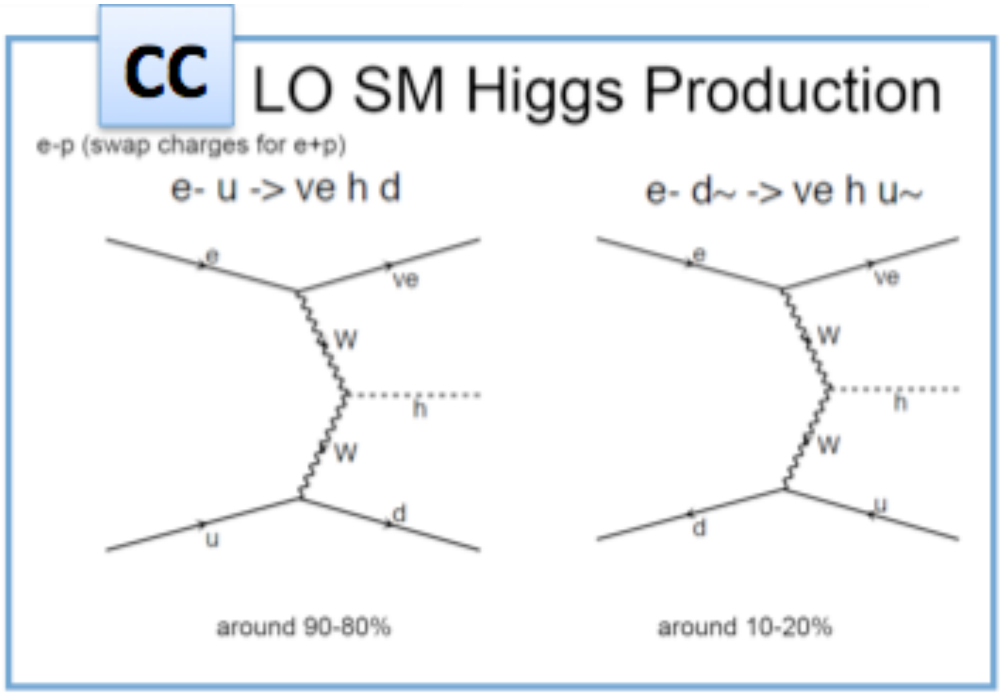

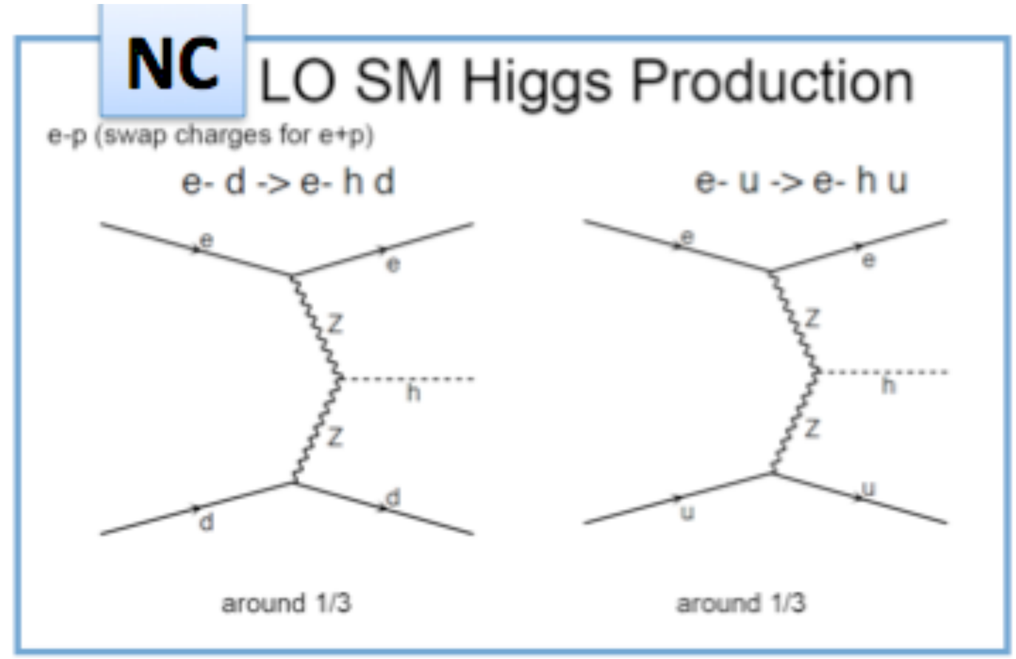

$H \rightarrow b\bar{b}$ results

Case study with higher electron energy: [M_H=120 GeV, E_p=7 TeV]

- Higgs invariant mass after all selection

E_e=150 GeV

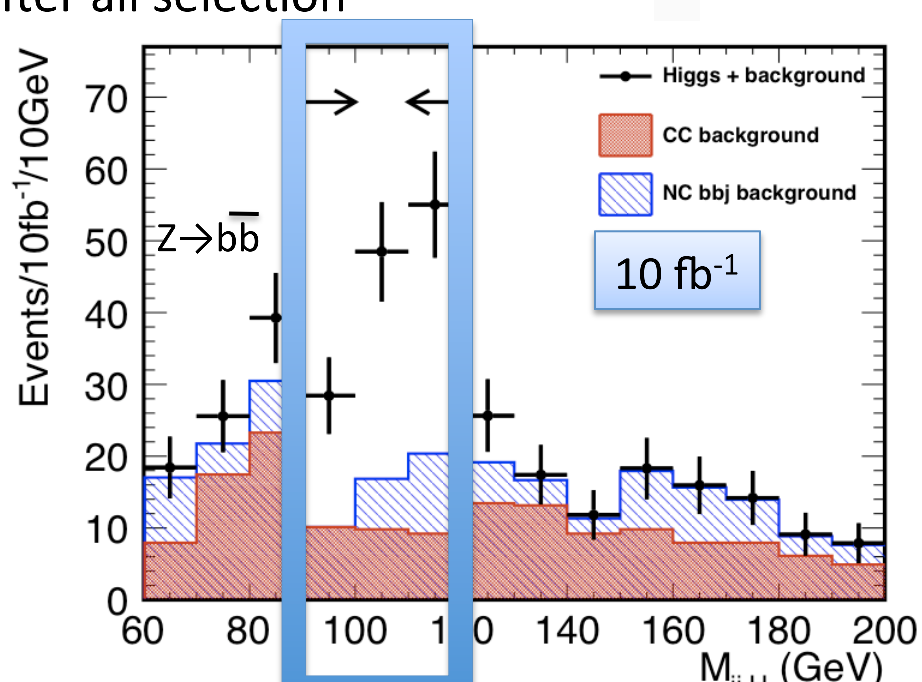

Clear signal obtained with cut-and-count based analysis!

Higgs production at LHeC

H→b$\bar{b}$ results

- Case study for electron beam energy of 60 GeV using same analysis strategy
  - luminosity values of 100 fb^{-1} are feasible

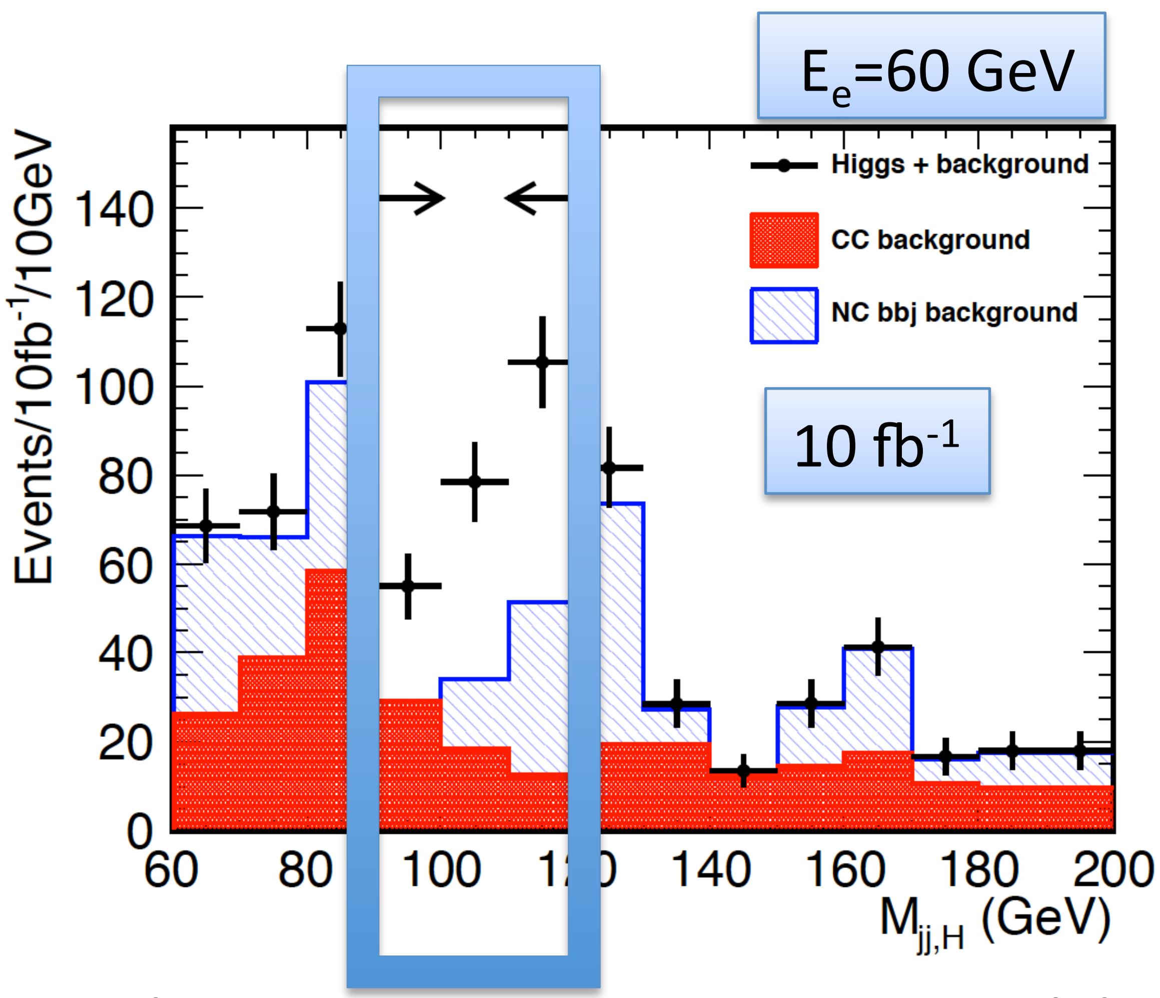

	E_e = 150 GeV (10 fb^{-1})	E_e = 60 GeV (100 fb^{-1})
H → bb signal	84.6	248
S/N	1.79*	1.05
S/√N	12.3	16.1

*Note: A parton-level study delivered S/N of 4.7.

- Electron energy recovery LINAC with high electron polarisation of 80% and 10^{34} cm^{-2} s^{-1} ➔ enhancement by factor 18 feasible, i.e. around 4500 Higgs candidates for E_e=60 GeV allowing to measure Hbb coupling with **0.8 %** statistical precision.

- S/N ~1 confirmed in independent analysis for M_H=125 GeV for E_e=60 GeV (master thesis by Sergio Mandelli, University of Liverpool 2013)

Higgs Physics with the LHeC

LHeC Higgs		CC (e^-p)	NC (e^-p)	CC (e^+p)
Polarisation		-0.8	-0.8	0
Luminosity [ab^{-1}]		1	1	0.1
Cross Section [fb]		196	25	58
Decay	BrFraction	N^H_{CC} e^-p	N^H_{NC} e^-p	N^H_{CC} e^+p
$H \to b\bar{b}$	0.577	113 100	13 900	3 350
$H \to c\bar{c}$	0.029	5 700	700	170
$H \to \tau^+\tau^-$	0.063	12 350	1 600	370
$H \to \mu\mu$	0.00022	50	5	–
$H \to 4l$	0.00013	30	3	–
$H \to 2l2\nu$	0.0106	2 080	250	60
$H \to gg$	0.086	16 850	2 050	500
$H \to WW$	0.215	42 100	5 150	1 250
$H \to ZZ$	0.0264	5 200	600	150
$H \to \gamma\gamma$	0.00228	450	60	15
$H \to Z\gamma$	0.00154	300	40	10

High precision partons and strong coupling to NNNLO remove QCD (''thy'') uncertainties
→LHC facility may be transformed into precisionHiggs factory [σ(pp→ HX) = 50 pb]

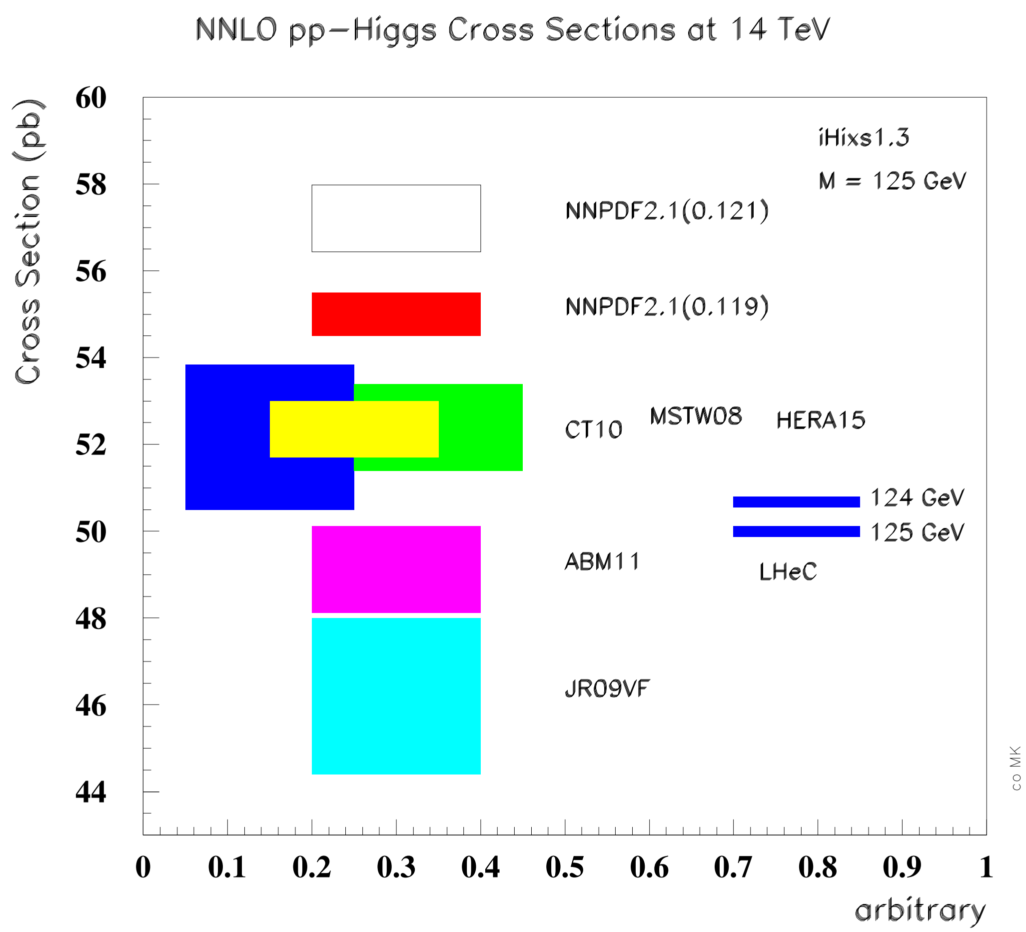

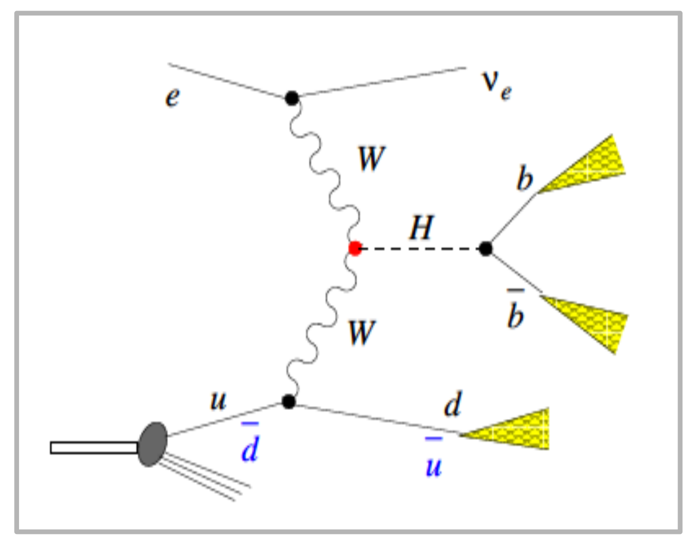

With L=O(10^{34})cm^{-2} s^{-1} the LHeC becomes a high precision H facility complementary to LHC.

H→ bb to 1%
cc, ττ under study

cf U.Klein. Talk at EPS Stockholm, July 2013

O.Brüning and M.Klein, ''The Large Hadron Electron Collider'' arXiv:1305.2090, MPLA A28(2013)16,1330011

cleaner FS than pp, no pile-up

- Sensitivity to H→bb is estimated by an initial simulation study :
  LHeC has the potential to measure H → bb coupling with an S/N of ~1 and to 1% (4%) accuracy with 60 GeV electron beam based on a luminosity of 10^{34} (10^{33}) cm^{-2} s^{-1}.
- At LHeC, various Higgs boson decays and Higgs CP eigenstates could be accessed via WW and ZZ fusion at c.m.s. energies of **1.3 TeV** and with **1 ab^{-1}** - complementary to LHC experiments.

Measurement of strong coupling

Unification of coupling constants?

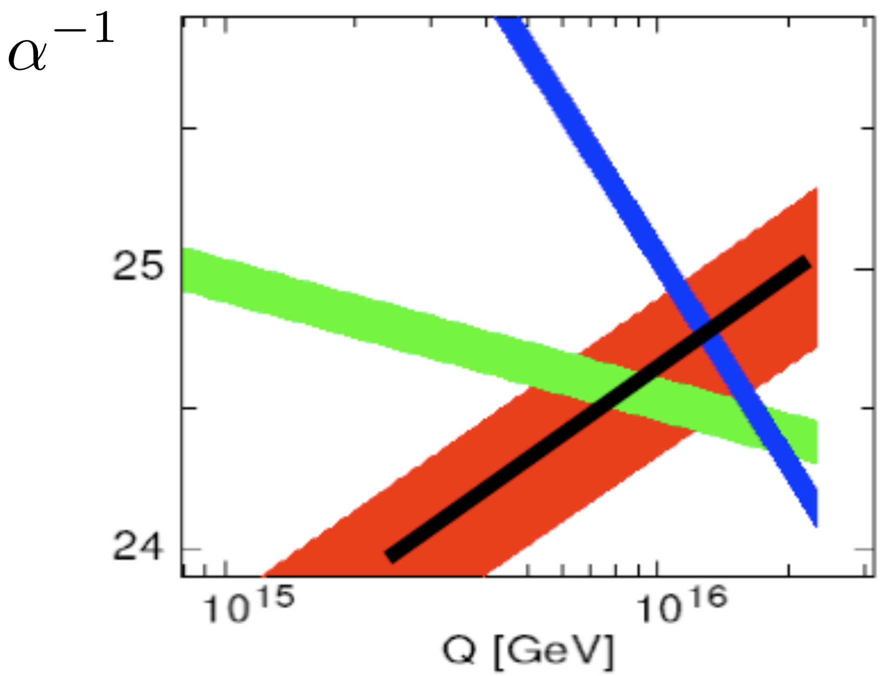

Strong coupling is least known of all couplings
Grand unification predictions suffer from uncertainty
DIS tends to be lower than the world average
LHeC: per mille accuracy (now percent accuracy)

A dedicated study was performed to determine the accuracy of alphas from the LHeC was performed using for the central values the SM prediction smeared within its uncertainties assuming Gauss distribution and taking into account correlations

case	cut [Q^2 (GeV^2)]	α_S	uncertainty	relative precision (%)
HERA only (14p)	$Q^2 > 3.5$	0.11529	0.002238	1.94
HERA+jets (14p)	$Q^2 > 3.5$	0.12203	0.000995	0.82
LHeC only (14p)	$Q^2 > 3.5$	0.11680	0.000180	0.15
LHeC only (10p)	$Q^2 > 3.5$	0.11796	0.000199	0.17
LHeC only (14p)	$Q^2 > 20.$	0.11602	0.000292	0.25
LHeC+HERA (10p)	$Q^2 > 3.5$	0.11769	0.000132	0.11
LHeC+HERA (10p)	$Q^2 > 7.0$	0.11831	0.000238	0.20
LHeC+HERA (10p)	$Q^2 > 10.$	0.11839	0.000304	0.26

F_2,F_L structure functions

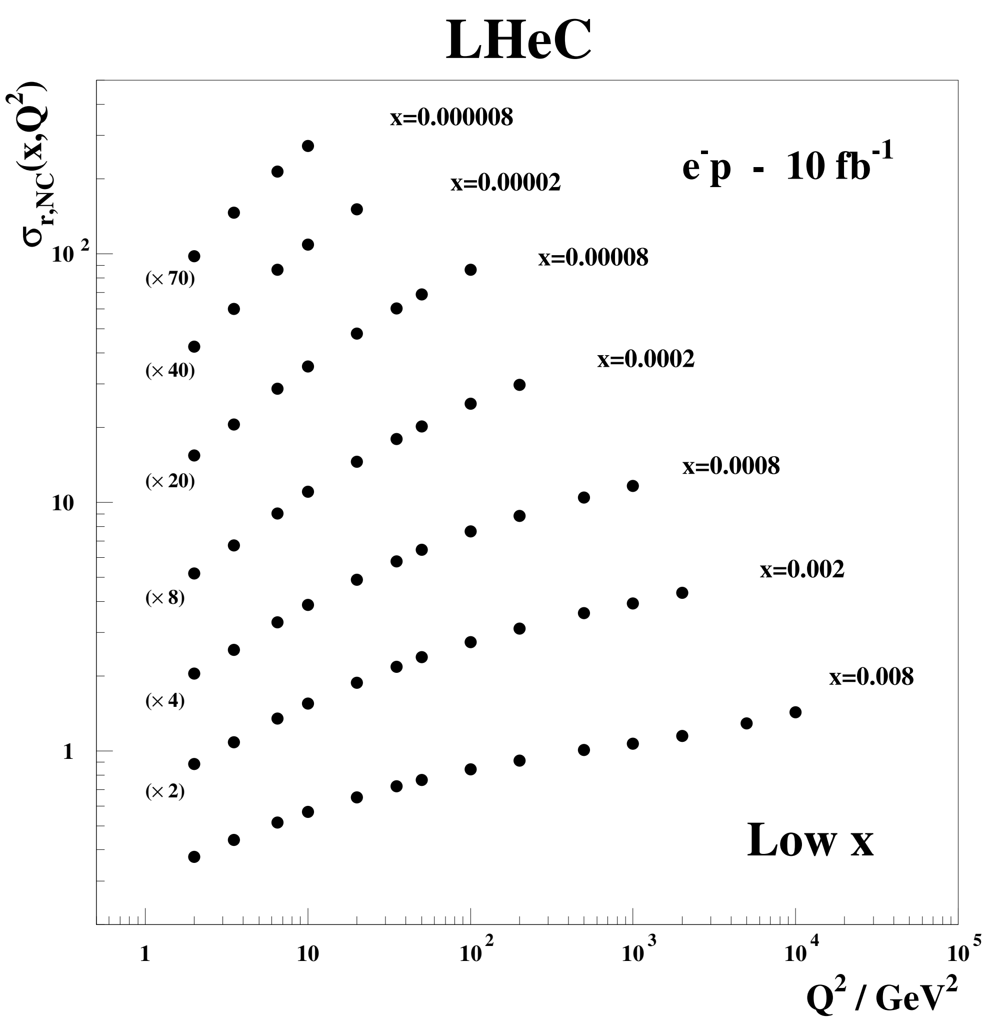

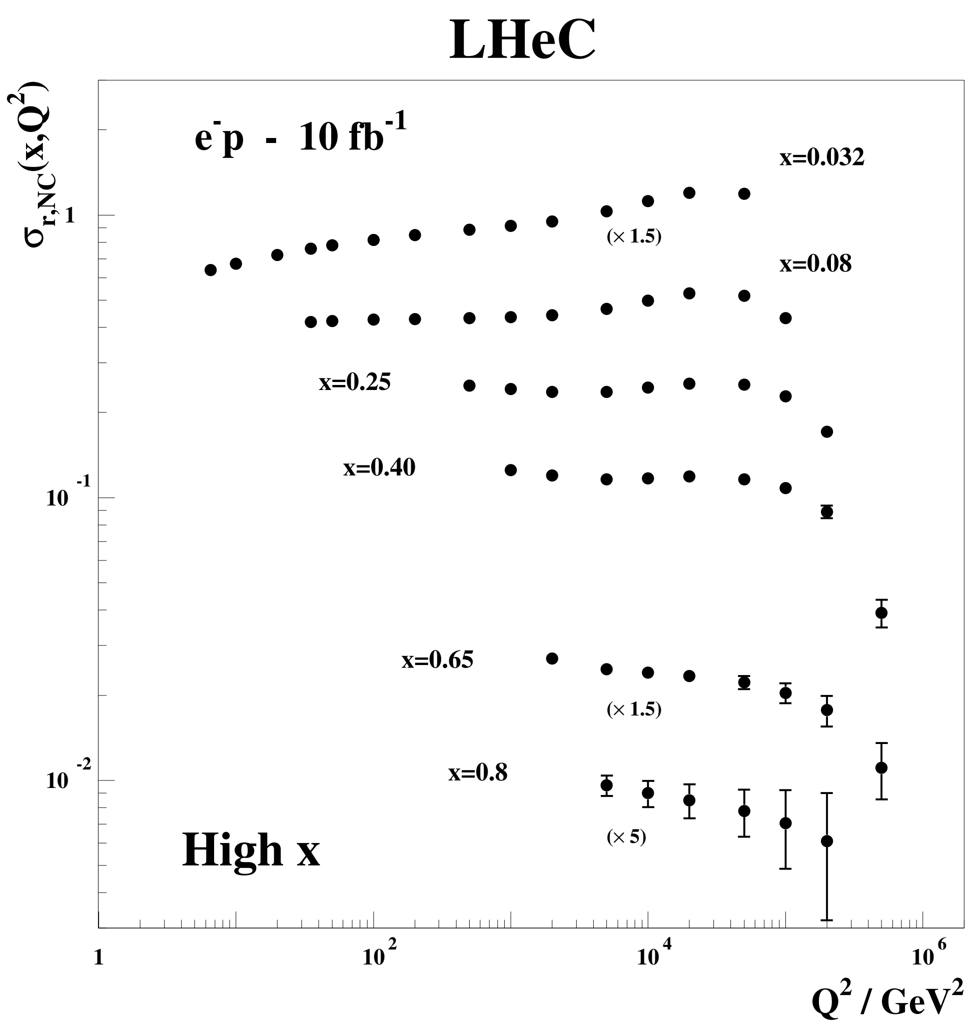

Reduced cross section: huge kinematic range and excellent accuracy

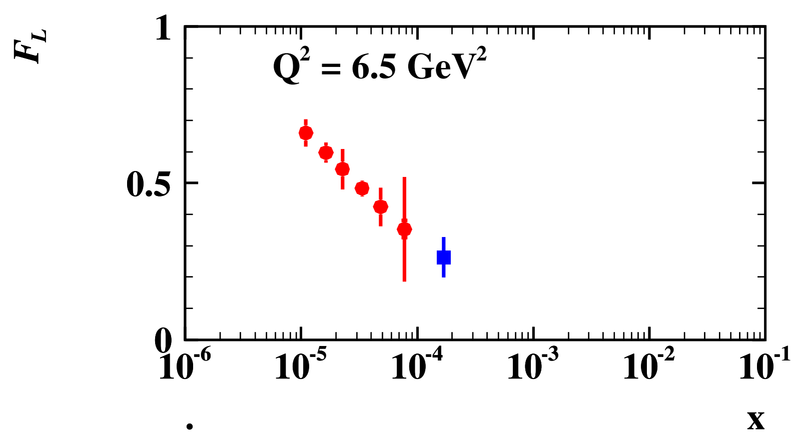

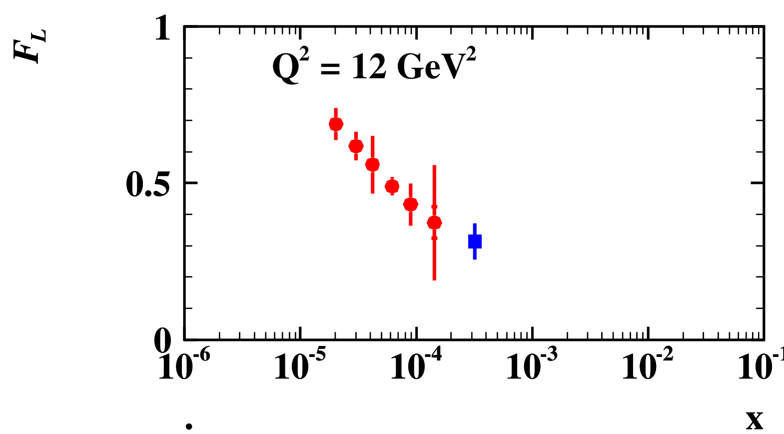

Longitudinal structure function: lowering electron energy

Constraining the pdfs

Gluon at small x: large uncertainties

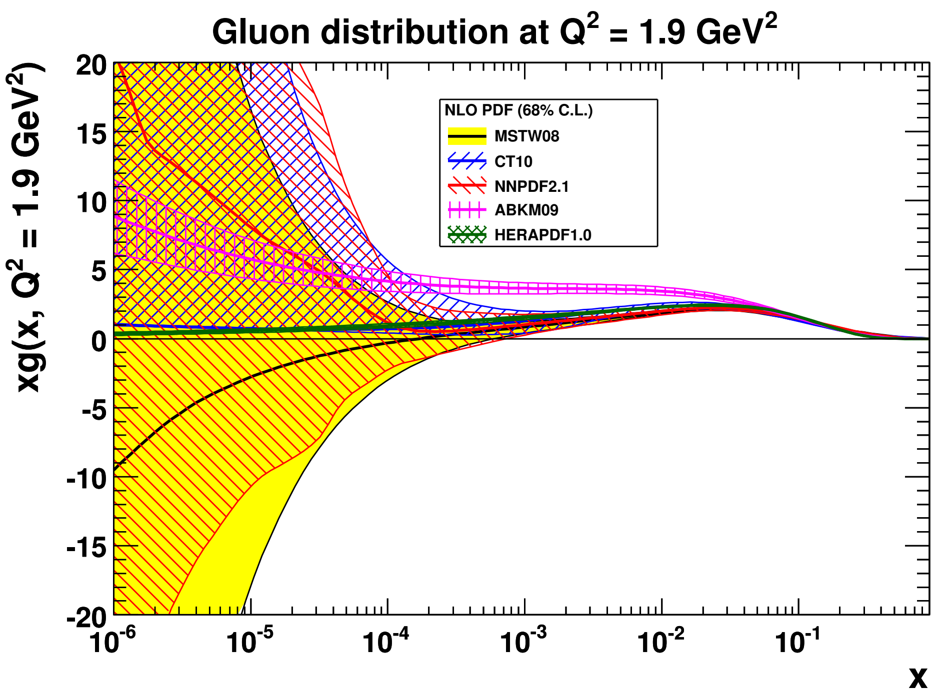

Constraints by including LHeC simulated data

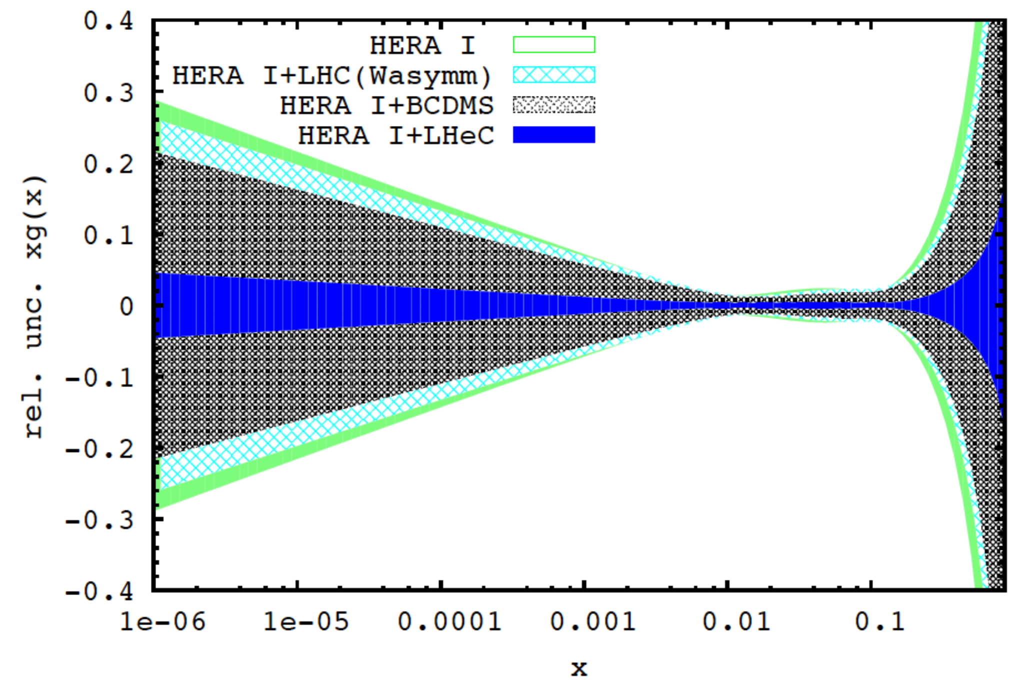

Constraints on valence at large x

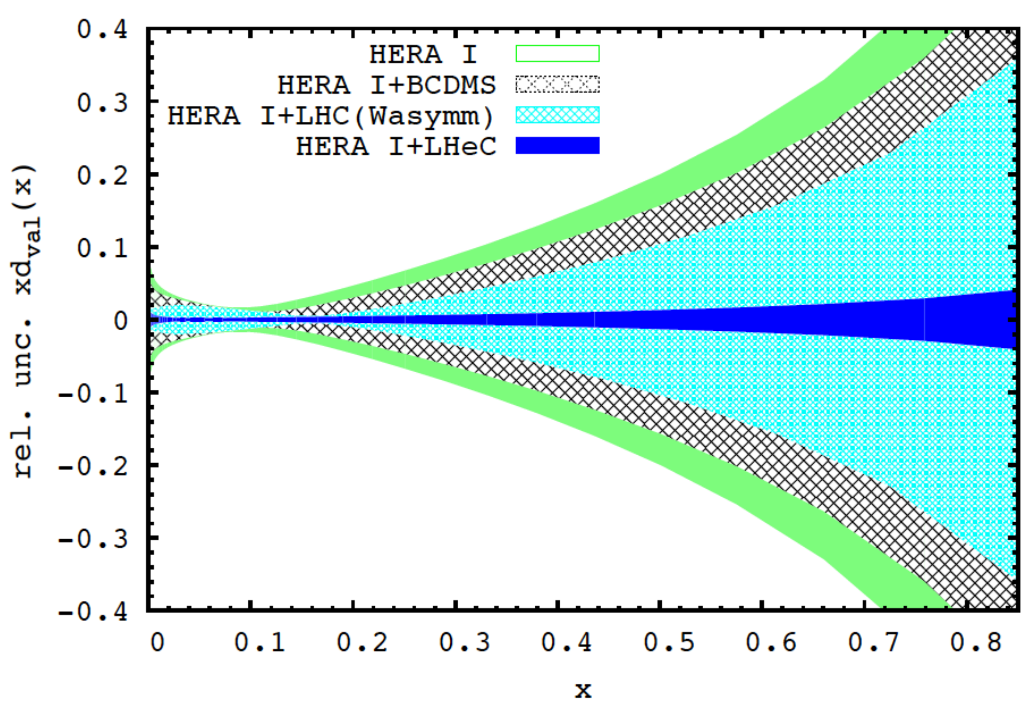

Constraints of strange quark density through charm tagging

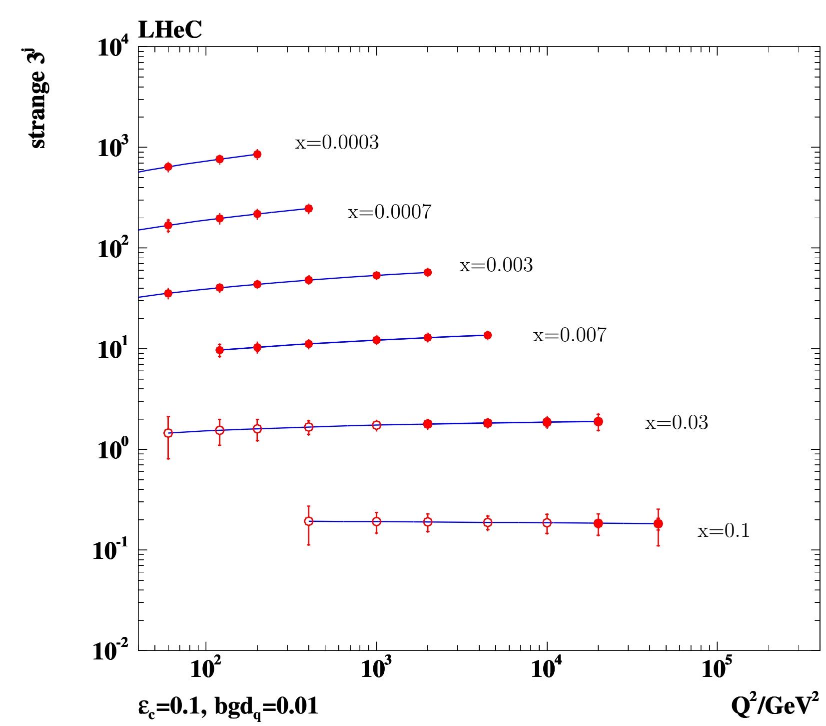

Mapping the Gluon Distribution

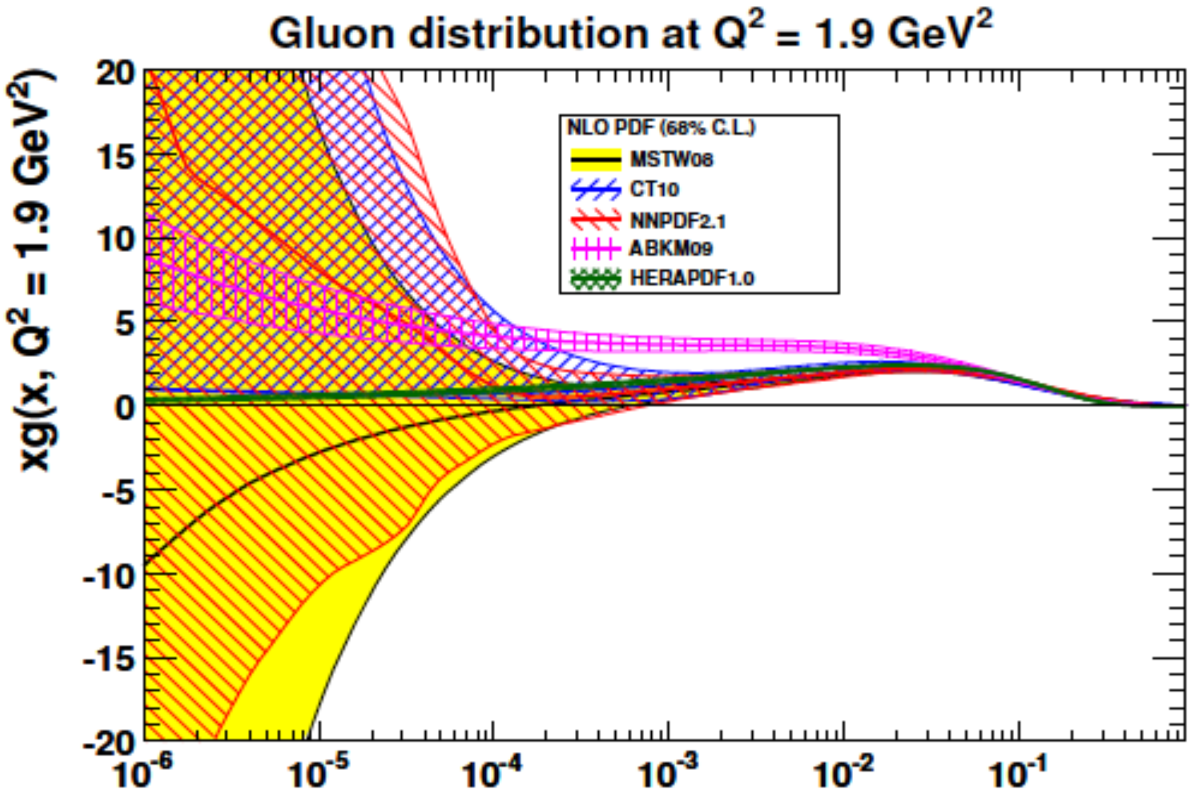

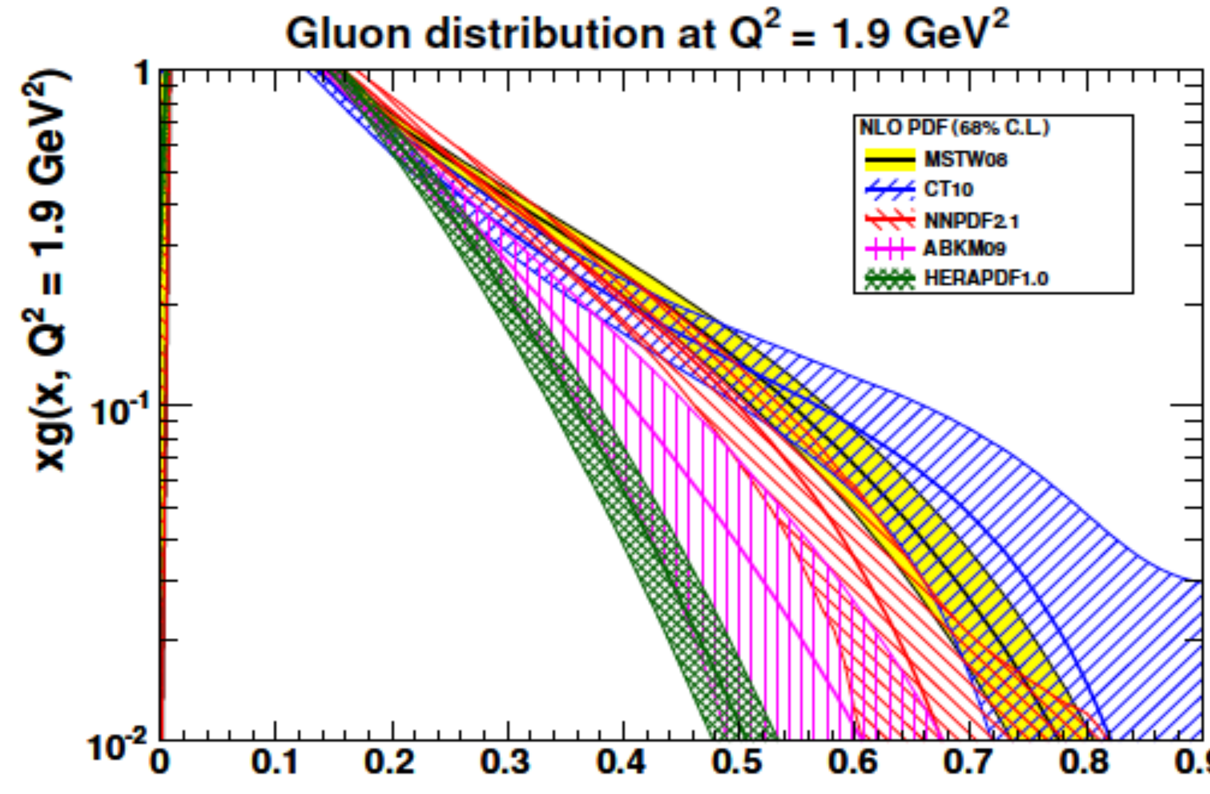

QCD fit analysis (default: NC,CC, LHeC only, following HERAPDF) with full experimental errors

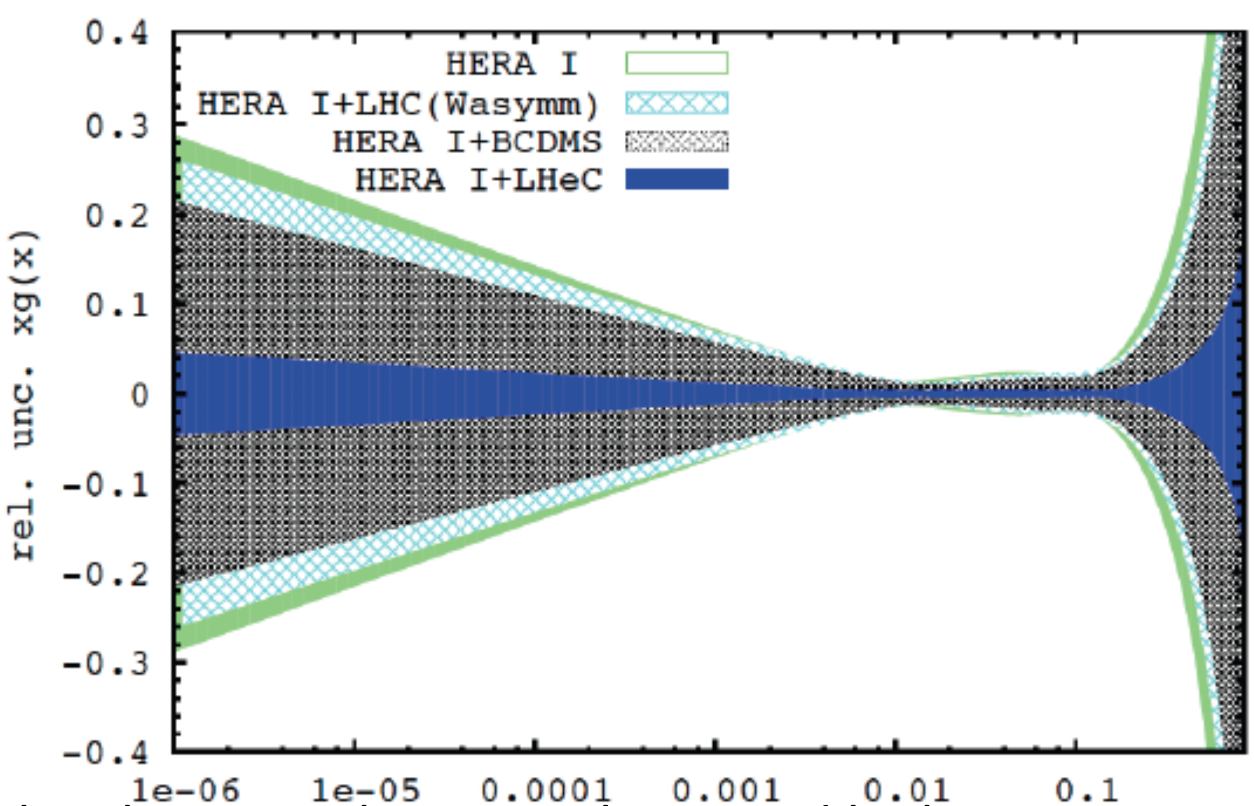

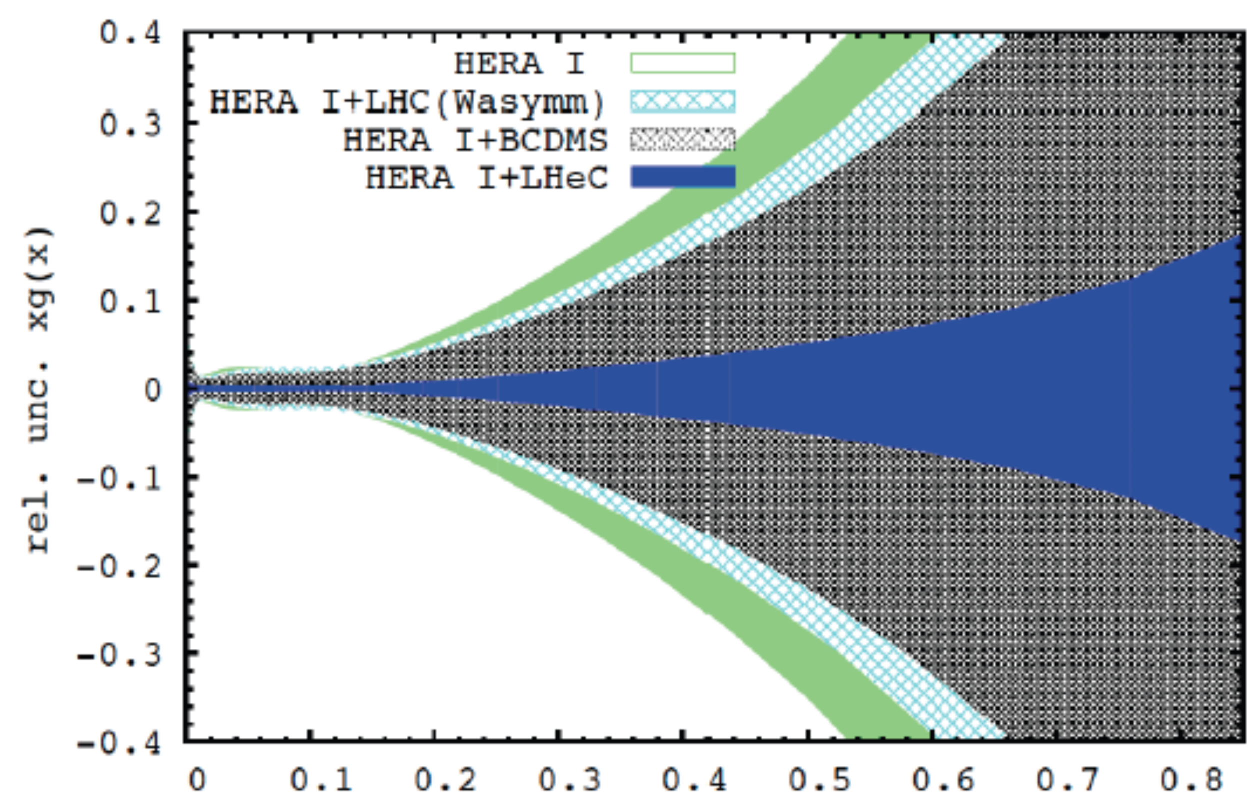

The gluon is unknown at low x and high x – QCD: non-linear evolution, resummation. BSM: hi M – HL-LHC!

Importance for NP searches

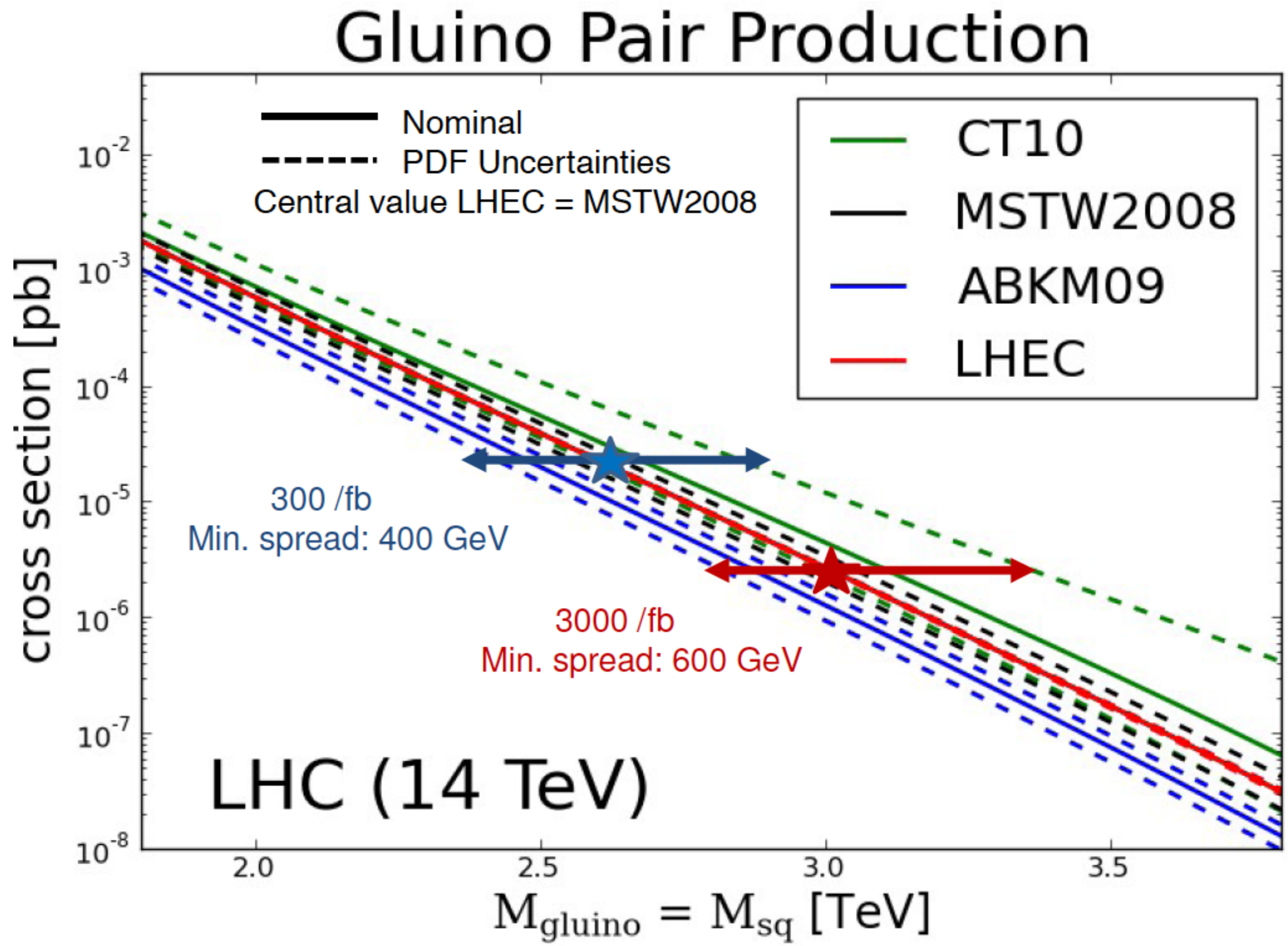

pp→ ğğX

Increase of pp luminosity moves searches to very high masses where the PDF uncertainties become very large. LHeC input will remove that.

M.D'Onofrio et al. LHeC Collaboration, ''New Physics with the LHeC", Poster at EPS Stockholm, July 18, 2013

Flavor decomposition

Charm

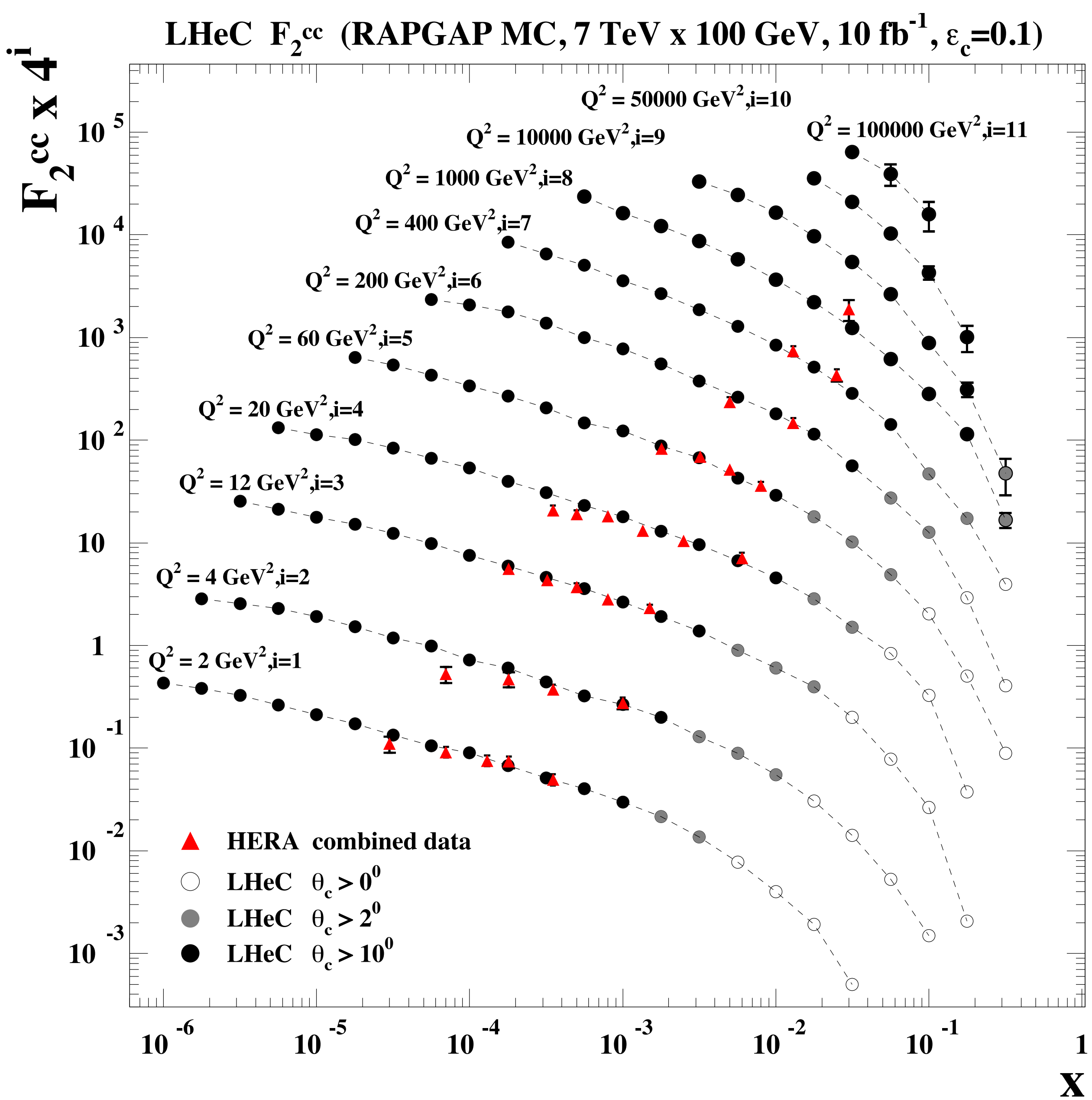

Beauty

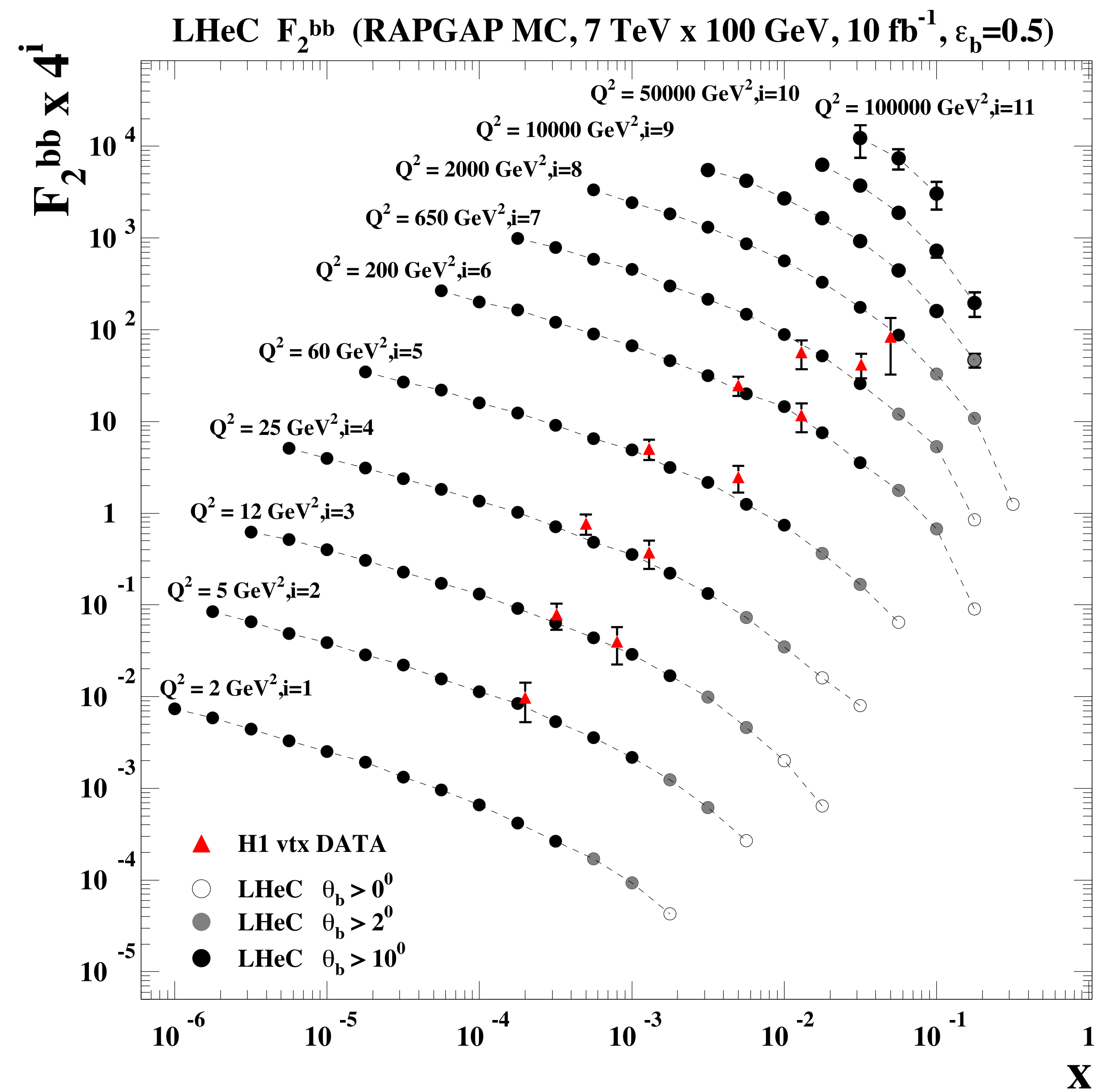

Diffraction

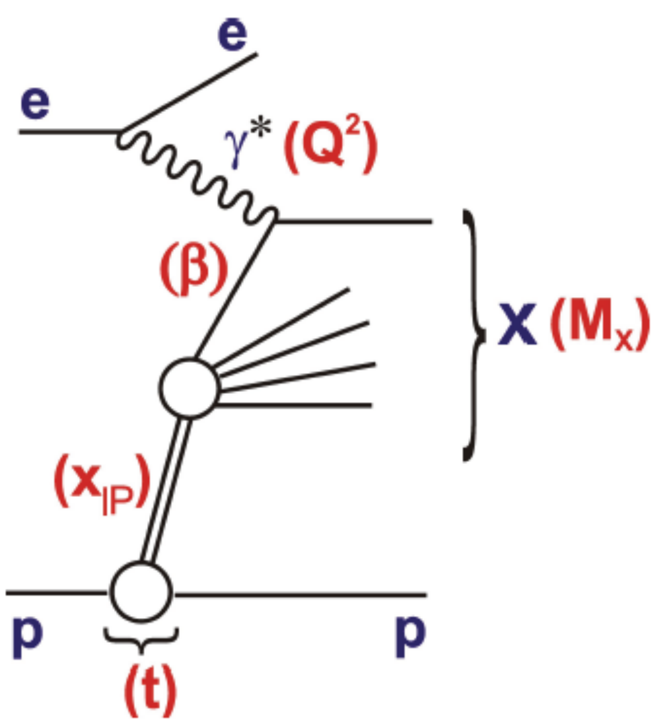

$$x_{IP} = \frac{Q^2 + M_X^2 - t}{Q^2 + W^2}$$

momentum fraction of the Pomeron w.r.t hadron

$$\beta = \frac{Q^2}{Q^2 + M_X^2 - t}$$

momentum fraction of parton w.r.t Pomeron

$$x_{Bj} = x_{IP}\beta$$

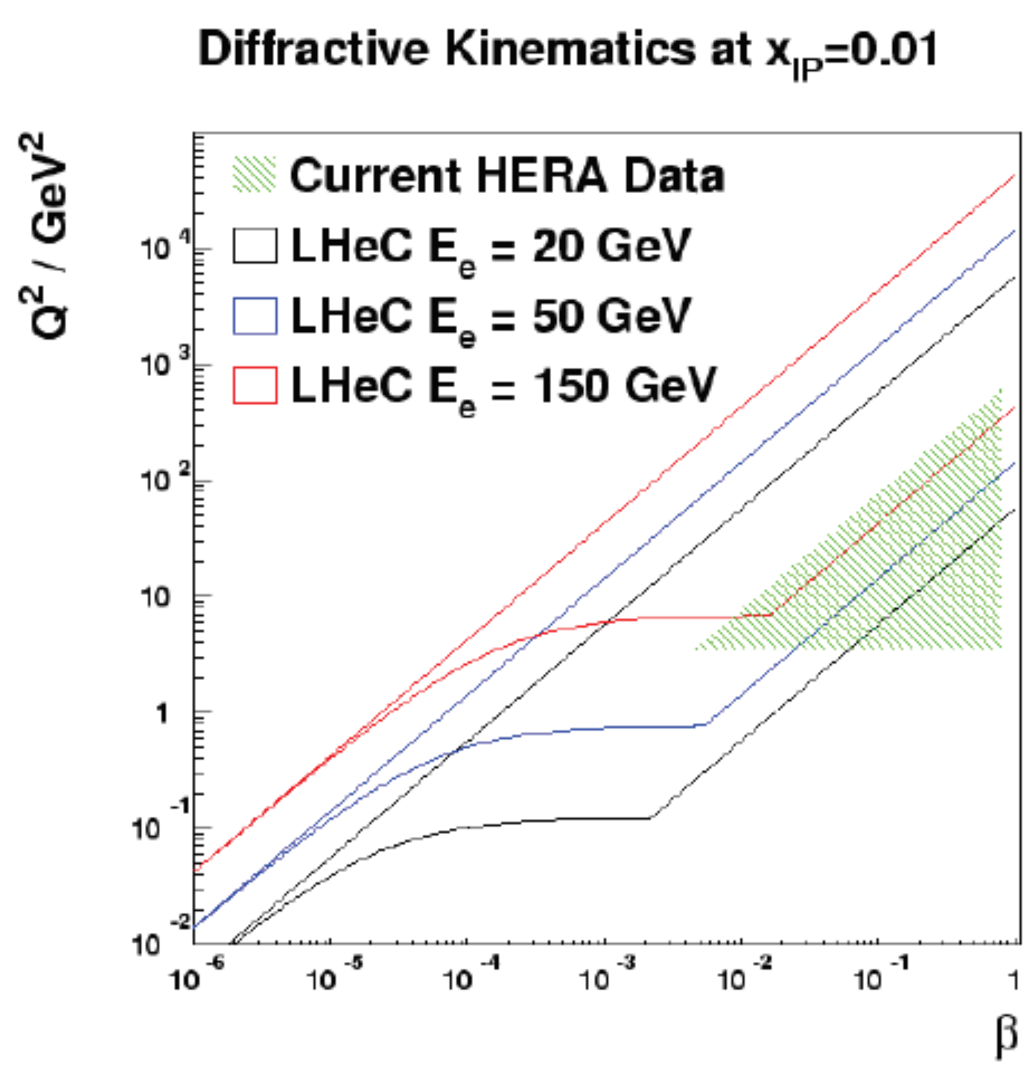

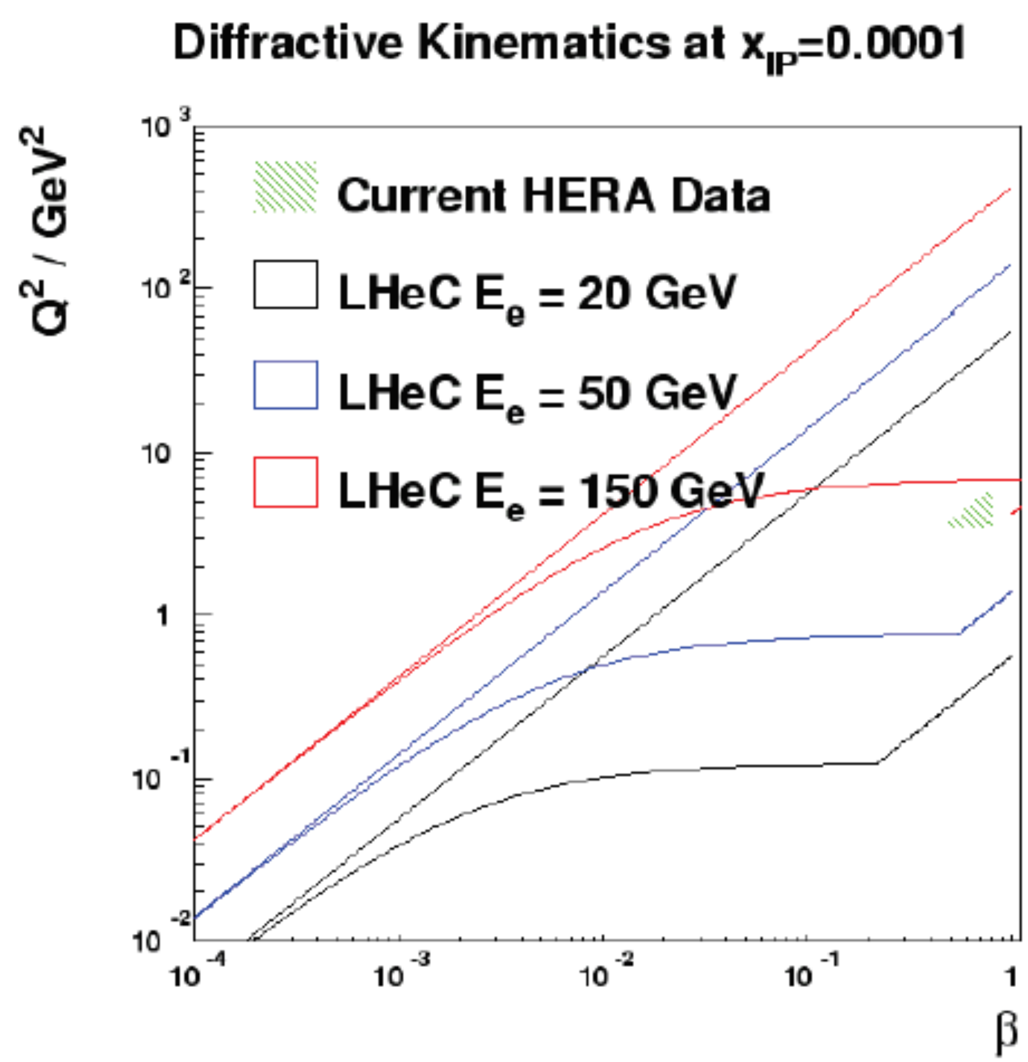

Diffractive event selection

Rapidity gap method

Exploit correlation between x_{IP} and $\eta_{\max}$
Assuming forward instrumentation down to 1^o
Could measure up to $\eta_{\max} < 5$
Limits the range in $x_{IP} < 0.01$
Misses region of large M_X

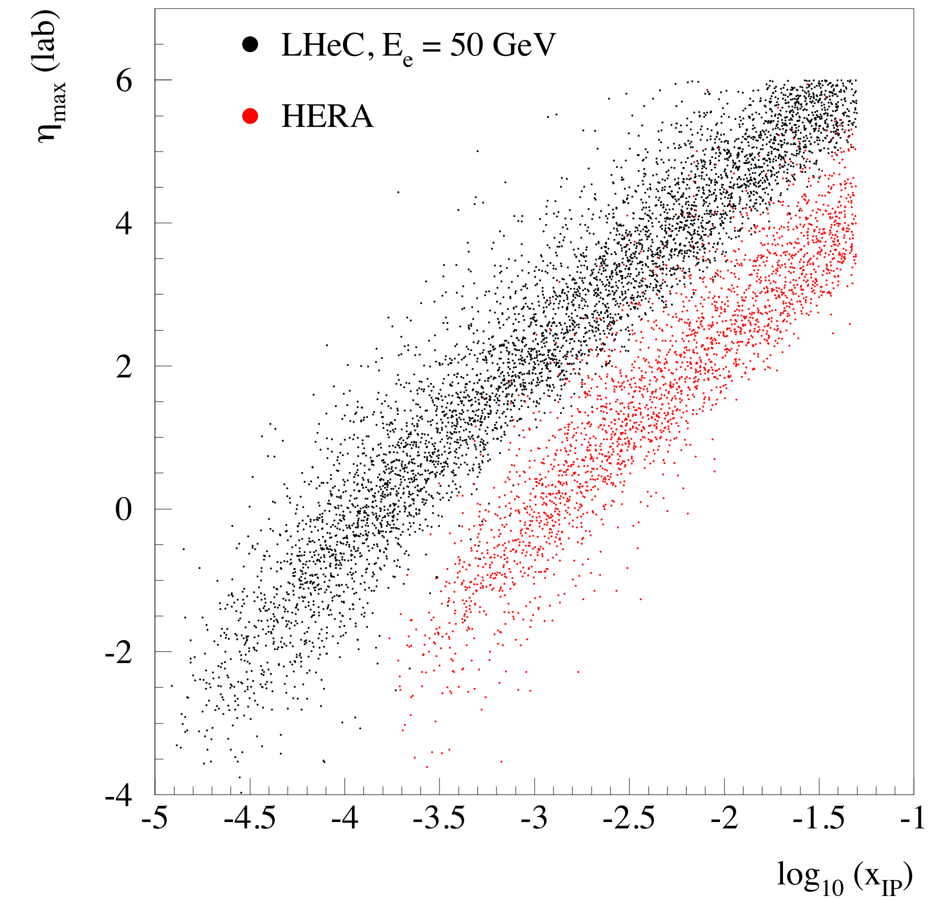

Leading proton tagging

Using proton spectrometer at 420m
Could reach higher values of x_{IP}
Overlap region between leading proton tagging method and rapidity gap method can be used as a cross check

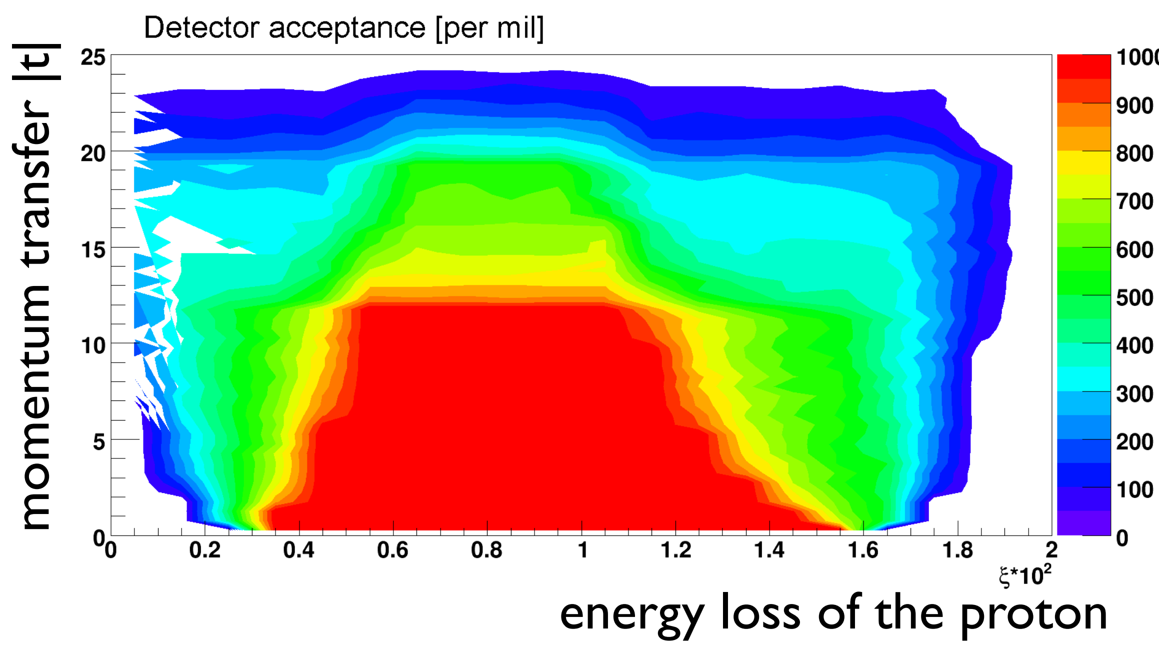

Diffractive mass distribution

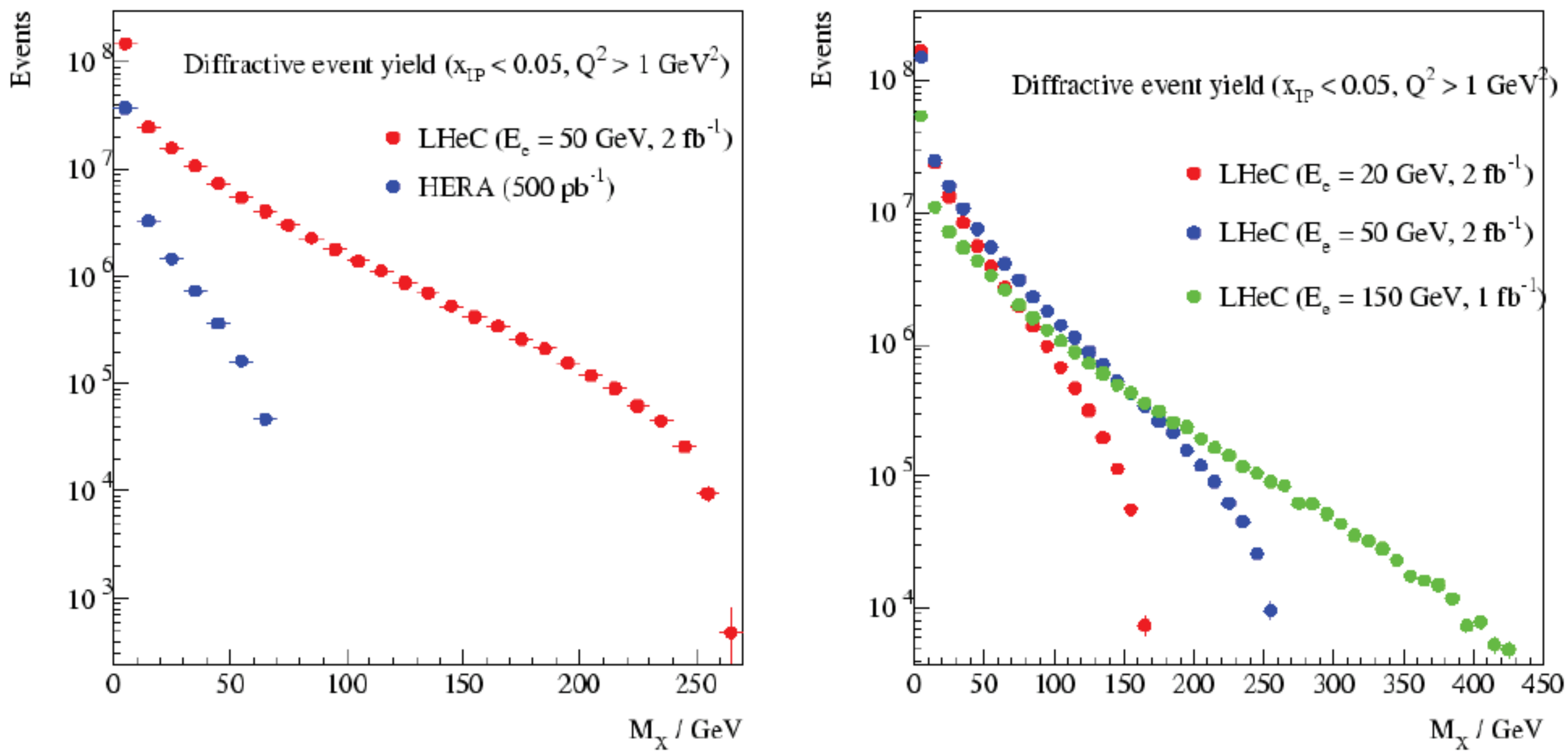

New domain of diffractive masses.
M_X can include W/Z/beauty

Neutral and charged current

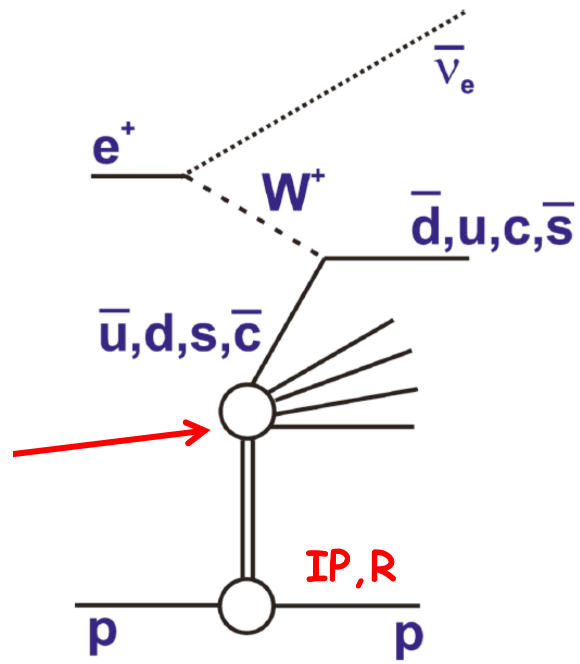

Diffraction with charged current sensitive to the flavor decomposition of the diffractive pdfs, not constrained by the neutral current data

Event selection:

Missing transverse energy
Rapidity gap selection

Different shapes of dσ/dy for W+ (q / $\bar{q}$) collisions

$$\frac{d\sigma}{dy}(e^- q) \propto 1 \qquad \frac{d\sigma}{dy}(e^- \bar{q}) \propto (1-y)^2$$

Suppressed in bwd region

$$\frac{d\sigma}{dxdy}(e^- p) \propto [(d+s)+(\bar{u}+\bar{c})(1-y)^2]$$

$$\frac{d\sigma}{dxdy}(e^+ p) \propto [(\bar{d}+\bar{s})+(u+c)(1-y)^2]$$

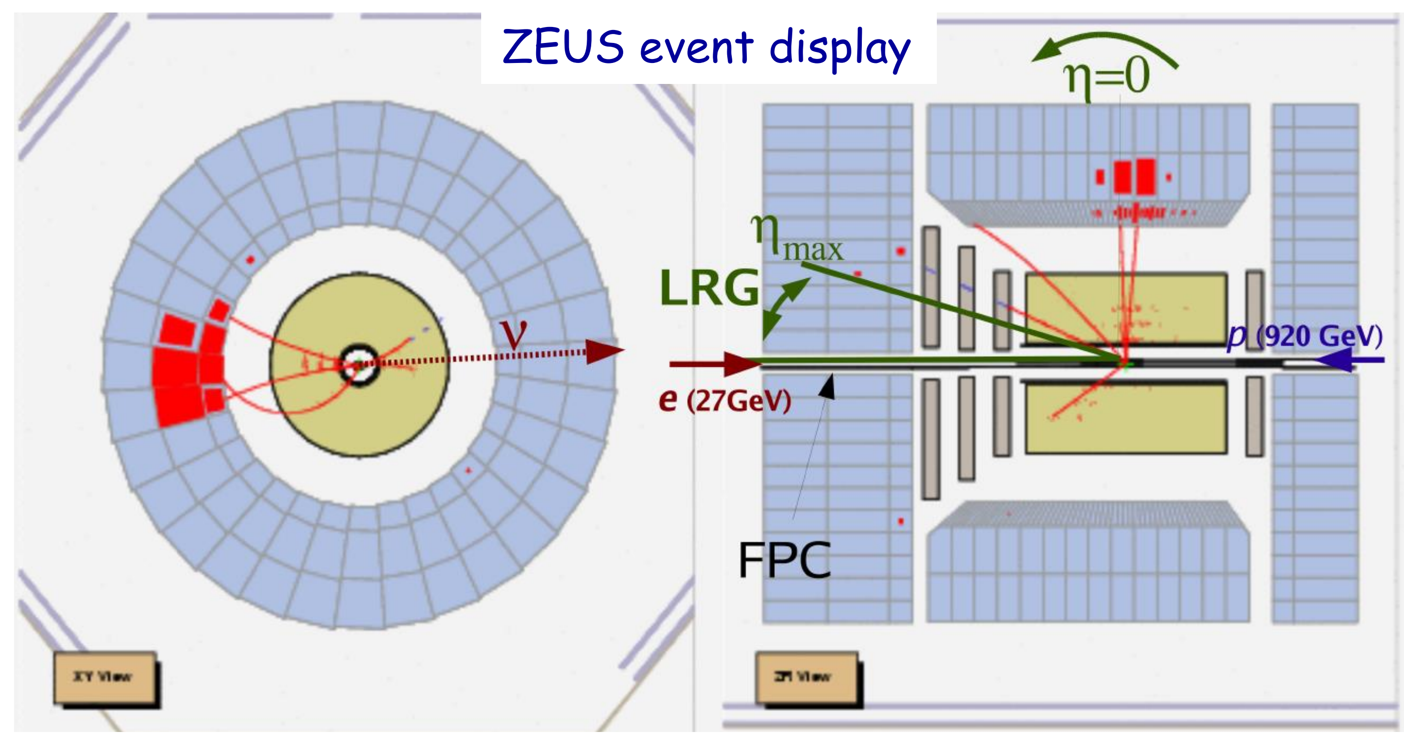

Kinematics calculable from the diffractive system

$$y = \frac{E^X - p_z^X}{2E_e} \qquad Q^2 = \frac{(p_T^X)^2}{1-y} \qquad x_{IP} = \frac{Q^2 + 2E_e(E^X + p_z^X)}{4E_e E_p} \qquad \beta = \frac{Q^2}{x_{IP}\, ys}$$

Charged current diffraction at HERA

H1

$$\sigma_{H1}^{CCdiff} = 0.39 \pm 0.12(stat) \pm 0.07(syst)\,\text{pb}$$

10 events

ZEUS

$$\sigma_{ZEUS}^{CCdiff} = 0.49 \pm 0.20(stat) \pm 0.13(syst)\,\text{pb}$$

9 events

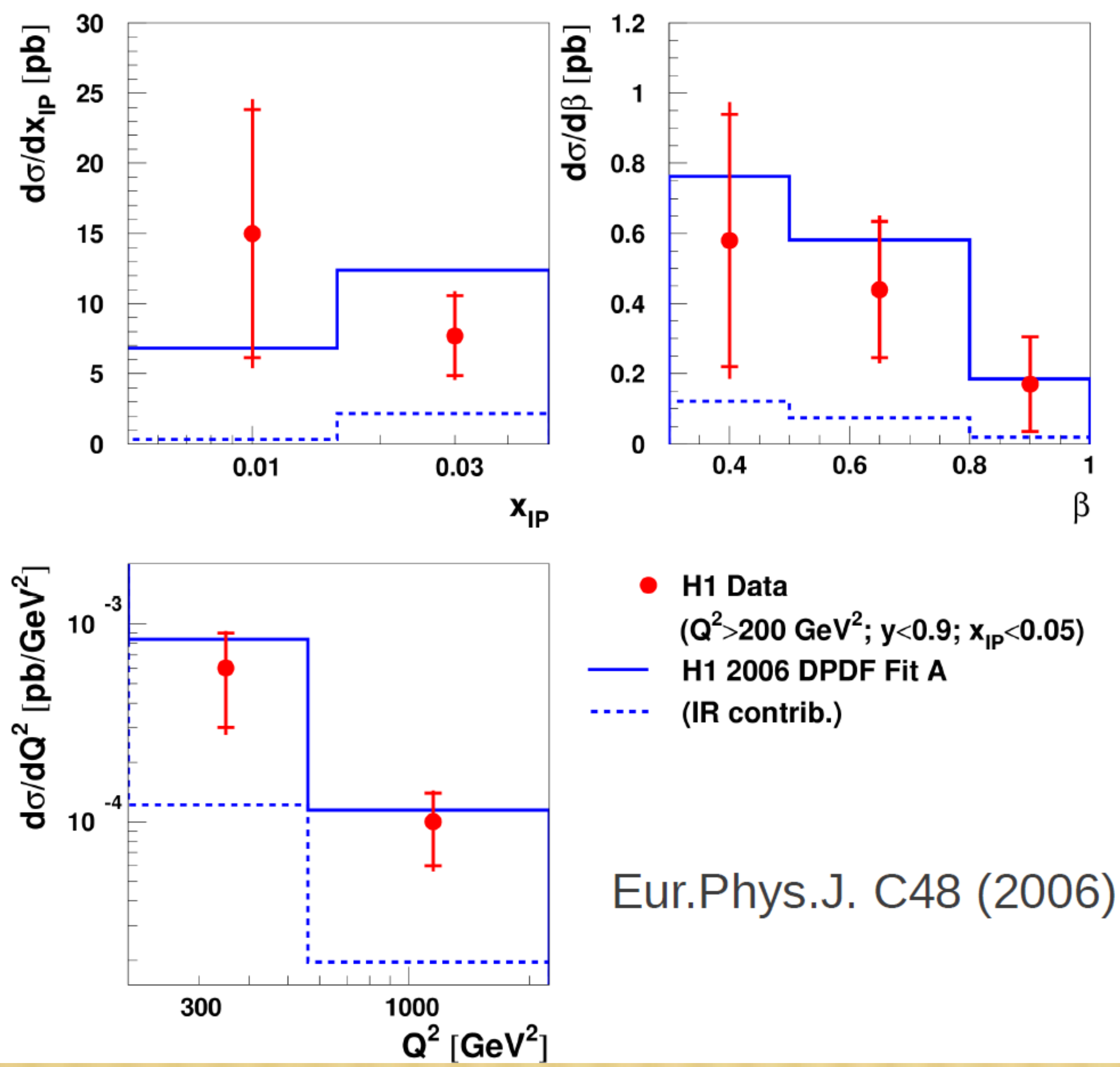

Eur.Phys.J. C48 (2006) 715-748

Analysis cuts

$$Q^2 > 200\,\text{GeV}^2$$
$$y < 0.9$$
$$x_{IP} < 0.05$$

Only about 2% of CC x-section !

Resolved Pomeron model with H1 fits A or B predicts zero e+e- assymmetry. Assymmetry not studied here....

Predictions for charged current diffraction at LHeC

HERA
920+27.5
$\sigma^{CCdiff}(MC) = 338fb$
~20 events ($60pb^{-1}$)

MC RAPGAP prediction

cuts:
$Q^2 > 700\ GeV^2$,
$0.005 < x_{IP} < 0.012$
$0.2 < y < 0.9$

Markéta Jansová,
Bachelor work, Prague 2013

LHeC
7000+60
$\sigma^{CCdiff}(MC) = 923fb$
~80000 events ($100fb^{-1}$)

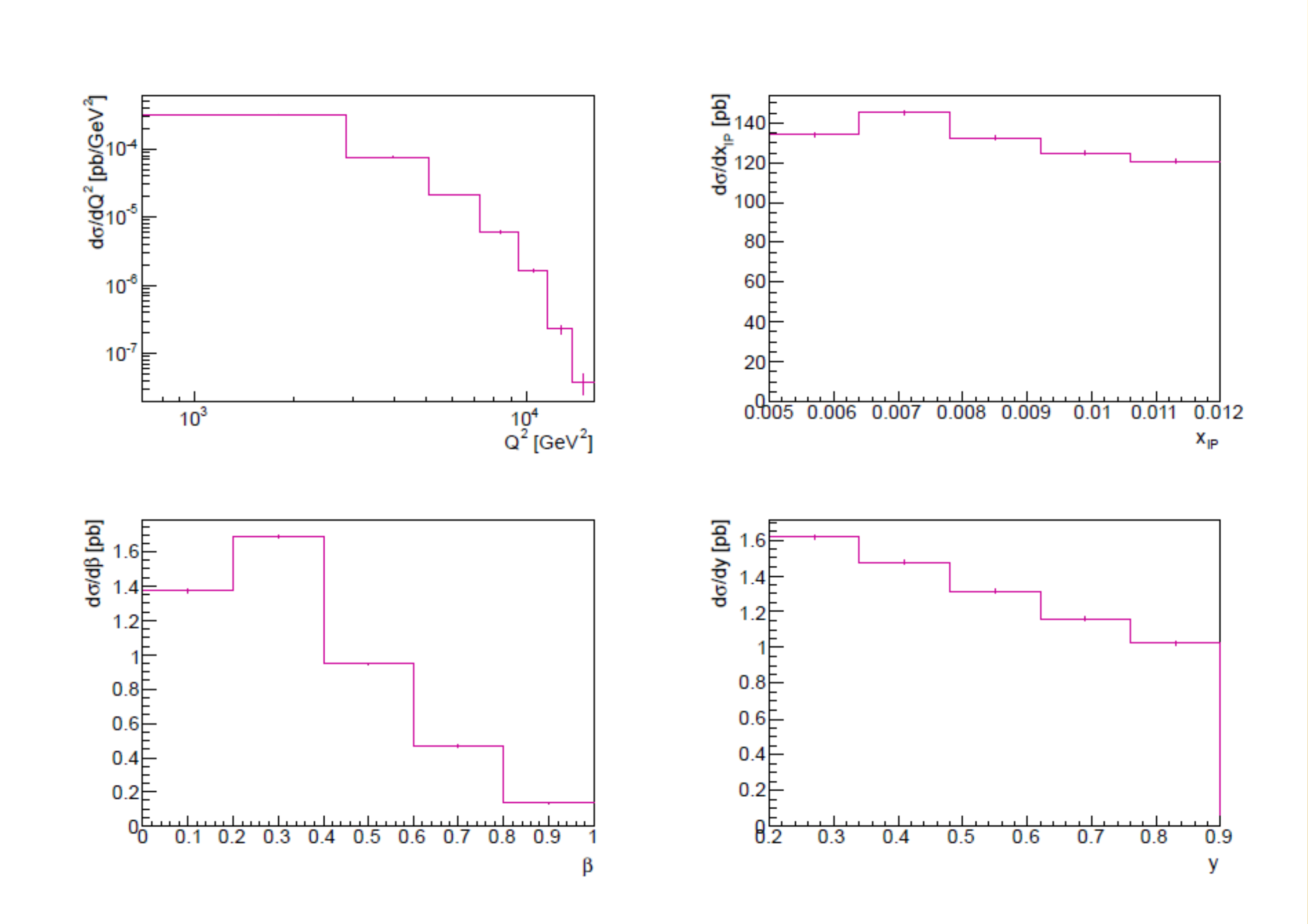

No corrections for detector acceptance and resolution!

Diffractive CC events could be studied in a more detailed way…

Factorization

Inclusive diffraction

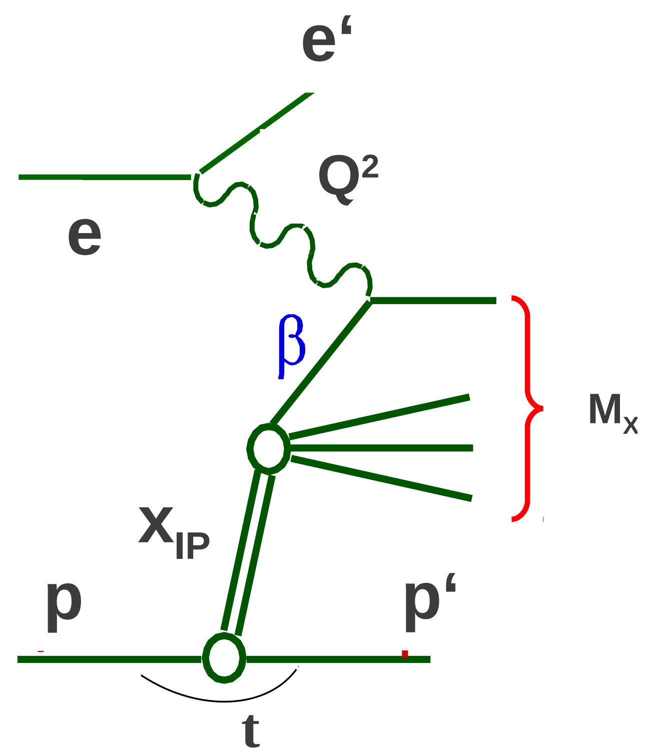

Diffractive dijets

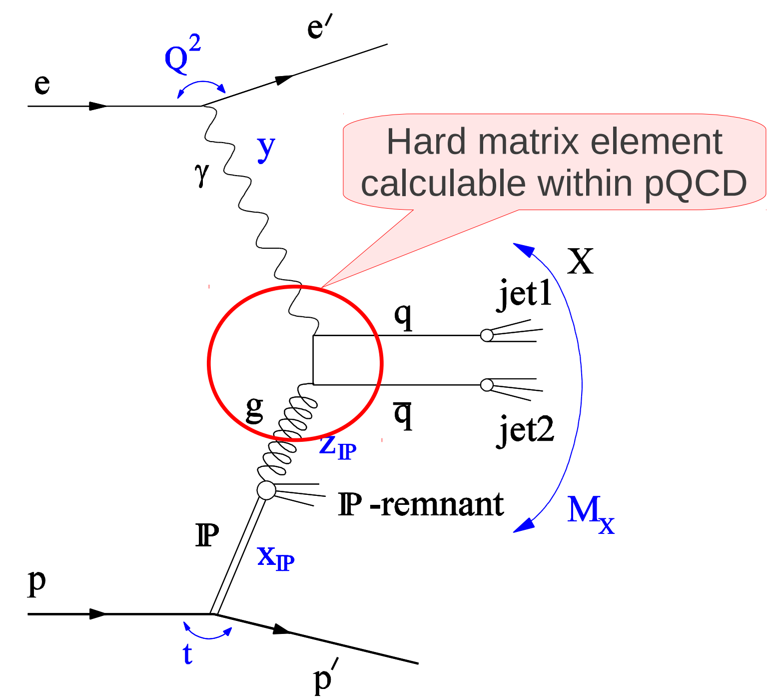

Factorization in Diffraction

QCD factorization holds for inclusive and exclusive processes if:

- photon is point-like (Q^2 is high enough)
- higher twist corrections are negligible (problems for small Q^2 around $\beta \simeq 1$)

  QCD factorization theoretically proven for DIS (Collins 1998)

$$d\sigma^D(\gamma p \to Xp) = \sum_{parton_i} f_i^D(\beta, Q^2, x_{IP}, t) * d\hat{\sigma}^{\gamma i}(x, Q^2)$$

f_i^D DPDFs, obeys DGLAP evolution, process independent

$d\hat{\sigma}^{\gamma i}$ Process dependent partonic x-section, calculable within pQCD

DIS Dijets HERA vs LHeC Comparison of Synthetic Data

- Higher CMS energy makes higher scales accessible

HERA		LHeC
$E_T^{\mathrm{jet1}} \sim 15\,\mathrm{GeV}$	→	$E_T^{\mathrm{jet1}} \sim 40\,\mathrm{GeV}$

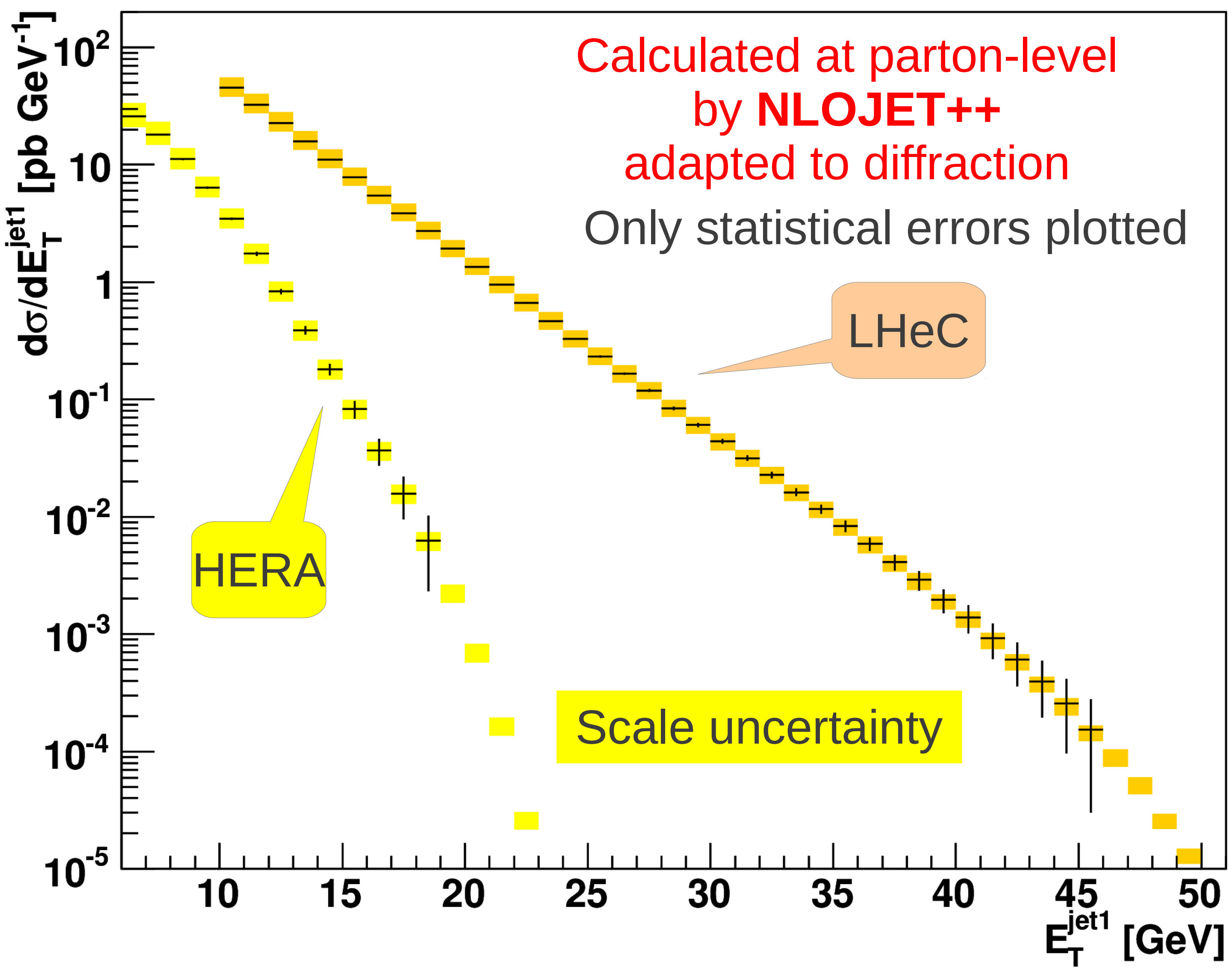

920 + 27.5 HERA ($400\,\mathrm{pb}^{-1}$)

$$Q^2 > 4\,\mathrm{GeV}^2 \wedge 0.1 < y < 0.7$$
$$x_{IP} < 0.03 \wedge |t| < 1\,\mathrm{GeV}^2$$
$$M_Y < 1.6\,\mathrm{GeV}$$
$$E_T^{\mathrm{jet1}} > 6\,\mathrm{GeV}$$
$$E_T^{\mathrm{jet2}} > 4\,\mathrm{GeV}$$
$$-1 < \eta^{\mathrm{jets}} < 2$$

7000 + 60 LHeC ($10\,\mathrm{fb}^{-1}$)

$$Q^2 > 2\,\mathrm{GeV}^2 \wedge 0.1 < y < 0.7$$
$$x_{IP} < 0.01 \wedge |t| < 1\,\mathrm{GeV}^2$$
$$M_Y < 1.6\,\mathrm{GeV}$$
$$E_T^{\mathrm{jet1}} > 10\,\mathrm{GeV}$$
$$E_T^{\mathrm{jet2}} > 6.5\,\mathrm{GeV}$$
$$-3 < \eta^{\mathrm{jets}} < 3$$

$$Q^2 > 2\,\mathrm{GeV}^2 \rightarrow \theta_{el} < 178.5^\circ$$
$$Q^2 > 4\,\mathrm{GeV}^2 \rightarrow \theta_{el} < 176.5^\circ$$

DIS dijets in diffraction

At LHeC xsection is dominated by small $z_{\mathbb{P}}$
The gluon part of the diffractive PDF dominates in that region, weakly constrained from inclusive measurement.

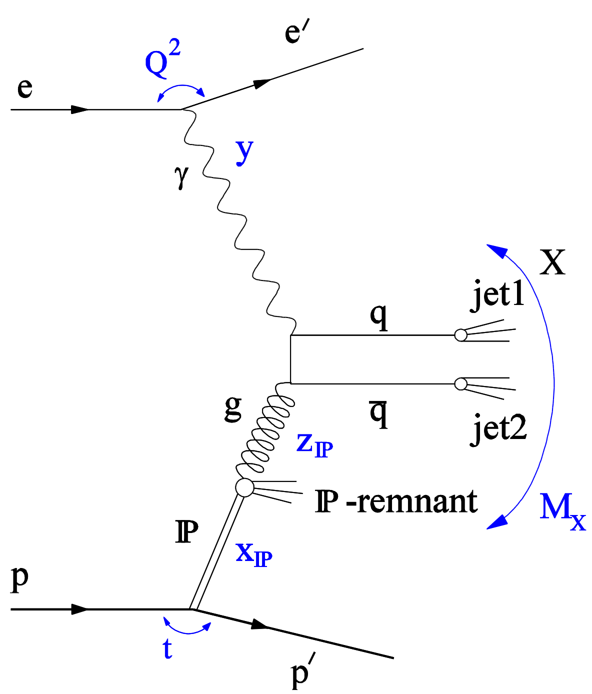

$$z_{IP}^{\min} \simeq \frac{\left(E_T^{\mathrm{jet1(min)}} + E_T^{\mathrm{jet1(min)}}\right)^2}{x_{IP}^{\max}\, y^{\max}\, s}$$

HERA	LHeC
$z_{IP} \sim 0.07$	$z_{IP} \sim 0.02$

Radek Žlebčík

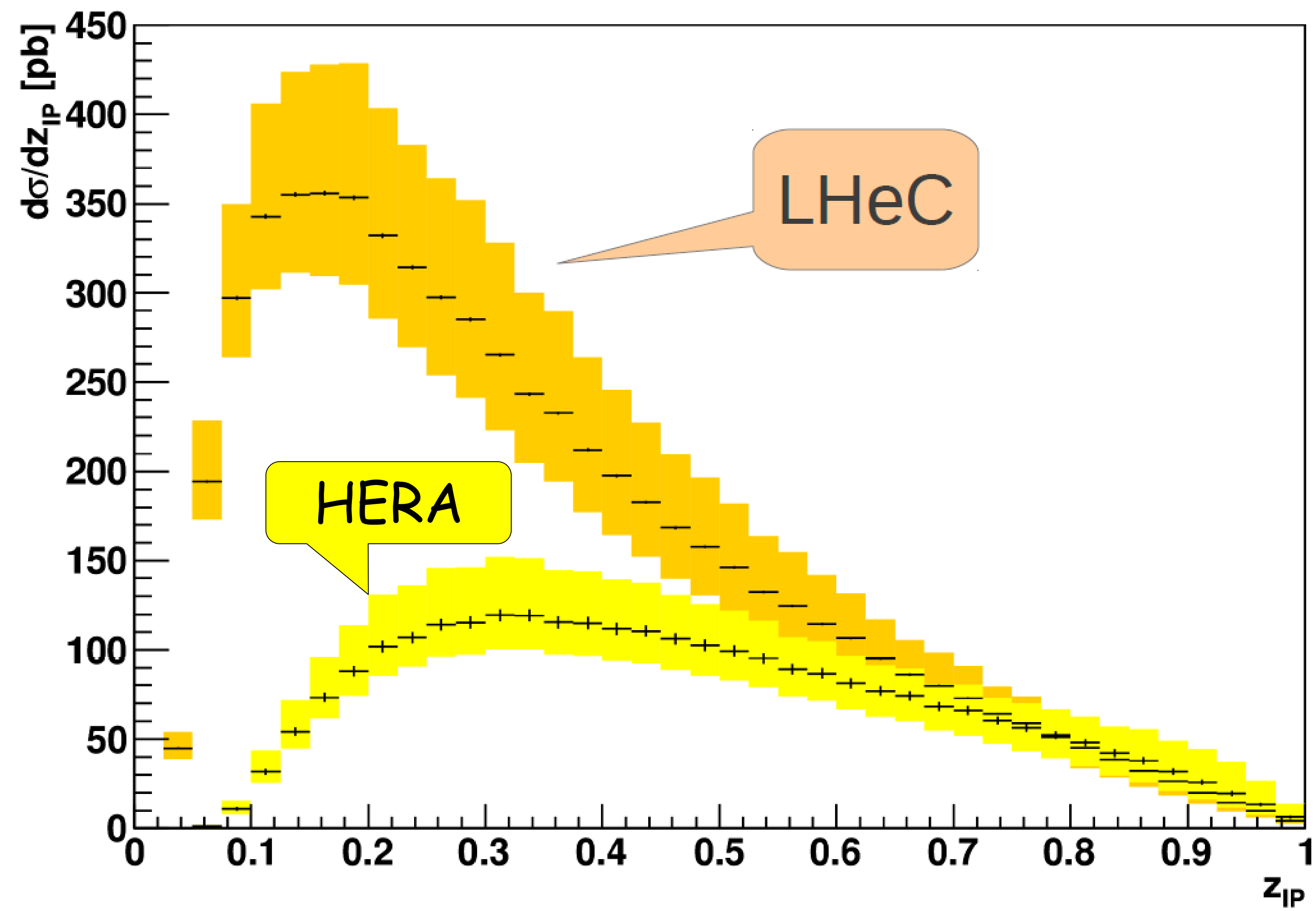

Diffractive Dijet Photoproduction

Direct
No photon remnant
$x_\gamma = 1$ (at parton-level)
Dominant for high Q^2
(near DIS region)

Resolved
photon remnant
$x_\gamma < 1$
Dominant for low Q^2, γ-PDF introduced:

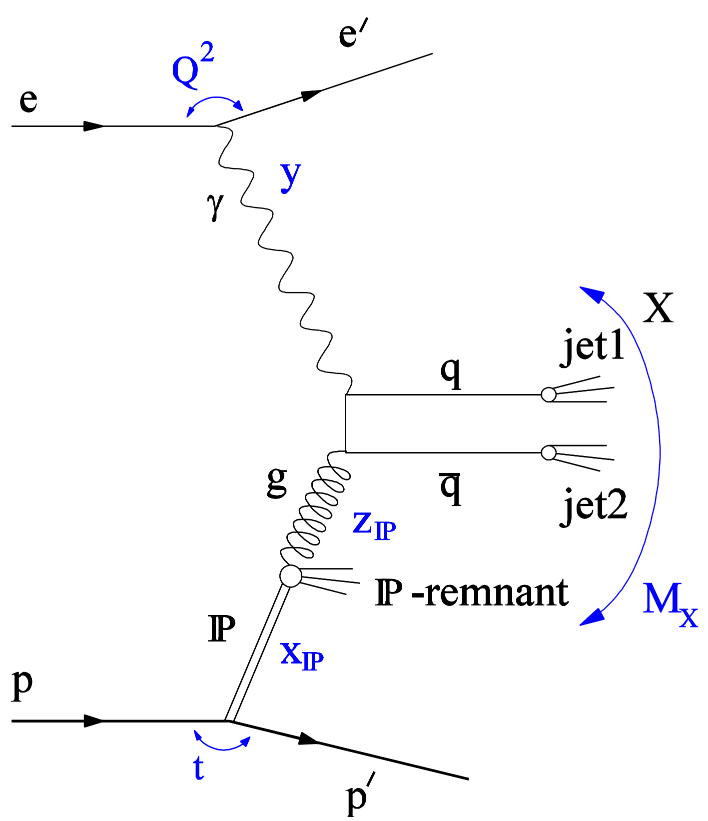

x_γ – photon momentum fraction

$$x_\gamma = \frac{E_T^{\text{jet1}} e^{-\eta^{\text{jet1}}} + E_T^{\text{jet2}} e^{-\eta^{\text{jet2}}}}{2y\, E_e^{\text{beam}}}$$

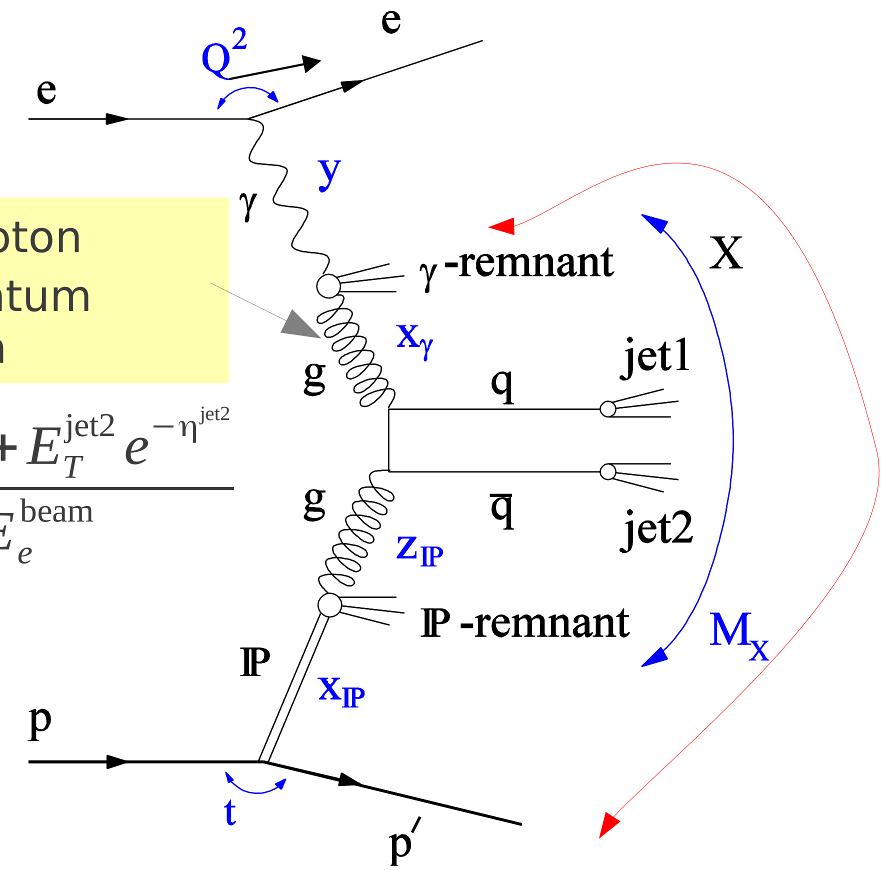

Additional interactions which spoil rap. Gap? (like in pp)

PHP Dijets HERA vs LHeC

- Due to much higher E_T^{jet} jets at LHeC is LHeC better tool to investigate possible factorisation breaking

HERA		LHeC
$E_T^{jet1} \sim 17\,\mathrm{GeV}$	→	$E_T^{jet1} \sim 42\,\mathrm{GeV}$

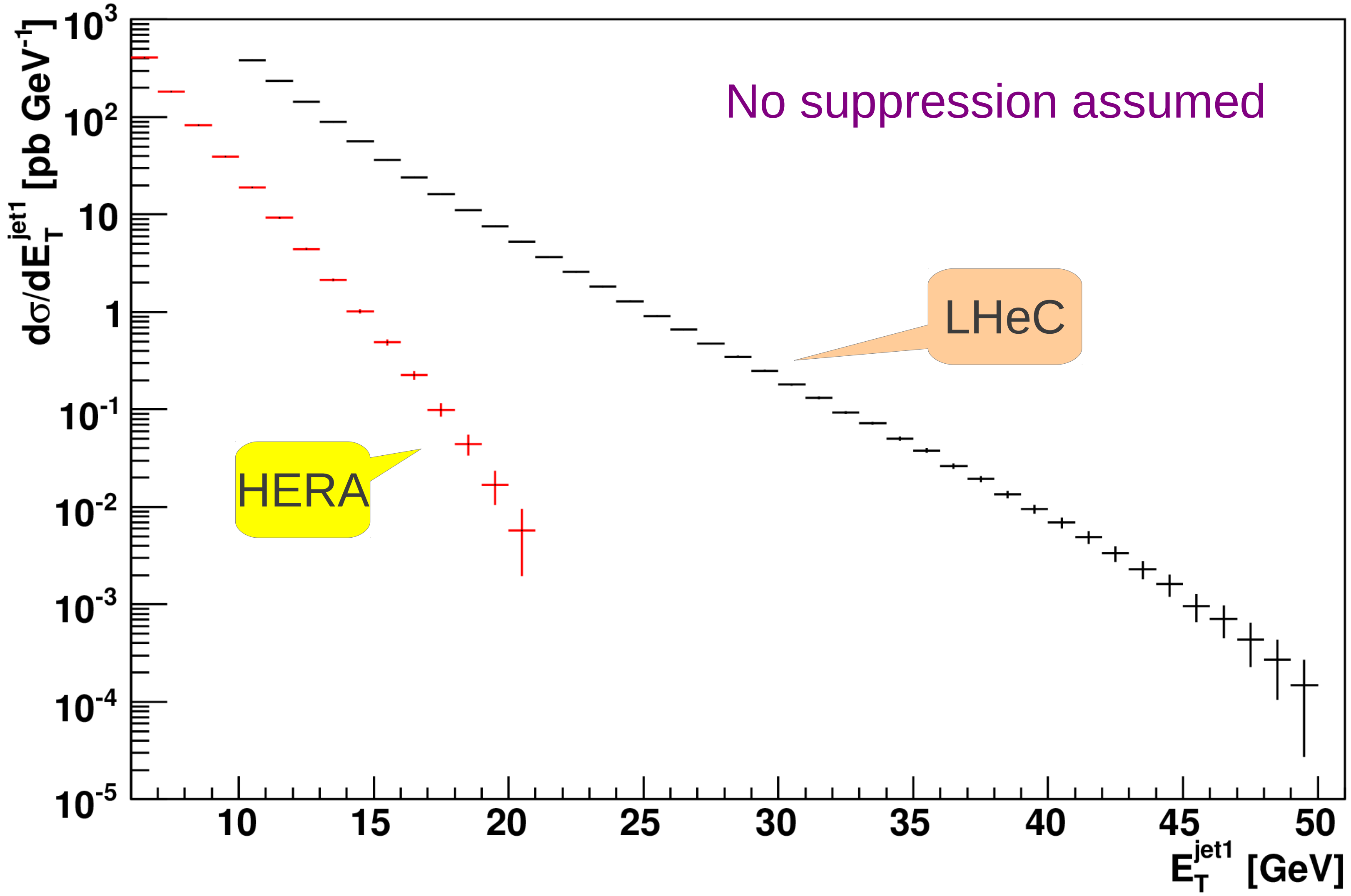

Only statistical errors of synthetic data depicted
No acceptance and detector smearing effects take into account

Calculated at parton-level by **Frixione NLO** adapted to diffraction

920 + 27.5 HERA $(400\,\mathrm{pb}^{-1})$

$$Q^2 < 2\,\mathrm{GeV}^2 \wedge 0.2 < y < 0.8$$
$$x_{IP} < 0.03 \wedge |t| < 1\,\mathrm{GeV}^2$$
$$M_Y < 1.6\,\mathrm{GeV}$$
$$E_T^{jet1} > 6\,\mathrm{GeV}$$
$$E_T^{jet2} > 4\,\mathrm{GeV}$$
$$-1 < \eta^{jets} < 2$$

7000 + 60 LHeC $(10\,\mathrm{fb}^{-1})$

$$Q^2 < 2\,\mathrm{GeV}^2 \wedge 0.2 < y < 0.8$$
$$x_{IP} < 0.01 \wedge |t| < 1\,\mathrm{GeV}^2$$
$$M_Y < 1.6\,\mathrm{GeV}$$
$$E_T^{jet1} > 10\,\mathrm{GeV}$$
$$E_T^{jet2} > 6.5\,\mathrm{GeV}$$
$$-3 < \eta^{jets} < 3$$

LHeC kinematics: acceptance

Kinematics in ePb

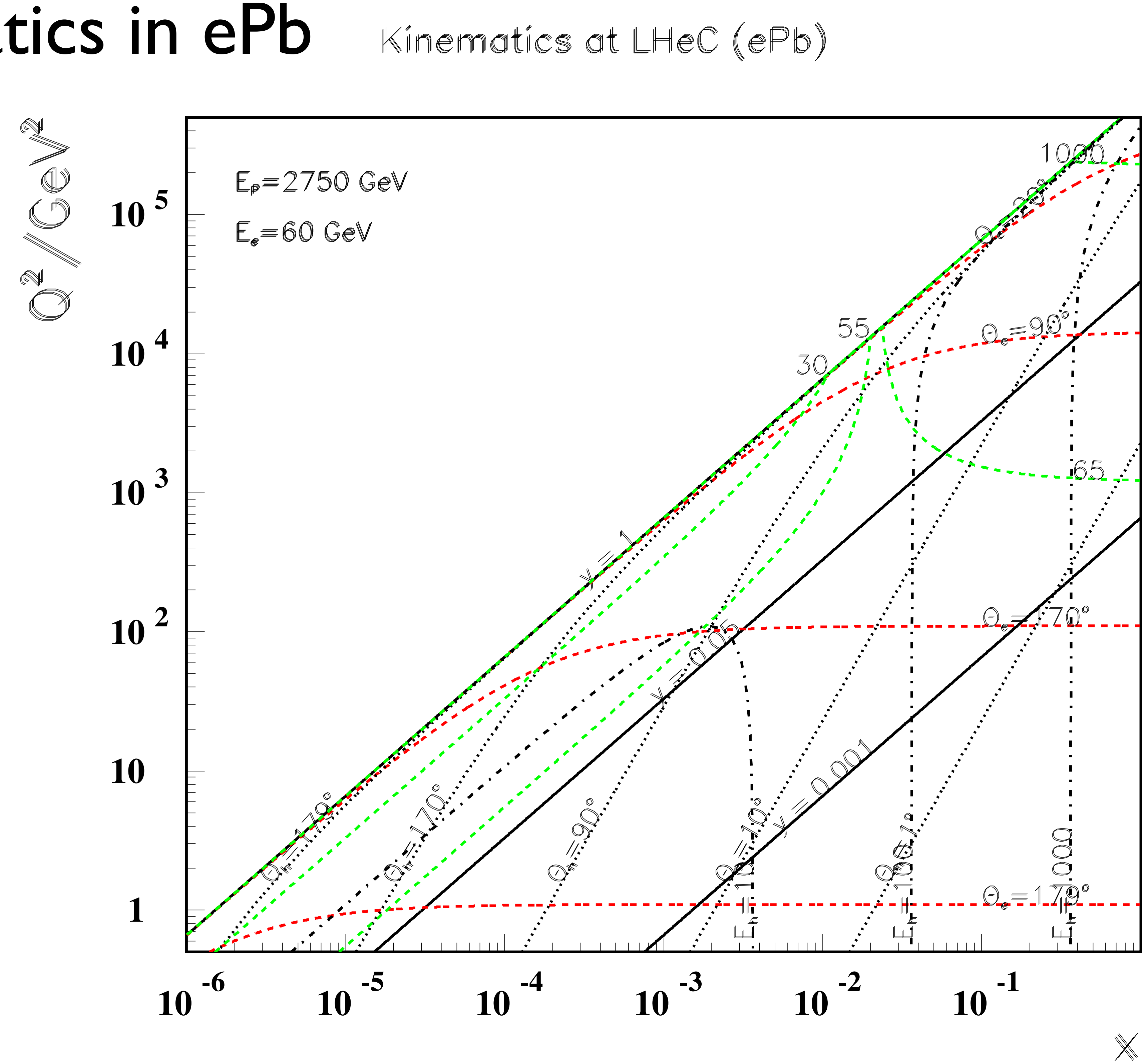

Similar requirements in the case of eA as in ep scattering.

Complementarity of pA and eA

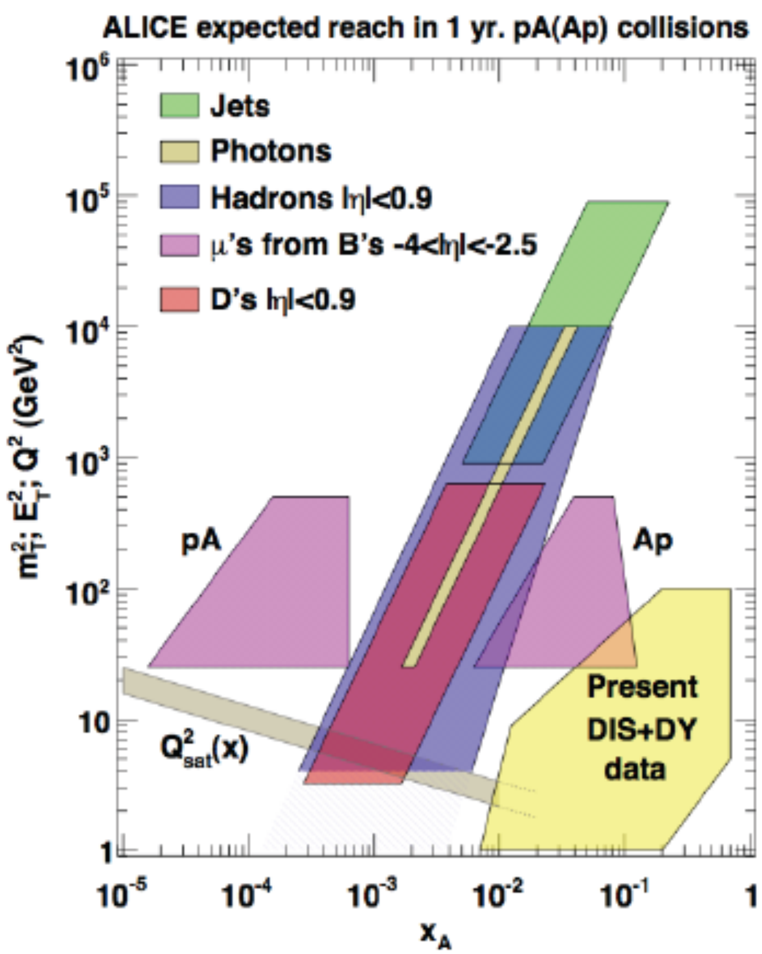

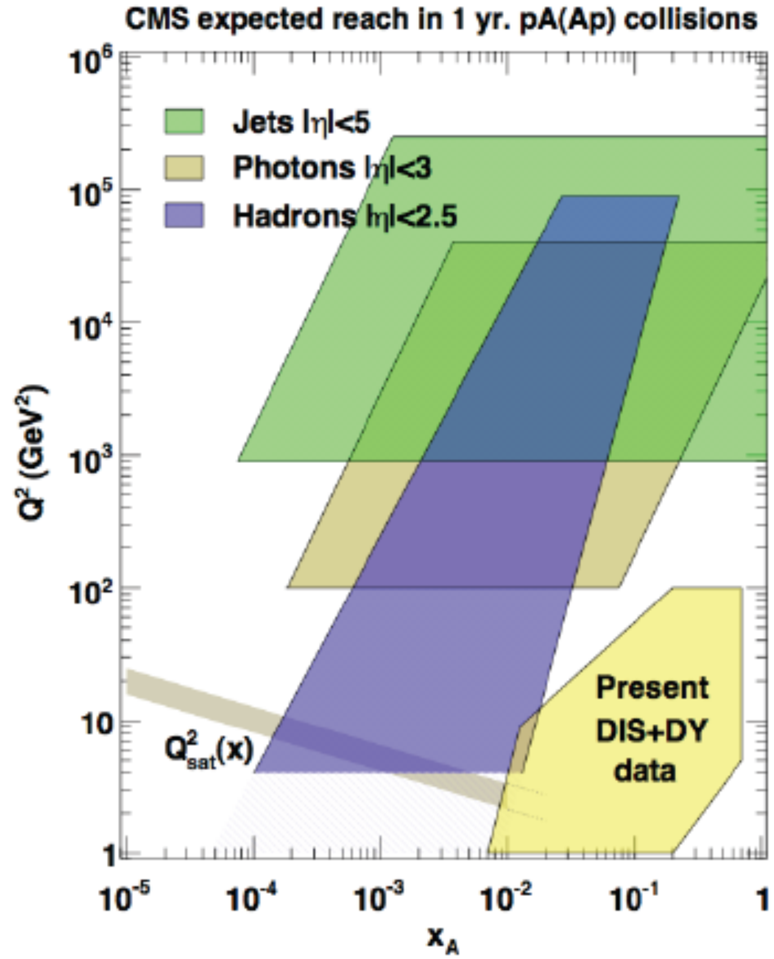

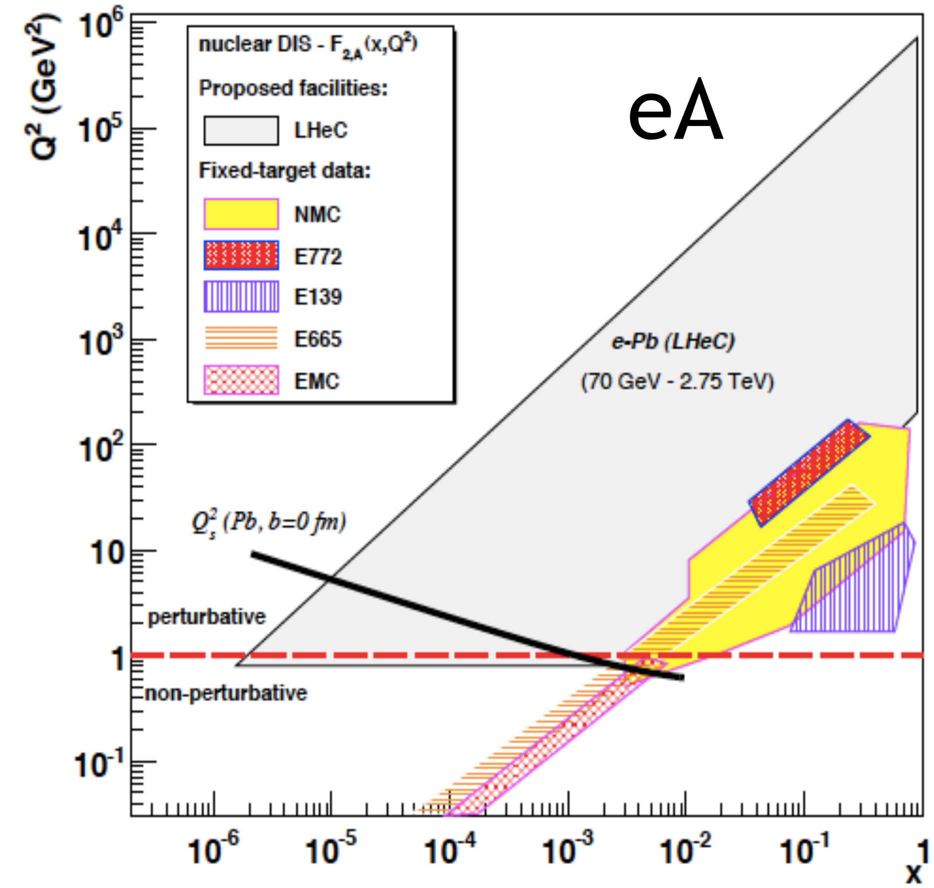

• **New effects likely to be revealed in tensions between eA and pA, AA, ep (breakdown of factorisation)**

• **Detailed precision understanding likely to come from eA**

- LHeC offers access to lower x than is realistically achievable in pA at the LHC
- Clean final states / theoretical control to (N)NLO in QCD

Nuclear parton distributions: uncertainty

Collinear factorization in DIS:

$$F_{2,L}^{A}(x,Q^2) = C_i(\alpha_s; x, Q^2/\mu^2) \otimes x f_i^A(x,\mu^2)$$

Current uncertainties of the parton distribution in nuclei

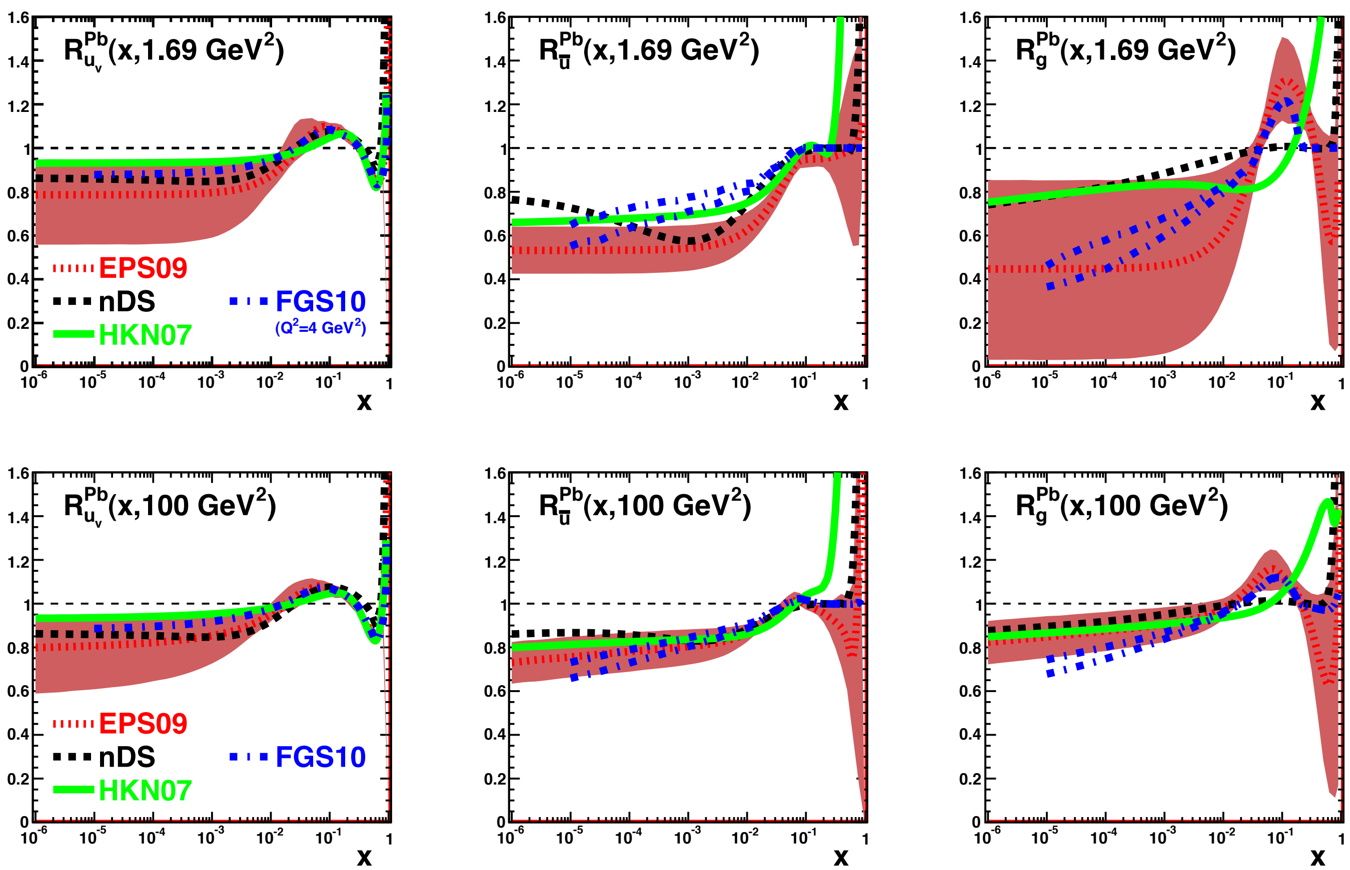

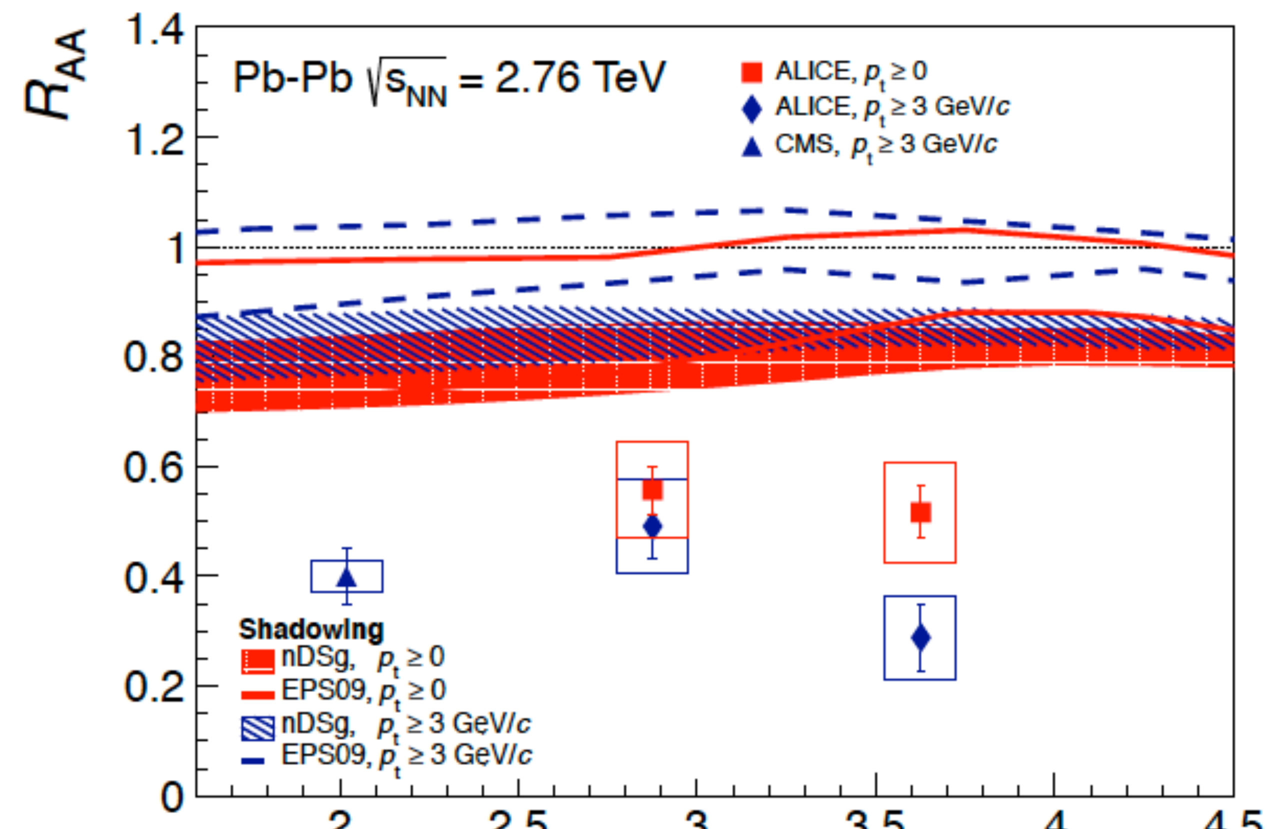

Inclusive J/ψ

Large uncertainty at small values of x especially in the gluon and sea quark sector
Translate into uncertainties in the evaluation of benchmarking for variety of processes at LHC and disentangling the effects of initial state from quark - gluon plasma in AA

Proton-lead surprises

1307.3237 – ALICE

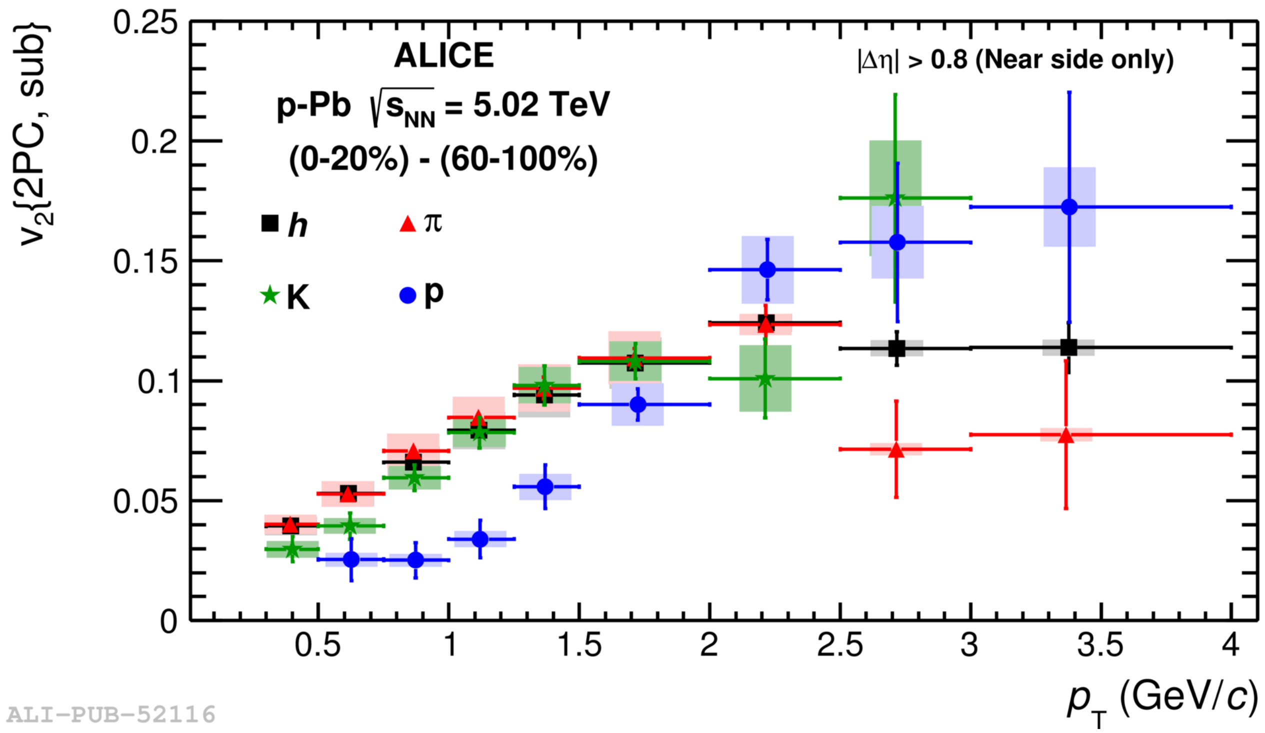

1303.2084 – ATLAS

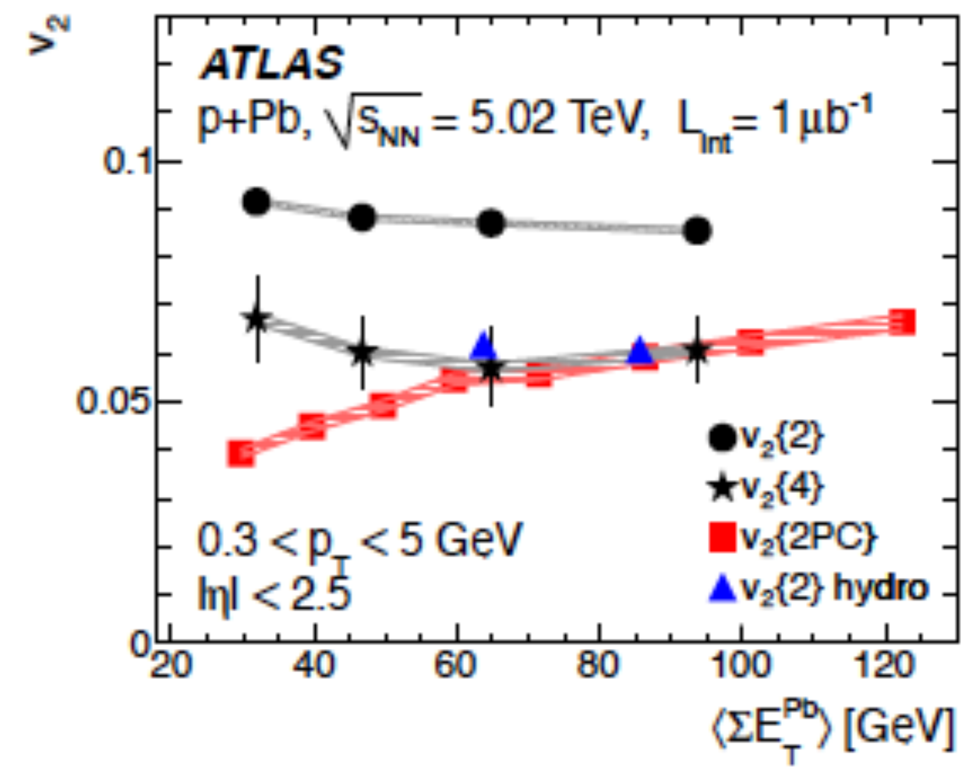

Flow in pPb resembles that of PbPb described by hydrodynamics?
How important are final state effects in pPb?
Are such collective effects present in eA?
Rises a lot of questions about extraction of npdfs from pPb: perhaps limited to W,Z...

Generated LHeC pseudodata for e-A

- A sample of pseudodata (by N. Armesto) for reduced cross-sections

$$\sigma_r^{NC} = \frac{Q^4 x}{2\pi\alpha^2 Y_+}\frac{d^2\sigma^{NC}}{dxdQ^2} = F_2\left[1 - \frac{y^2}{Y_+}\frac{F_L}{F_2}\right] \qquad Y_+ = 1 + (1-y)^2$$

was generated from using assuming:

E_{lepton} = 50 GeV, E_p = 7000 GeV, E_{Pb} = 2750 GeV , E_{Ca} = 3500 GeV

in the kinematical window: $x < 0.01$ & $Q^2 < 1000$ GeV^2

- The e+p cross-sections from a pQCD based simulation, nuclear effects according to a dipole model (Eur. Phys. J. C26 (2002) 35-43)

- The inclusive cross-sections were combined to ratios

$$\frac{\sigma^{\mathrm{Ca}}_{\mathrm{reduced}}(x,Q^2)}{\sigma^{\mathrm{p}}_{\mathrm{reduced}}(x,Q^2)}, \quad \text{and} \quad \frac{\sigma^{\mathrm{Pb}}_{\mathrm{reduced}}(x,Q^2)}{\sigma^{\mathrm{p}}_{\mathrm{reduced}}(x,Q^2)}$$

- Flavor-decomposed quantities were also considered

$$\frac{\sigma^{\mathrm{Ca,\,Pb}}_{\mathrm{reduced,\,charm}}(x,Q^2)}{\sigma^{\mathrm{p}}_{\mathrm{reduced,\,charm}}(x,Q^2)} \quad \text{and} \quad \frac{\sigma^{\mathrm{Ca,\,Pb}}_{\mathrm{reduced,\,bottom}}(x,Q^2)}{\sigma^{\mathrm{p}}_{\mathrm{reduced,\,bottom}}(x,Q^2)}$$

Before the LHeC pseudodata vs EPS09

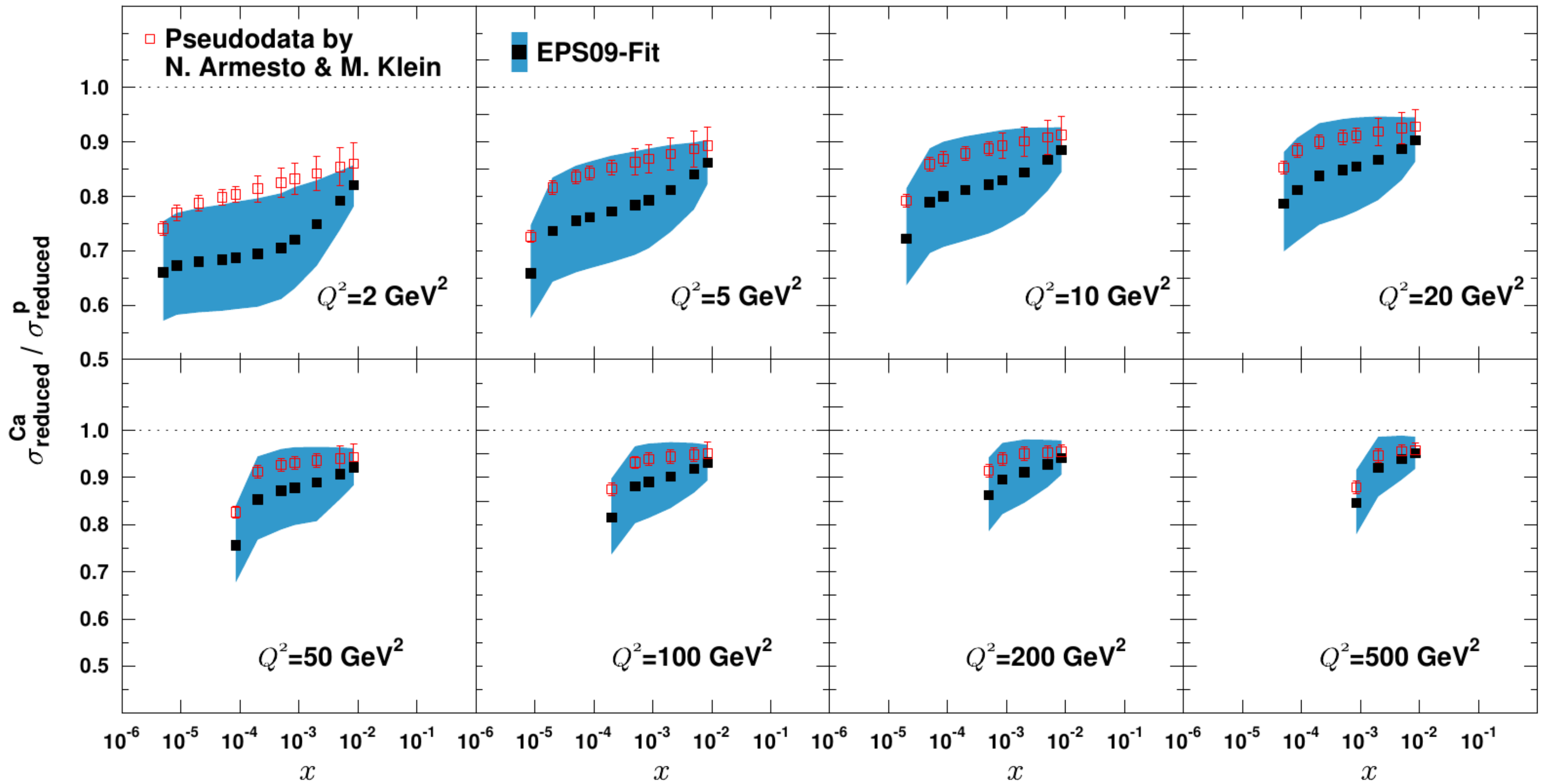

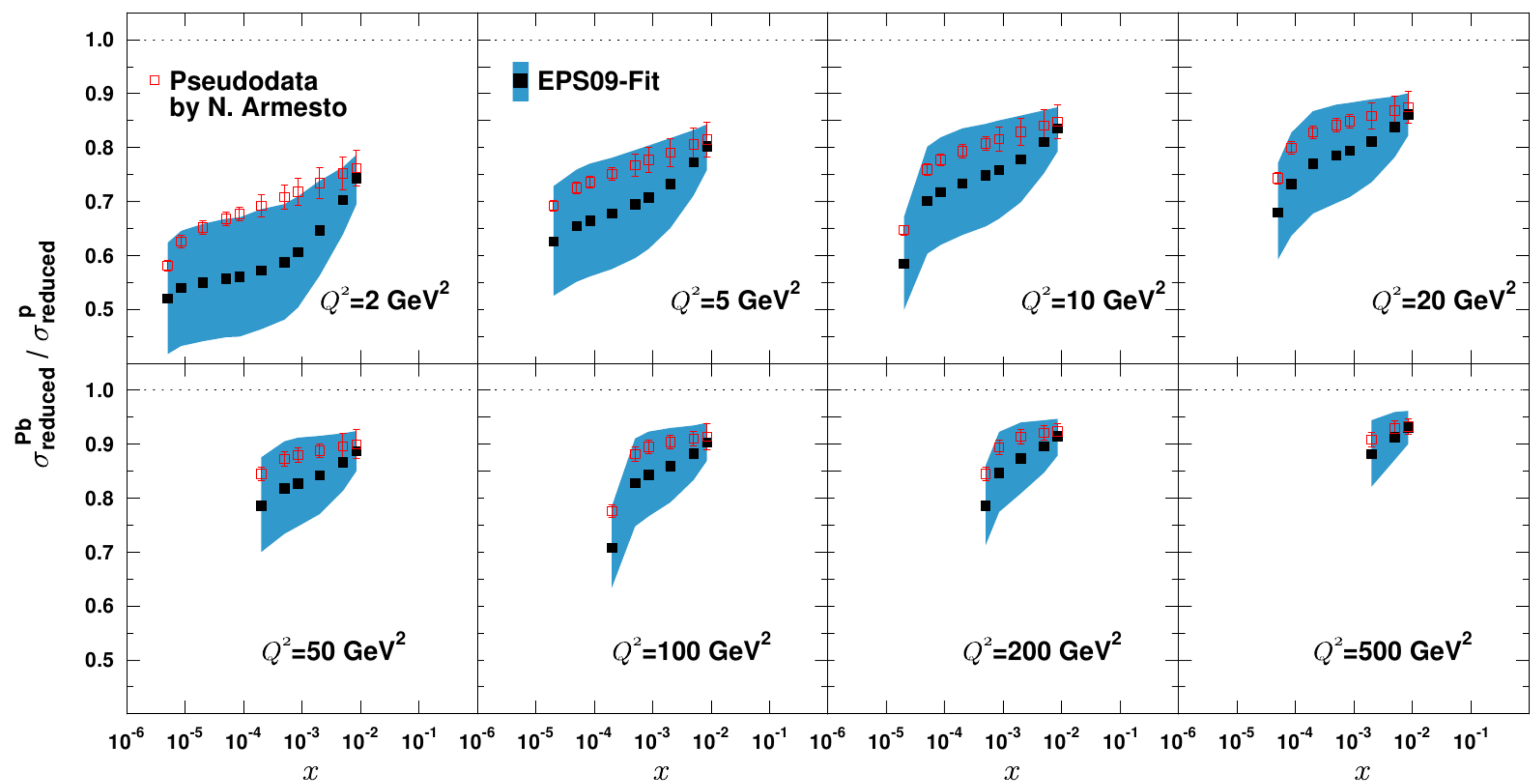

After the LHeC pseudodata vs EPS09

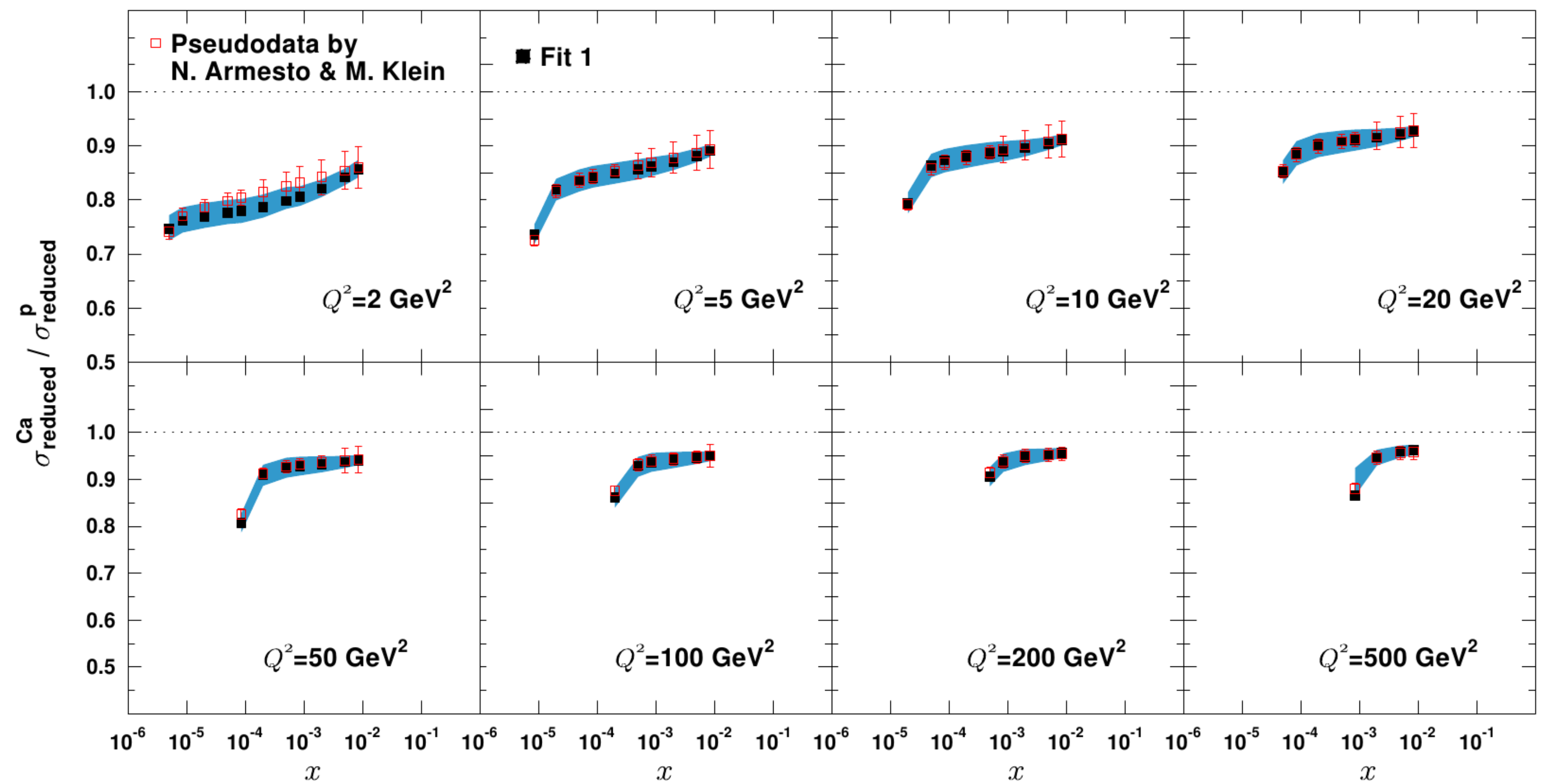

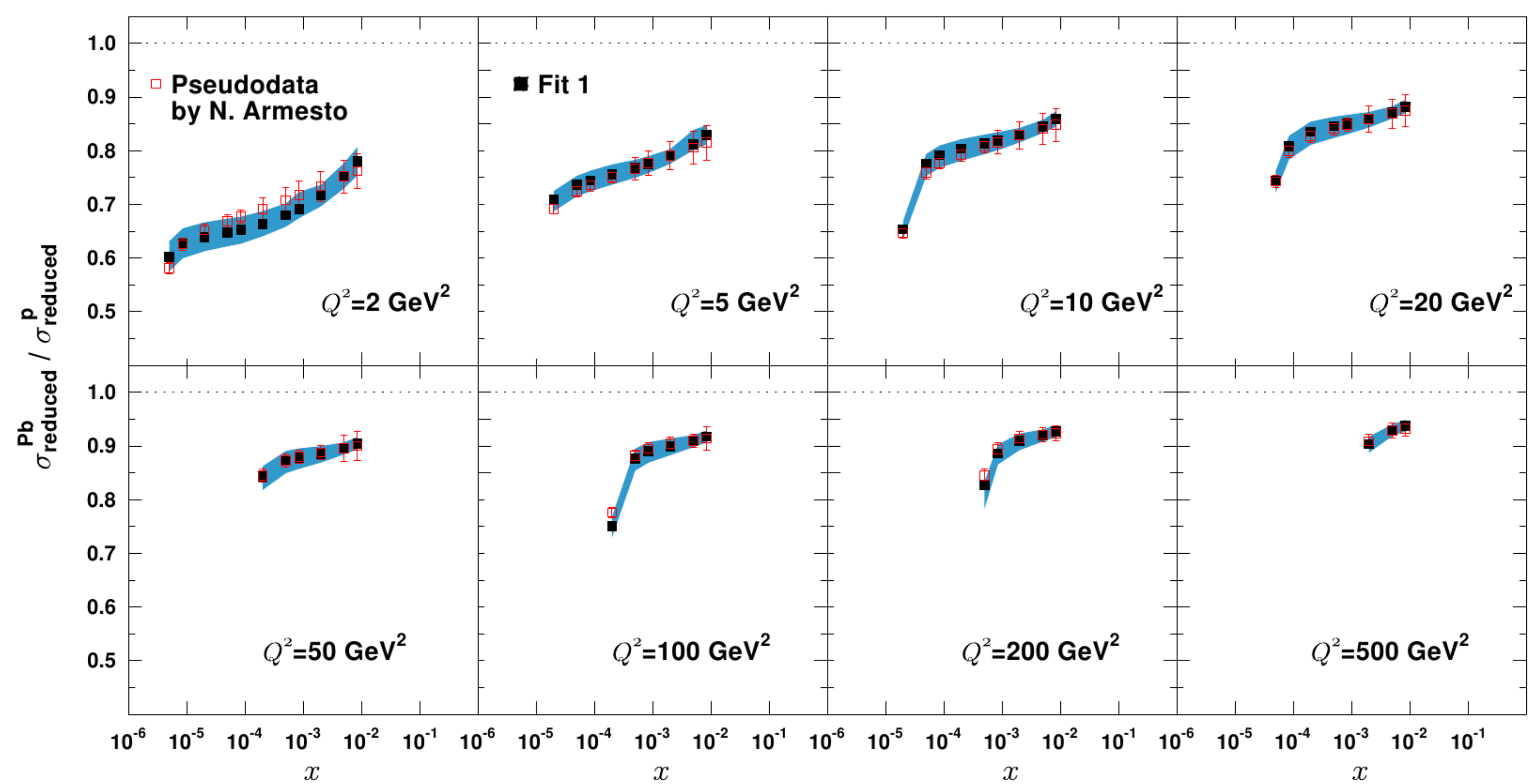

Deuterons: constraints on light quark sea asymmetry

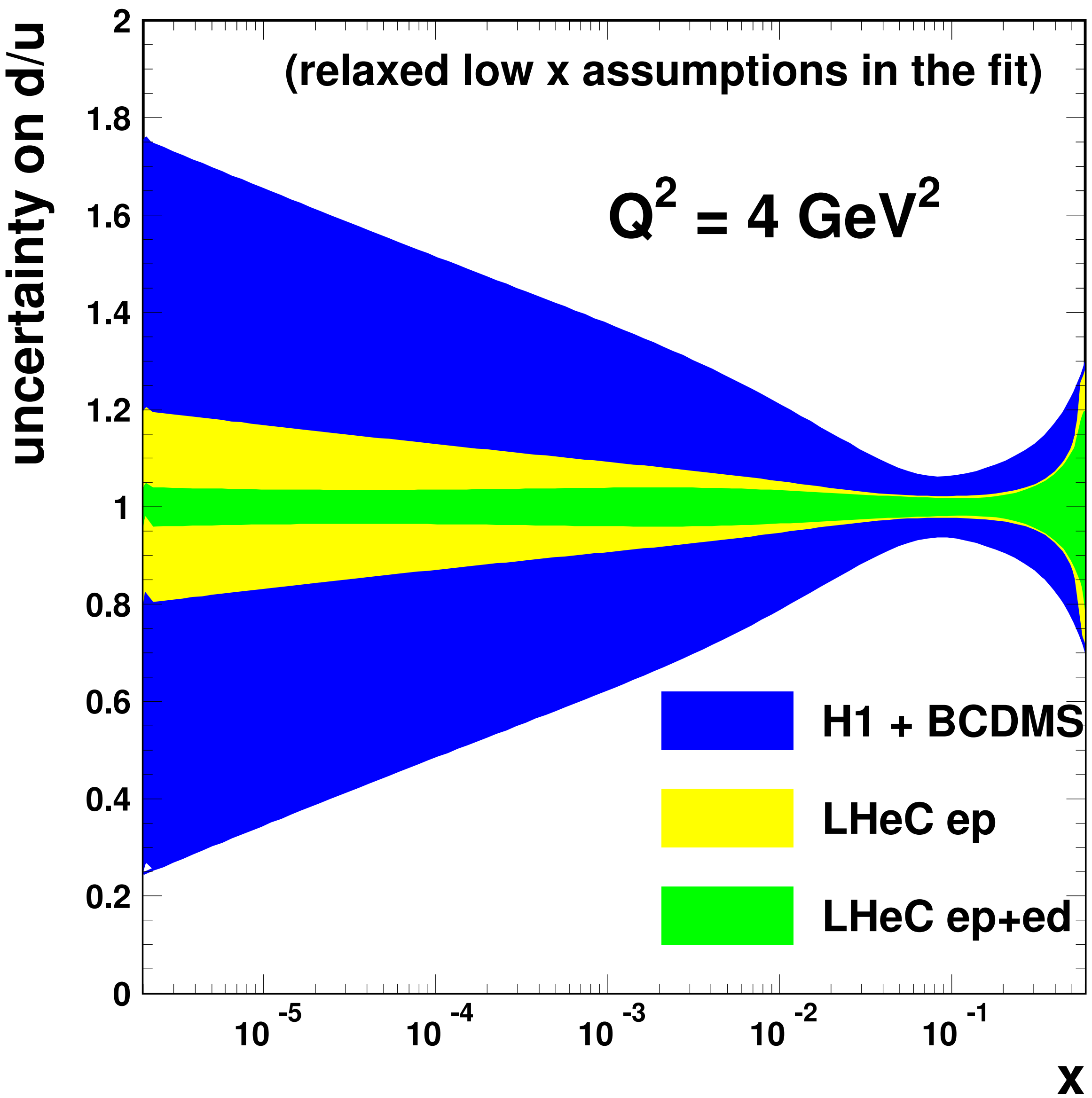

- ✳ Relaxing assumptions about dbar/ubar ratio in the fit.
- ✳CC high precision/statistics LHeC data from ep can constrain the ratio.
- ✳Further constraint from measuring additionally neutron pdfs from deuteron scattering.

Tests of charge symmetry using electrons and positrons in CC interactions:

$$R^{-} = 2\frac{W_2^{-D} - W_2^{+D}}{W_2^{-p} + W_2^{+p}}$$

Sensitive to u and d distributions in the proton and neutron respectively.

Radiation and Hadronization

- LHeC can provide information on radiation and hadronization.
- Large lever arm in energy allows probing different timescales: parton radiation, pre-hadron formation, hadron.
- Different stages can happen inside or outside nuclear matter depending on the energy of the parton.
- Important for heavy ion collisions .

Low energy: hadronization inside

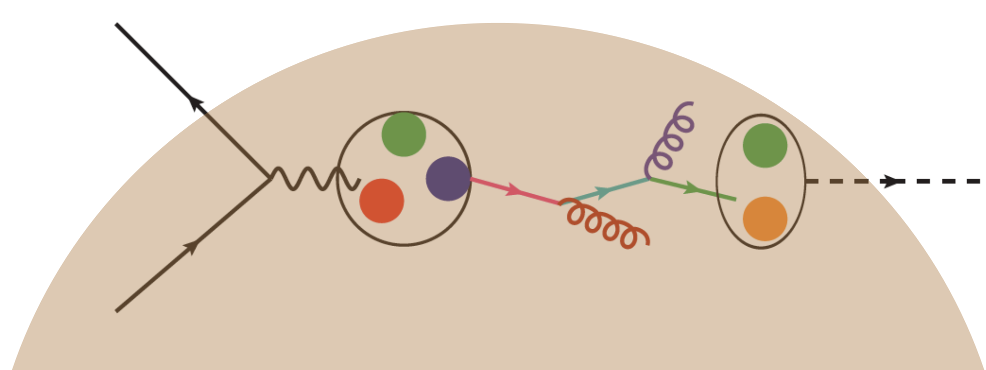

High energy: partonic evolution altered in nuclear medium

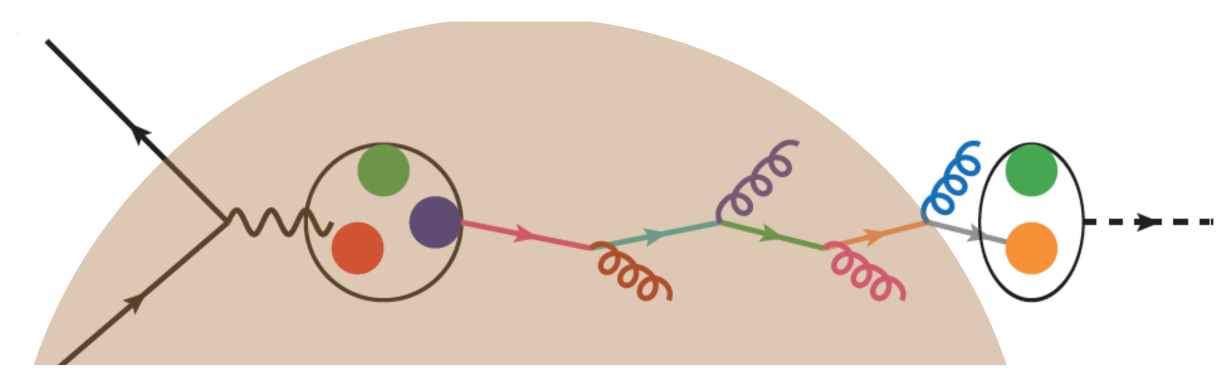

Radiation and Hadronization

$$R_A^k(\nu, z, Q^2) = \frac{1}{N_A^e}\frac{dN_A^k}{d\nu dz} \Big/ \frac{1}{N_p^e}\frac{dN_p^k}{d\nu dz} \qquad z = E_h/\nu$$

N^e number of scattered electrons at given photon energy and Q

Ratio becomes sensitive to ratio of fragmentation functions in nucleus and proton

Ratio is close to one for large energies as energy losses are becoming smaller.

Suppression larger for larger z due to steepness of the fragmentation function.

Formation time effects are non-negligible only at smallest energies.

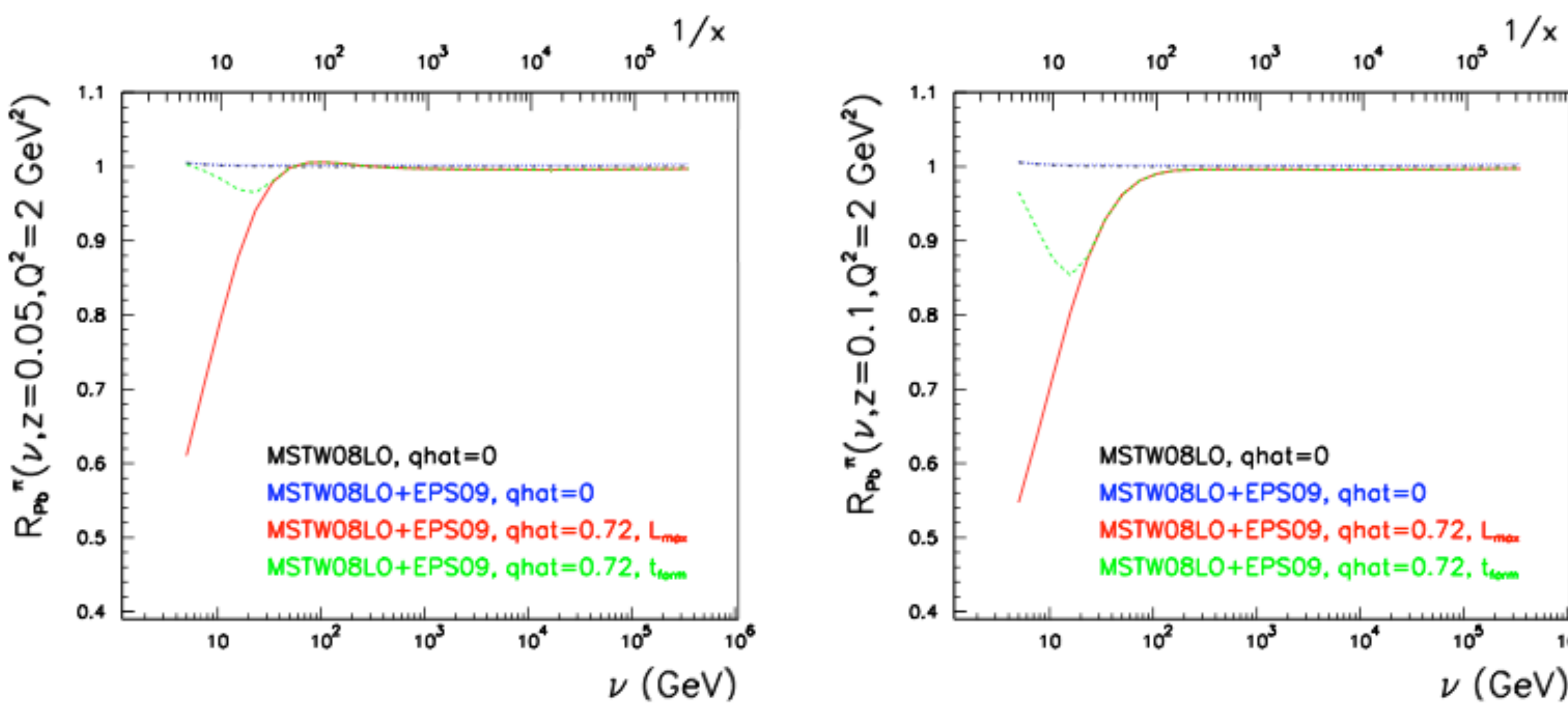

Summary

- New prospects for luminosity range at LHeC $\mathcal{L} = 10^{34} \frac{1}{\mathrm{cm}^2\,\mathrm{s}}$
- This has important impact onto Higgs production. $H \to b\bar{b}$ with 1% precision at luminosity of. More dedicated studies needed here.
- Precision pdfs needed for new physics.
- Prospects of charged current diffraction. Access to flavor decomposition of diffractive pdfs.
- Dijets in diffraction, due to smaller z_{IP} , sensitivity to gluon component.
- Diffractive dijets in DIS and photoproduction, factorization tests.
- d/u ratio constraints in ep and in eD.
- A proposal for ERL test facility with energy 900 MeV is under development.
- Next LHeC workshop 20/21st January 2014

backup

Design Parameters

parameter [unit]	LHeC	
species	e	p, $^{208}Pb^{82+}$
beam energy (/nucleon) [GeV]	60	7000, 2760
bunch spacing [ns]	25, 100	25, 100
bunch intensity (nucleon) [10^{10}]	0.1 (0.2), 0.4	17 (22), 2.5
beam current [mA]	6.4 (12.8)	860 (1110), 6
rms bunch length [mm]	0.6	75.5
polarization [%]	90 (e^+ none)	none, none
normalized rms emittance [μm]	50	3.75 (2.0), 1.5
geometric rms emittance [nm]	0.43	0.50 (0.31)
IP beta function $\beta^*_{x,y}$ [m]	0.12 (0.032)	0.1 (0.05)
IP spot size [μm]	7.2 (3.7)	7.2 (3.7)
synchrotron tune Q_s	—	1.9×10^{-3}
hadron beam-beam parameter	0.0001 (0.0002)	
lepton disruption parameter D	6 (30)	
crossing angle	0 (detector-integrated dipole)	
hourglass reduction factor H_{hg}	0.91 (0.67)	
pinch enhancement factor H_D	1.35 (0.3 for e^+)	
CM energy [TeV]	1.3, 0.81	
luminosity / nucleon [10^{33} cm^{-2}s^{-1}]	1 (10), 0.2	

arXiv:1211:5102

Designed for synchronous ep and pp operation during the HL-LHC phase.

CDR chapter on low x and nuclei:

Low x and saturation

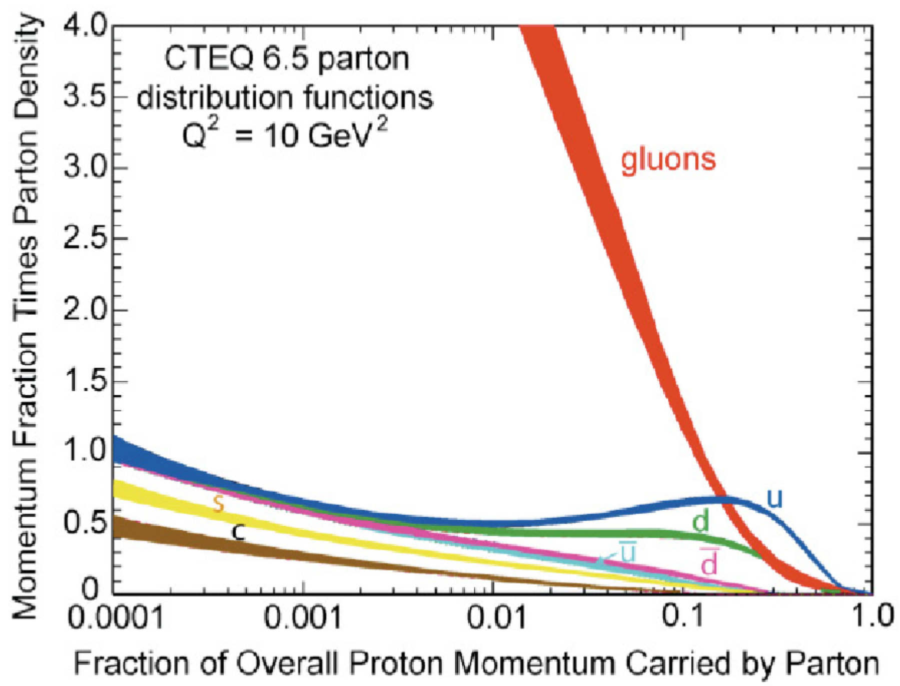

HERA established strong growth of the gluon density towards small x
Parton saturation: recombination of gluons at sufficiently high densities leading to nonlinear modification of the evolution equations.
Emergence of a dynamical scale: saturation scale dependent on energy.

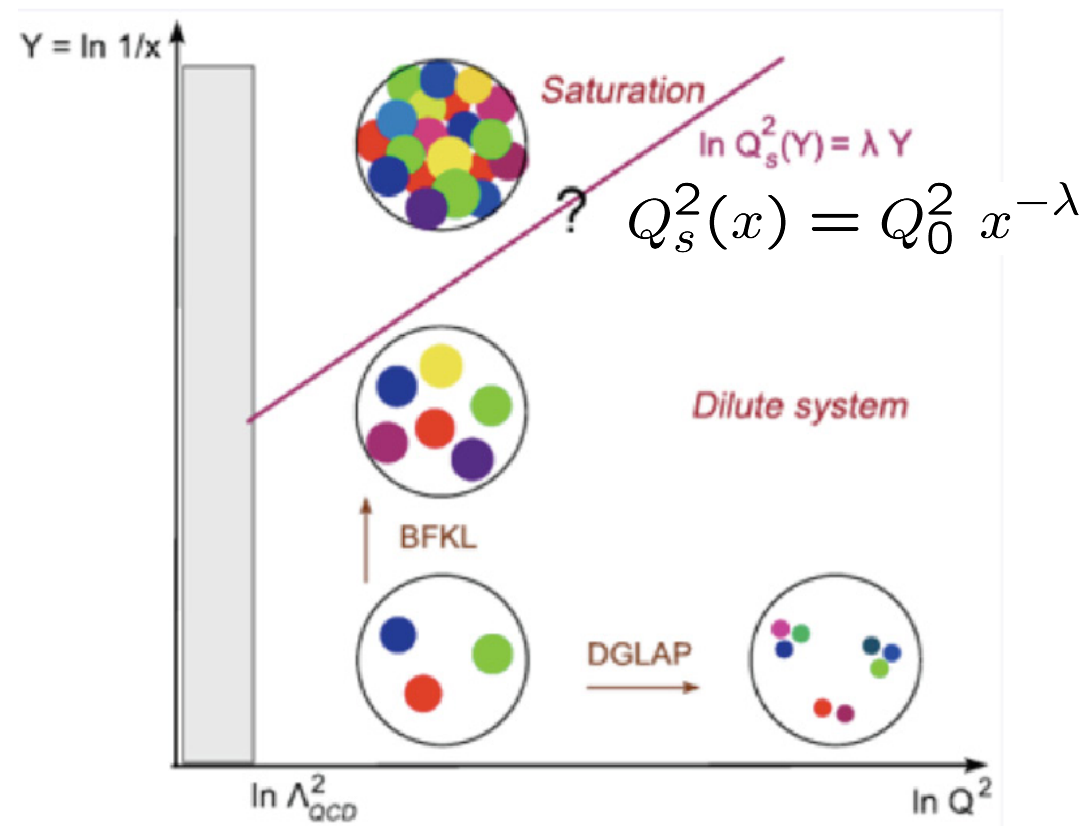

What we learned from HERA about saturation?

Linear DGLAP evolution works well at HERA.
Hints of saturation at low Q and low x: deterioration of the global fit in that region.
Large diffractive component.
Success of the dipole models in the description of the data.
The models point at the low value of the saturation scale
LHeC would provide an access to a kinematic regime where the saturation scale is perturbative

Strategy for making target more ‘black’

LHeC would deliver a two-pronged approach:

Probing lower x in ep. Evolution of a single source

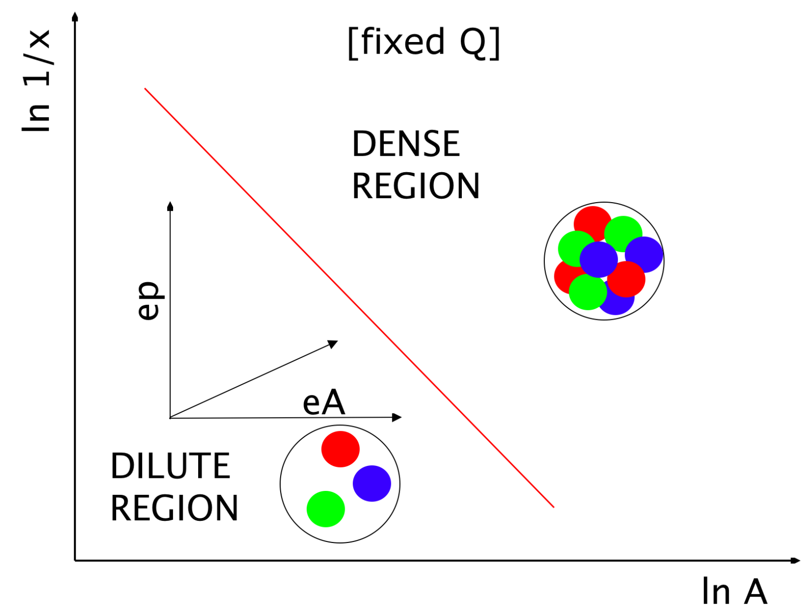

More nucleons: eA scattering. Many sources overlapping in impact parameter .

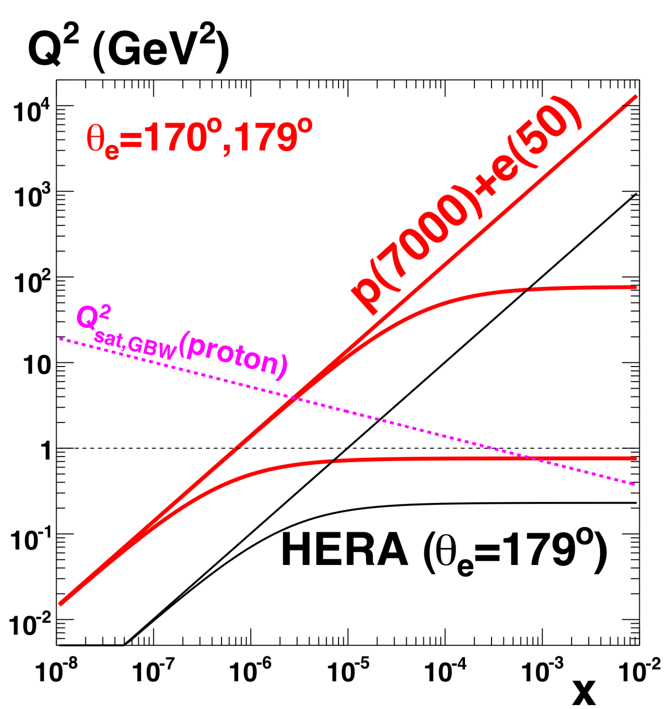

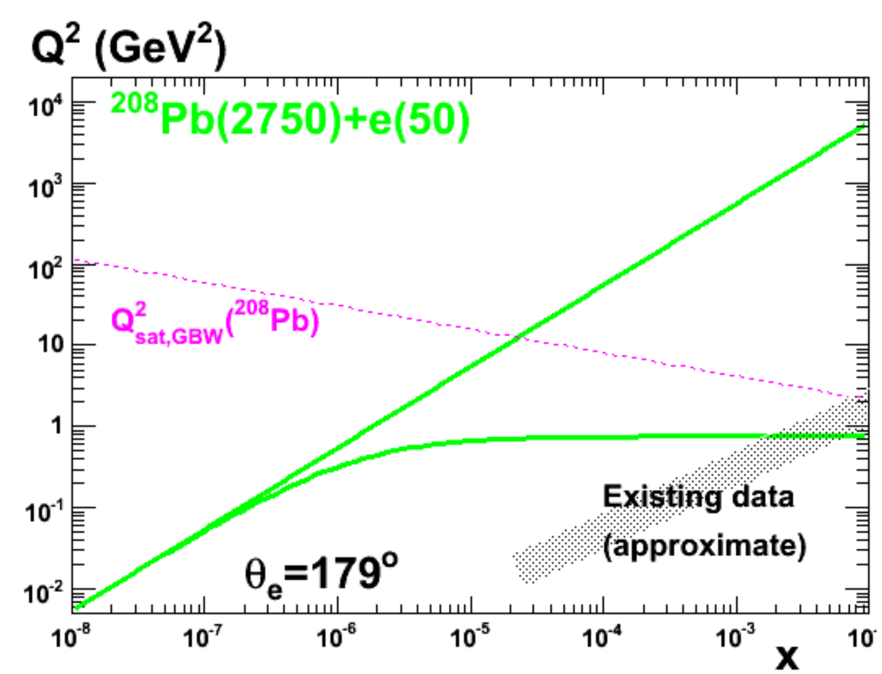

F_2, F_L structure functions

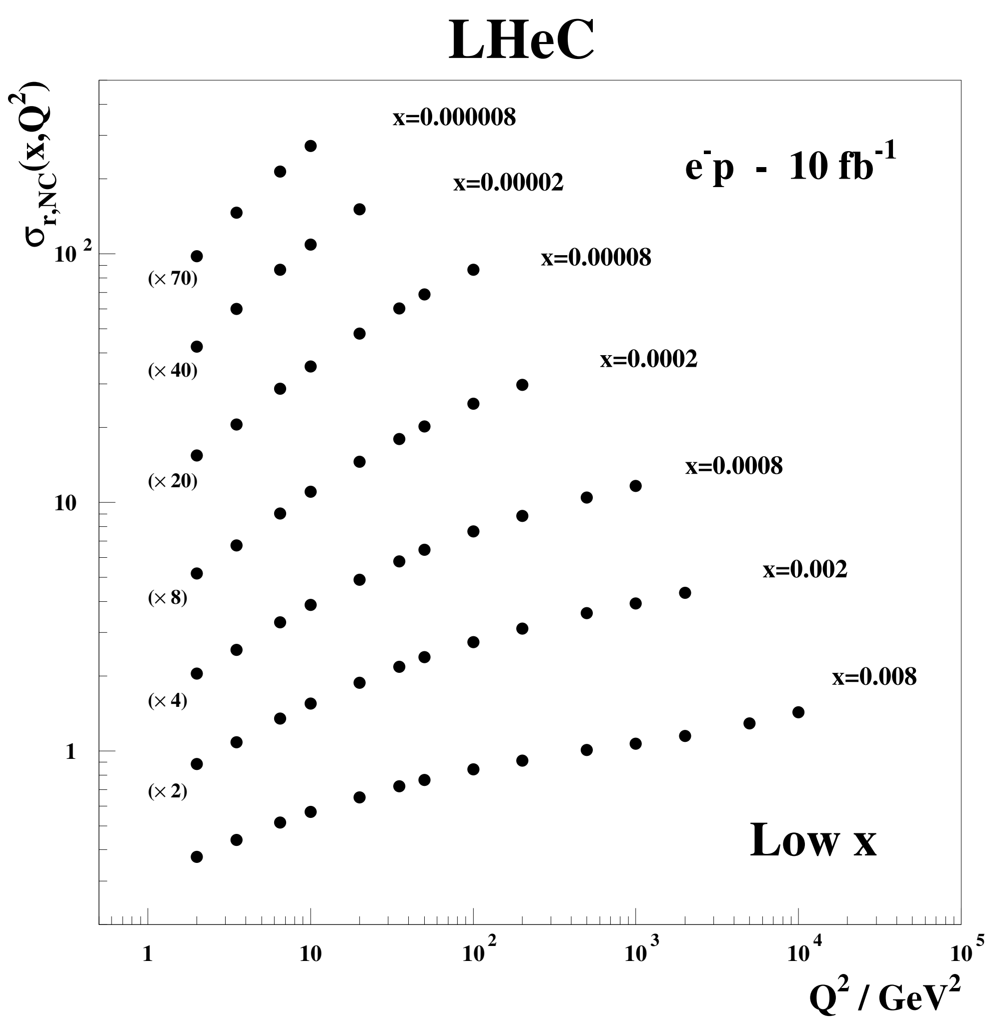

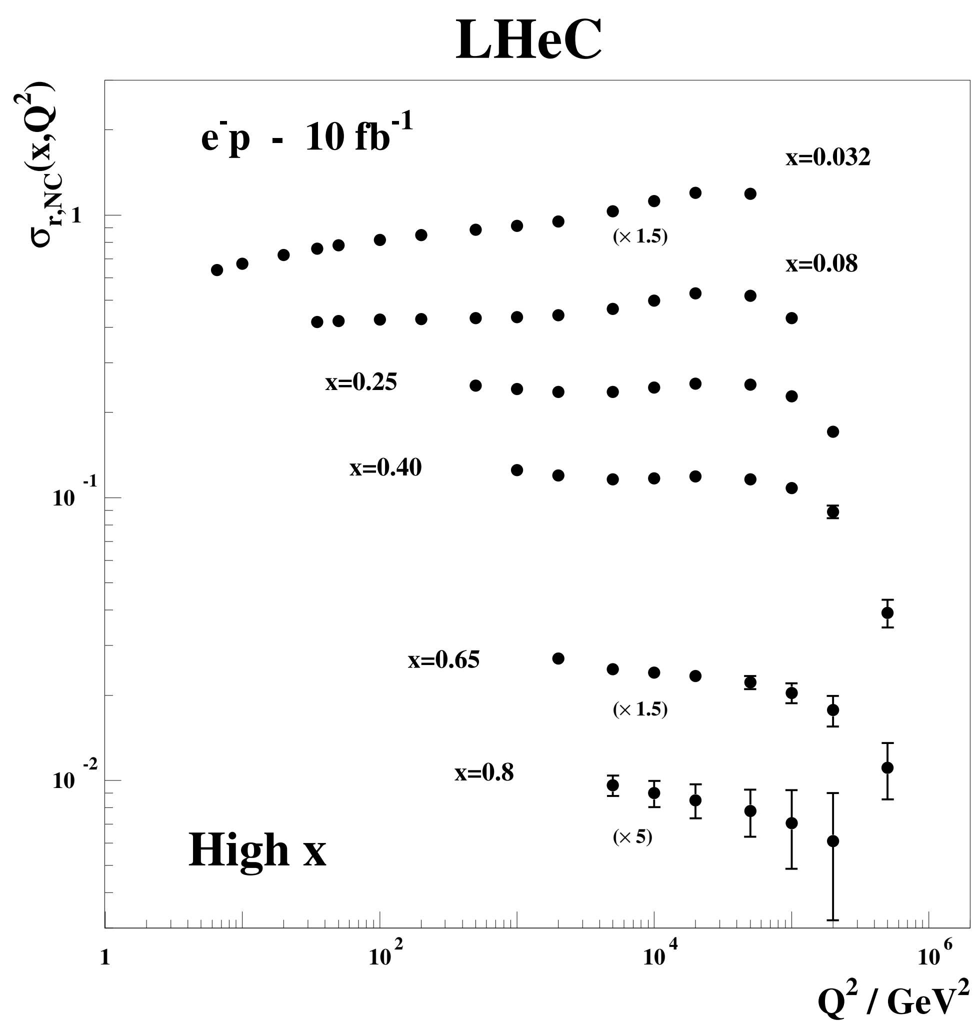

Reduced cross section: huge kinematic range and excellent accuracy

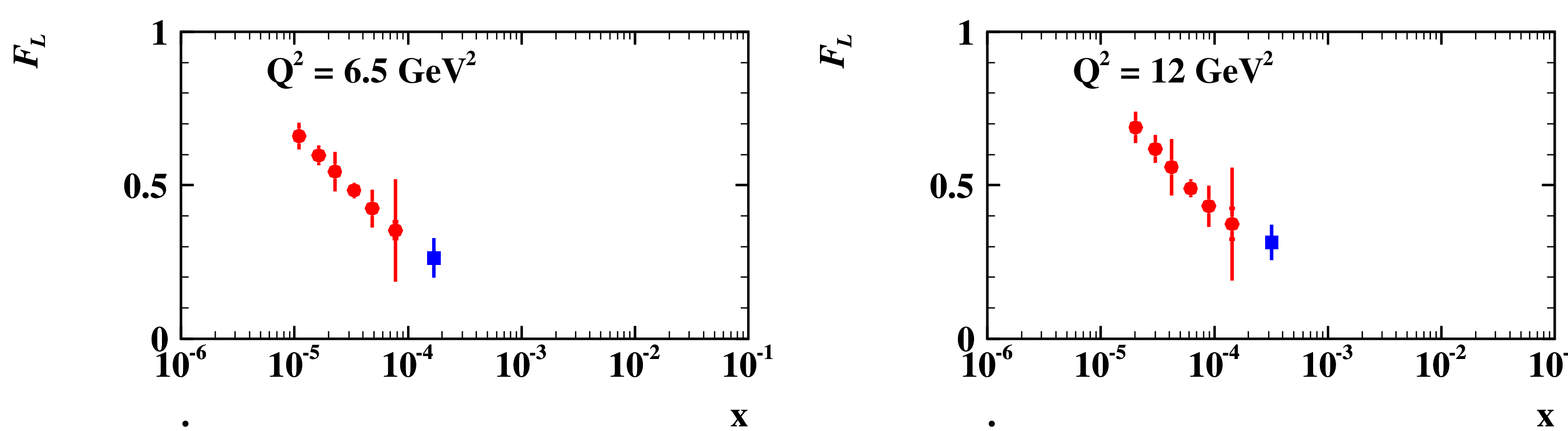

Longitudinal structure function: lowering electron energy

F_2, F_L structure functions at low x

Precision measurements of structure functions at very low x: test DGLAP, small x, saturation inspired approaches.

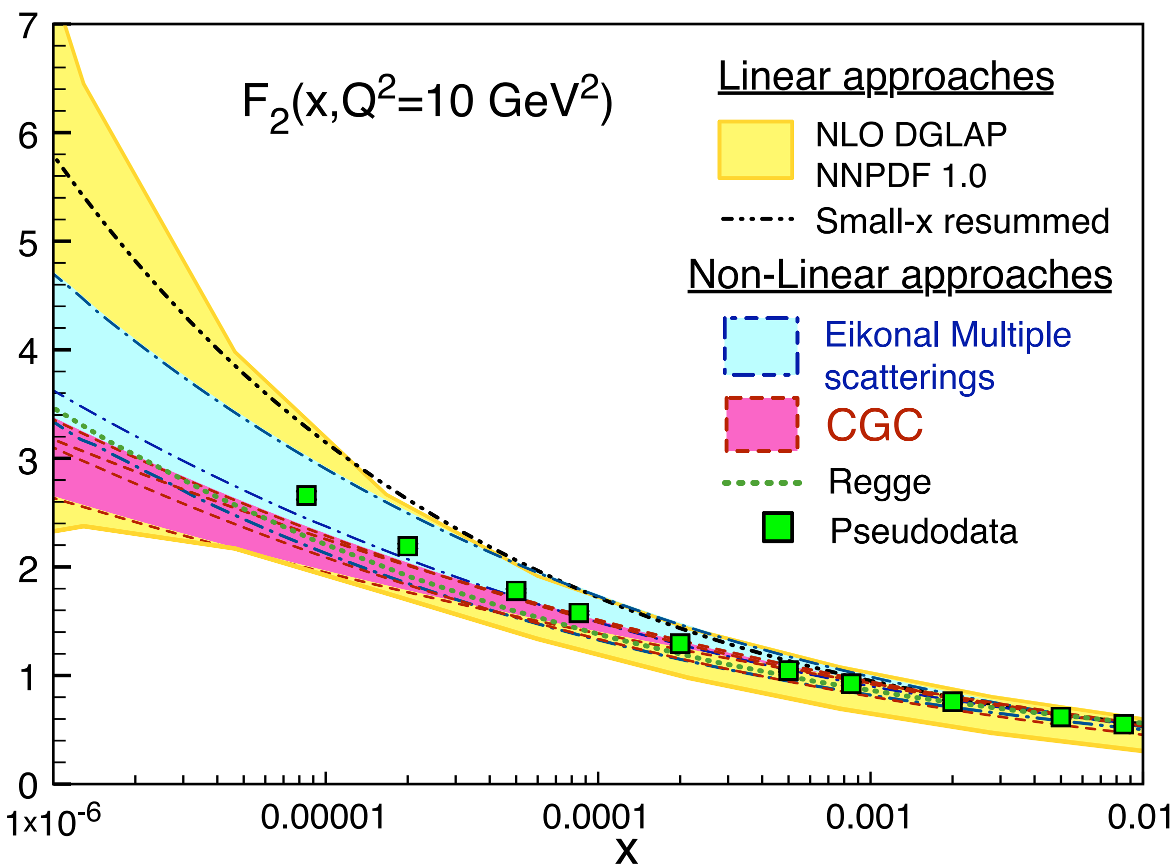

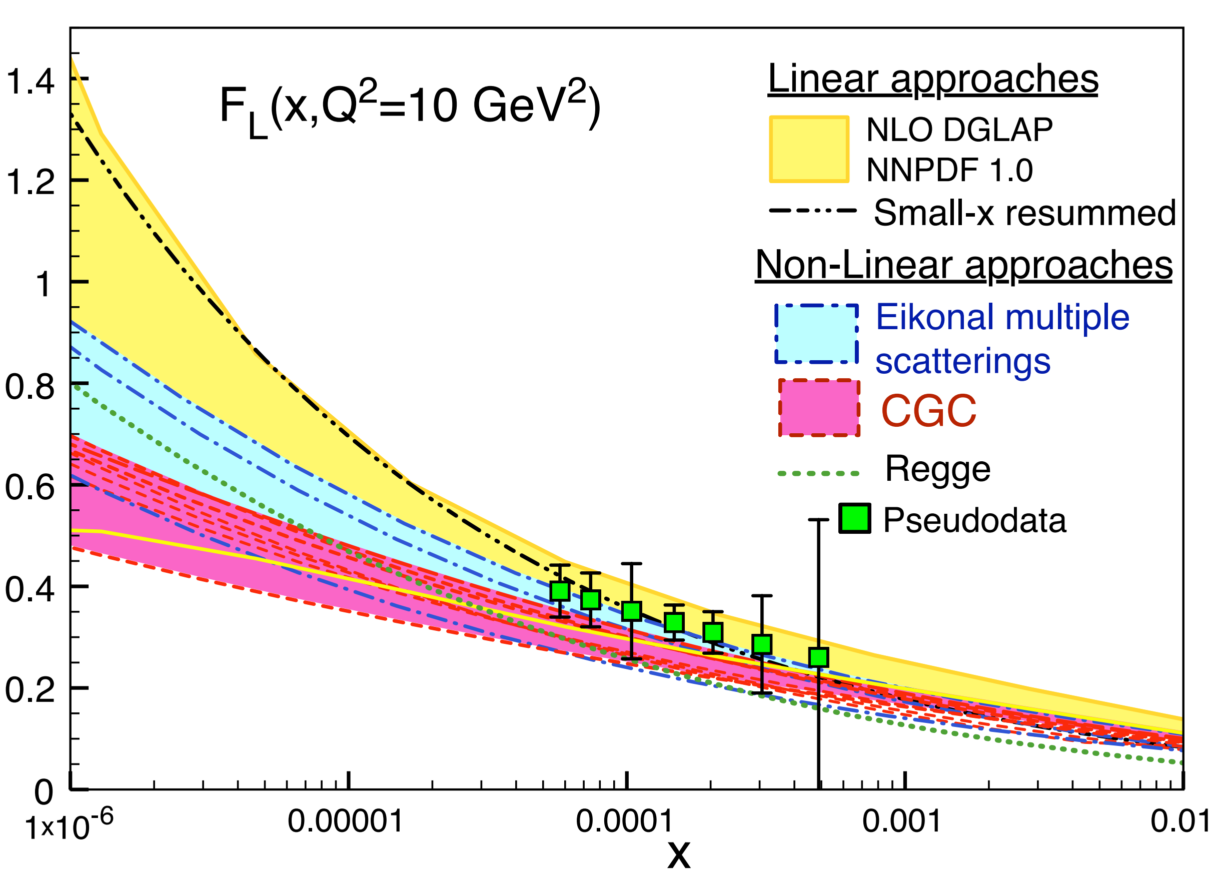

Interestingly, rather small band of uncertainties for models based on saturation as compared with the calculations based on the linear evolution. Possible cause: the nonlinear evolution washes out any uncertainties due to the initial conditions, or too constrained parametrization used within the similar framework.

approx. 2% error on the F2 pseudodata, and 8% on the FL pseudodata ,should be able to distinguish between some of the scenarios.

Testing nonlinear dynamics in ep

Simulated LHeC data using the nonlinear evolution which leads to the parton saturation at low x.

DGLAP fits (using the NNPDF) cannot accommodate the nonlinear effects if F2 and FL are simultaneously fitted.

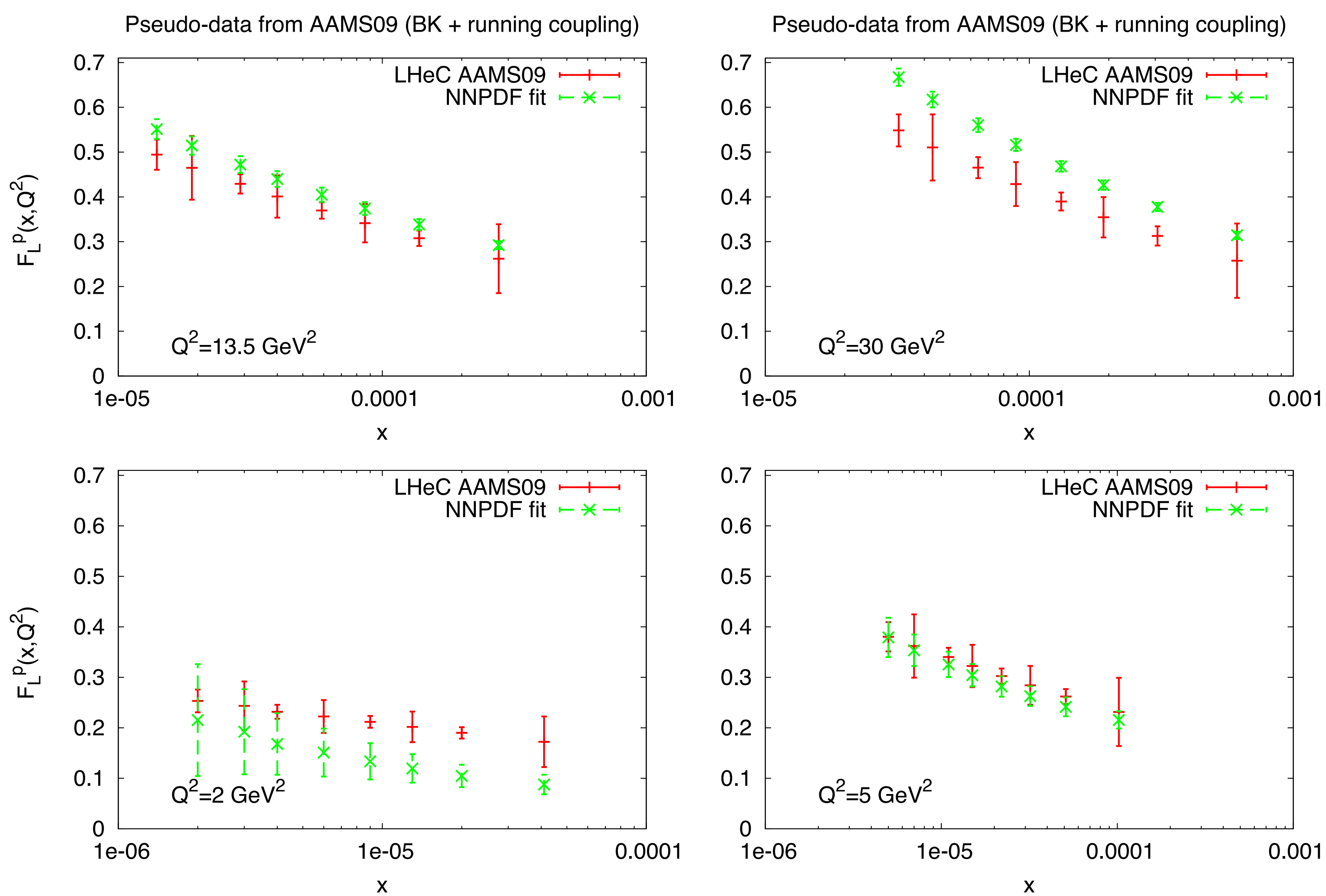

Albacete,Rojo

Additional constraints (apart from F2) are FL and F2 charm, which can help pin down the gluon distribution at small x.

DIS on deuterons

- Deuteron can serve as an effective neutron beam through the spectator proton tagging. The resulting neutron structure function data are essentially free from nuclear corrections.

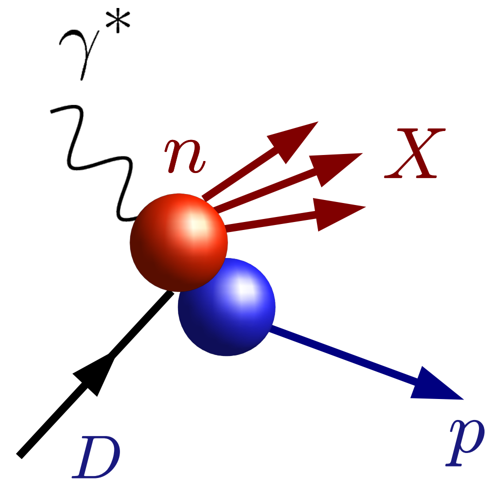

- Can perform quark flavor decomposition. Important at large x

$$F_2(p) \sim (4u + d)$$

$$F_2(n) \sim (u + 4d)$$

- Testing important relation between diffraction in ep and shadowing in eD (Gribov)

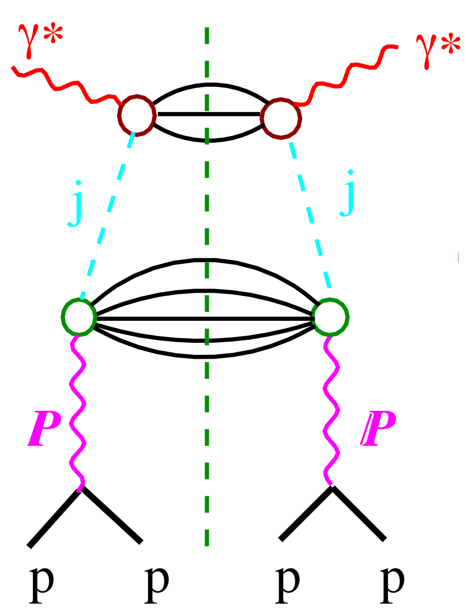

Diffraction in ep

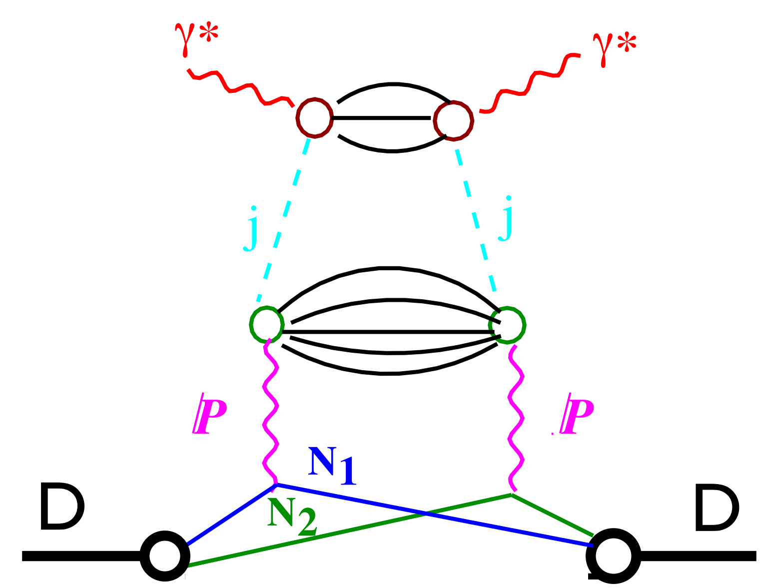

Double scattering in eD

Nuclear physics in eA complementarity to pA, AA at LHC

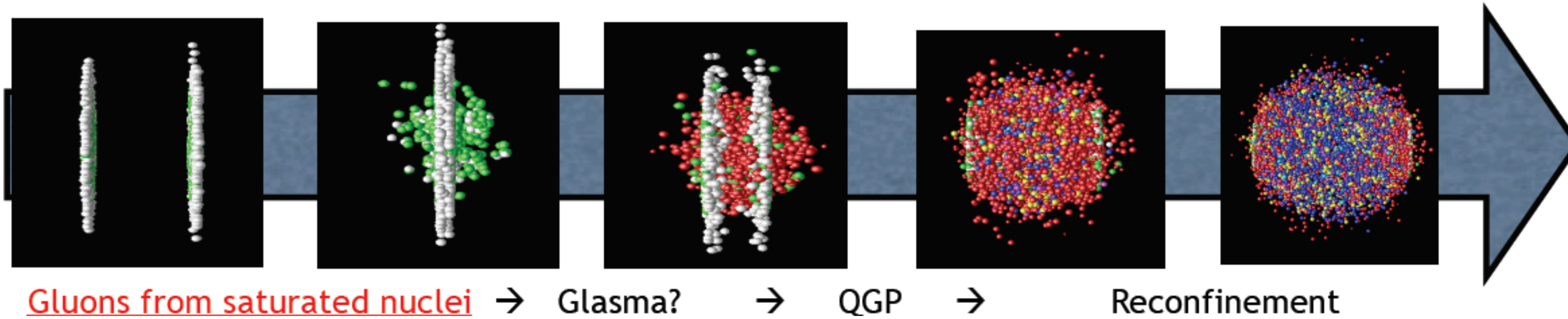

Precision measurement of the initial state.

Nuclear structure functions.

Particle production in the early stages.

Factorization eA/pA/AA.

Modification of the QCD radiation and hadronization in the nuclear medium.

Nuclear structure

Deep Inelastic Scattering : $$\frac{d^2\sigma^{ep\to eX}}{dxdQ^2} = \frac{4\pi\alpha_{e.m.}^2}{xQ^4}\left[\left(1-y+\frac{y^2}{2}\right)F_2(x,Q^2)-\frac{y^2}{2}F_L(x,Q^2)\right]$$

Nuclear ratio for structure function $$R^A_{F_2}(x,Q^2) = \frac{F_2^A(x,Q^2)}{A\,F_2^{\text{nucleon}}(x,Q^2)}$$

Nuclear effects $$R^A \neq 1$$

- Fermi motion $x \geq 0.8$
- EMC region $0.25-0.3 \leq x \leq 0.8$
- Antishadowing region $0.1 \leq x \leq 0.25-0.3$
- Shadowing region $x \leq 0.1$

Schematic picture

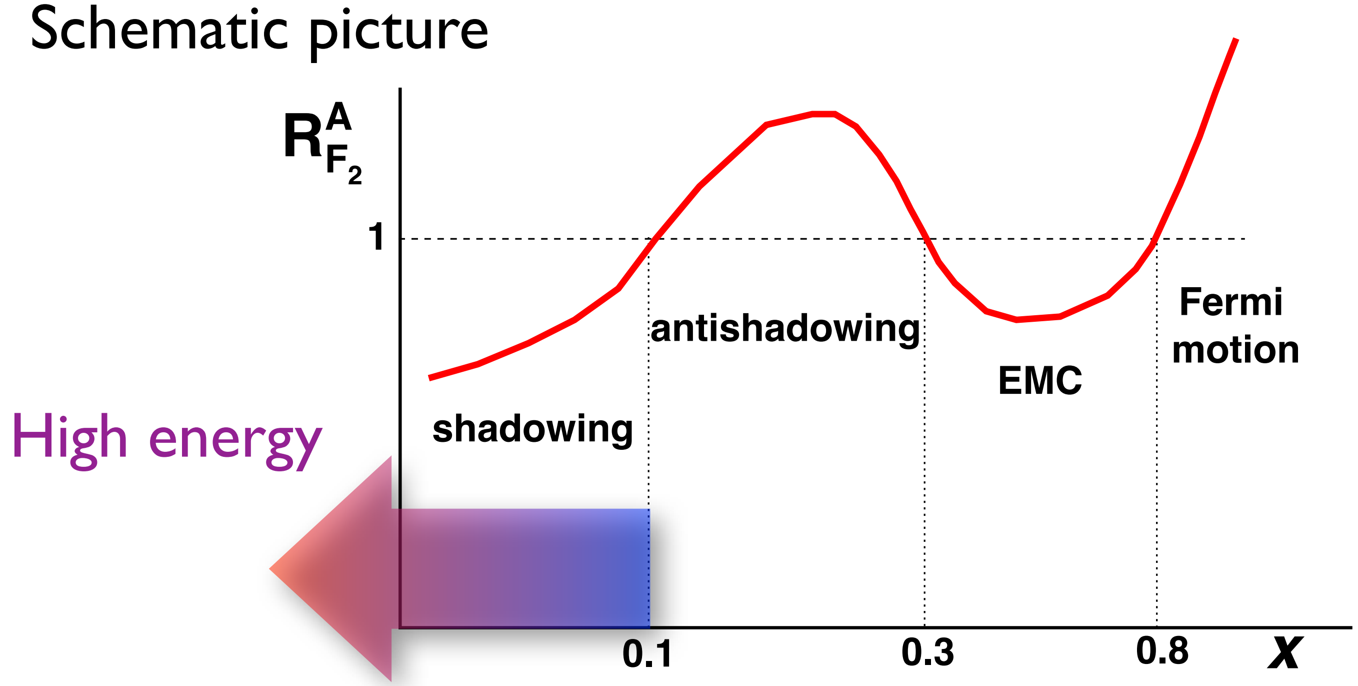

What the nuclear DIS data tell us?

Kinematic coverage in nuclear DIS and DY

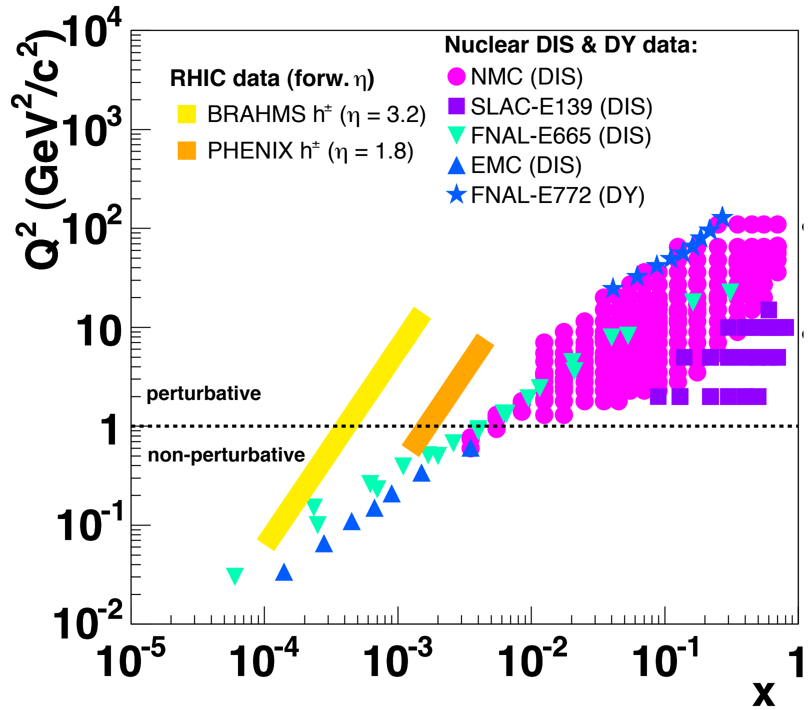

Shadowing increases with A

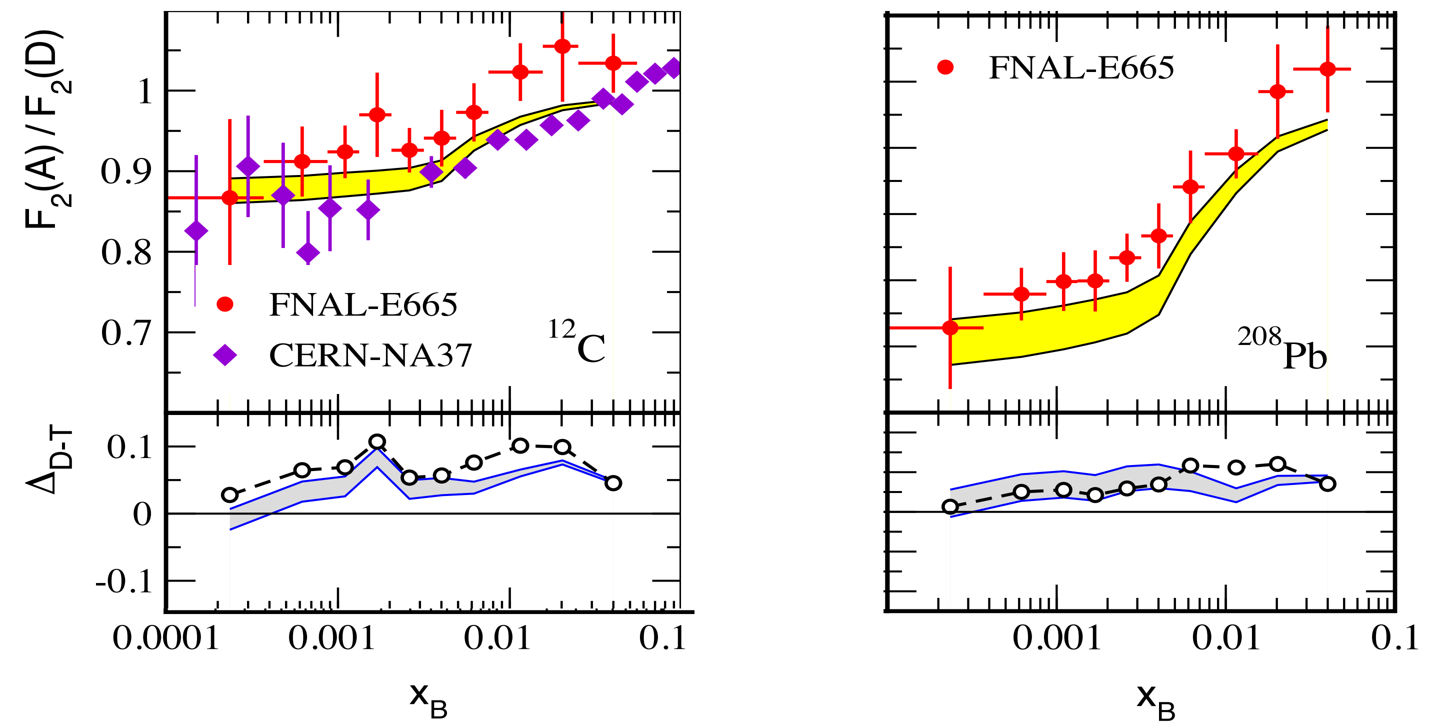

Shadowing increases with decreasing x

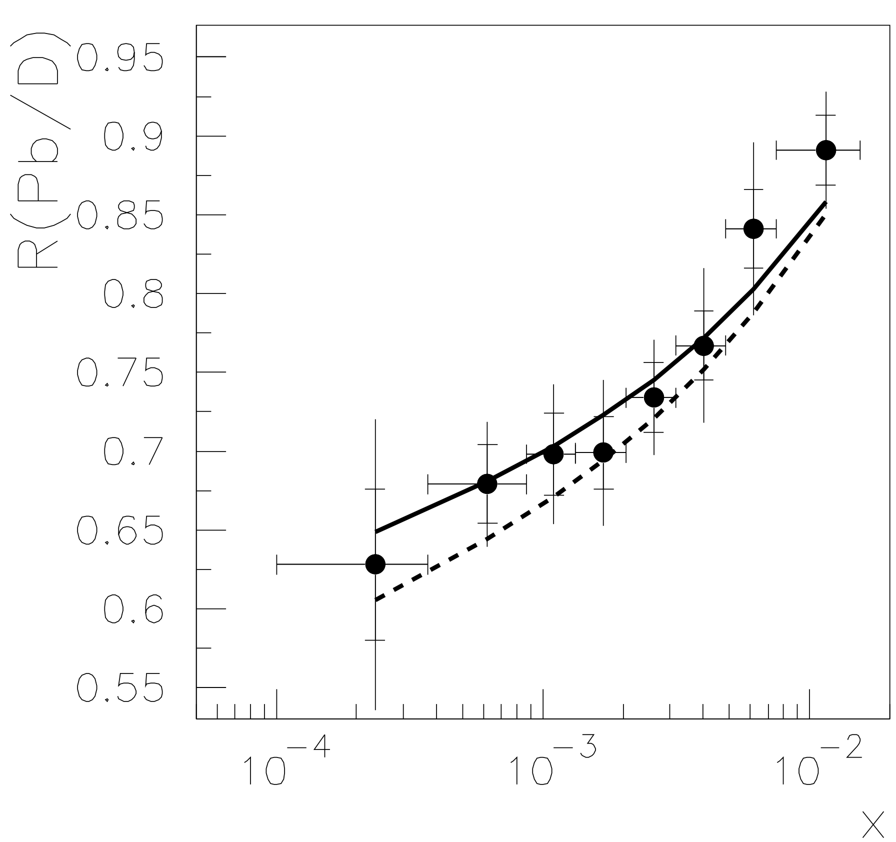

Shadowing decreases with increasing Q

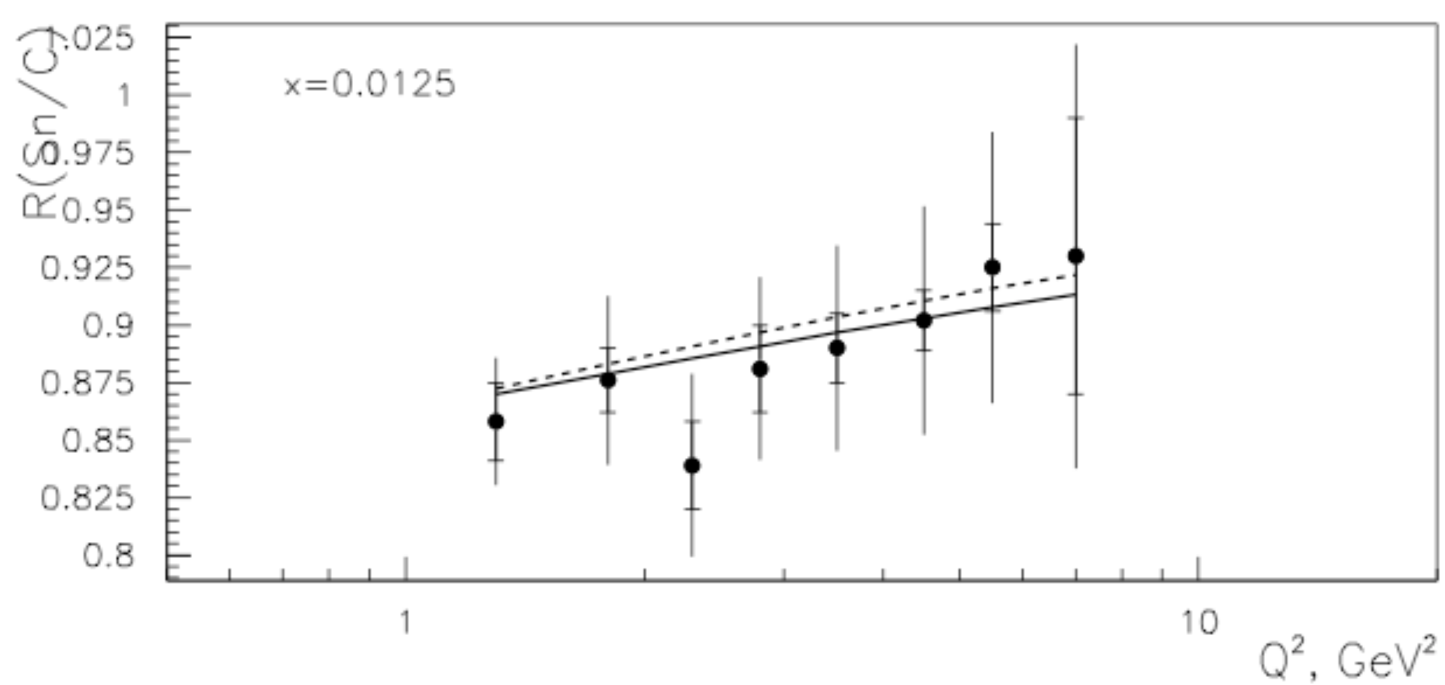

Nuclear structure functions at LHeC

Nuclear ratio for structure function or a parton density:

$$R_f^A(x,Q^2) = \frac{f^A(x,Q^2)}{A \times f^N(x,Q^2)}$$

LHeC potential: precisely measure partonic structure of the nuclei at small x.

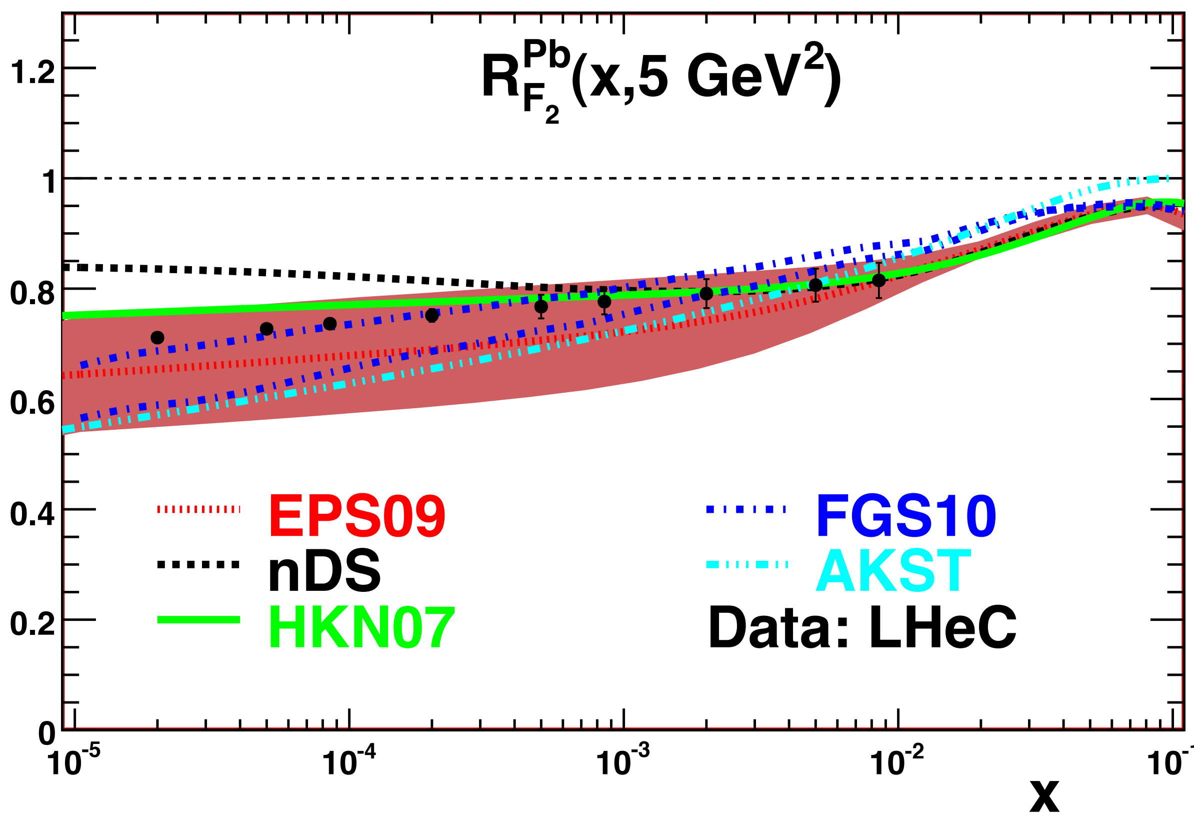

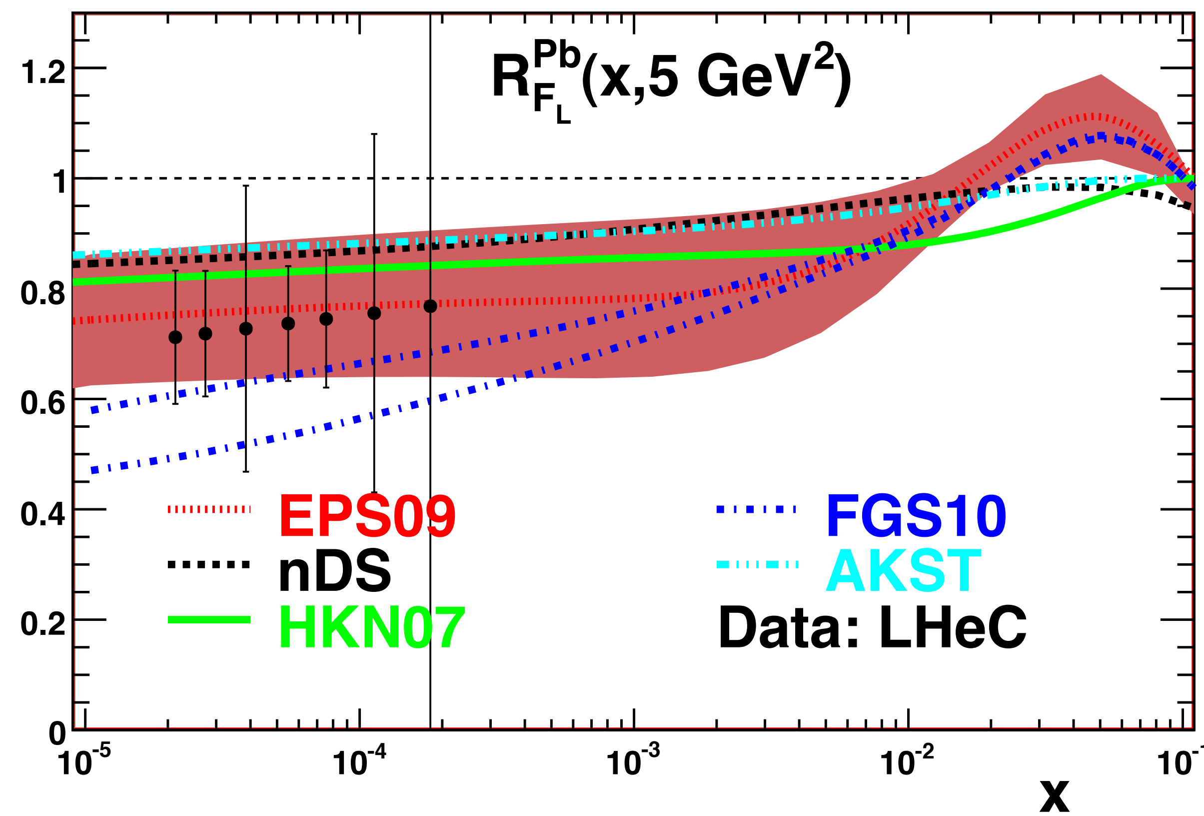

Nuclear parton distributions at LHeC

Global NLO fit with the LHeC pseudodata included. DGLAP NLO, VFNS SACOT prescription, CTEQ6.6 for free proton pdf.

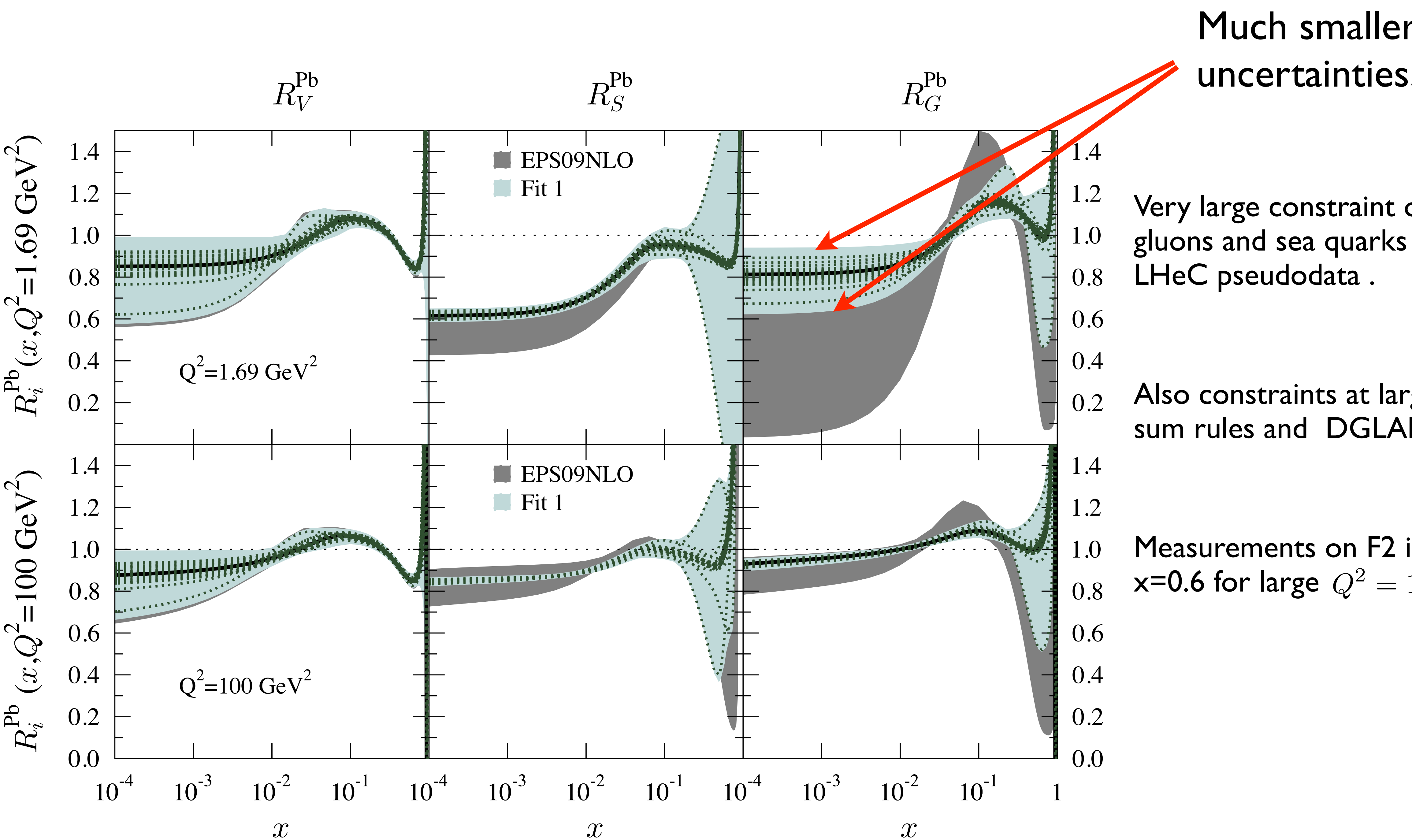

Very large constraint on the low x gluons and sea quarks with the LHeC pseudodata .

Also constraints at large x through sum rules and DGLAP evolution.

Measurements on F2 in eA up to x=0.6 for large $Q^2 = 1000\ \mathrm{GeV}^2$

Nuclear parton distributions at LHeC

Global NLO fit with the LHeC pseudodata included. DGLAP NLO, VFNS SACOT prescription, CTEQ6.6 for free proton pdf.

Including information on charm and beauty contributions in eA DIS

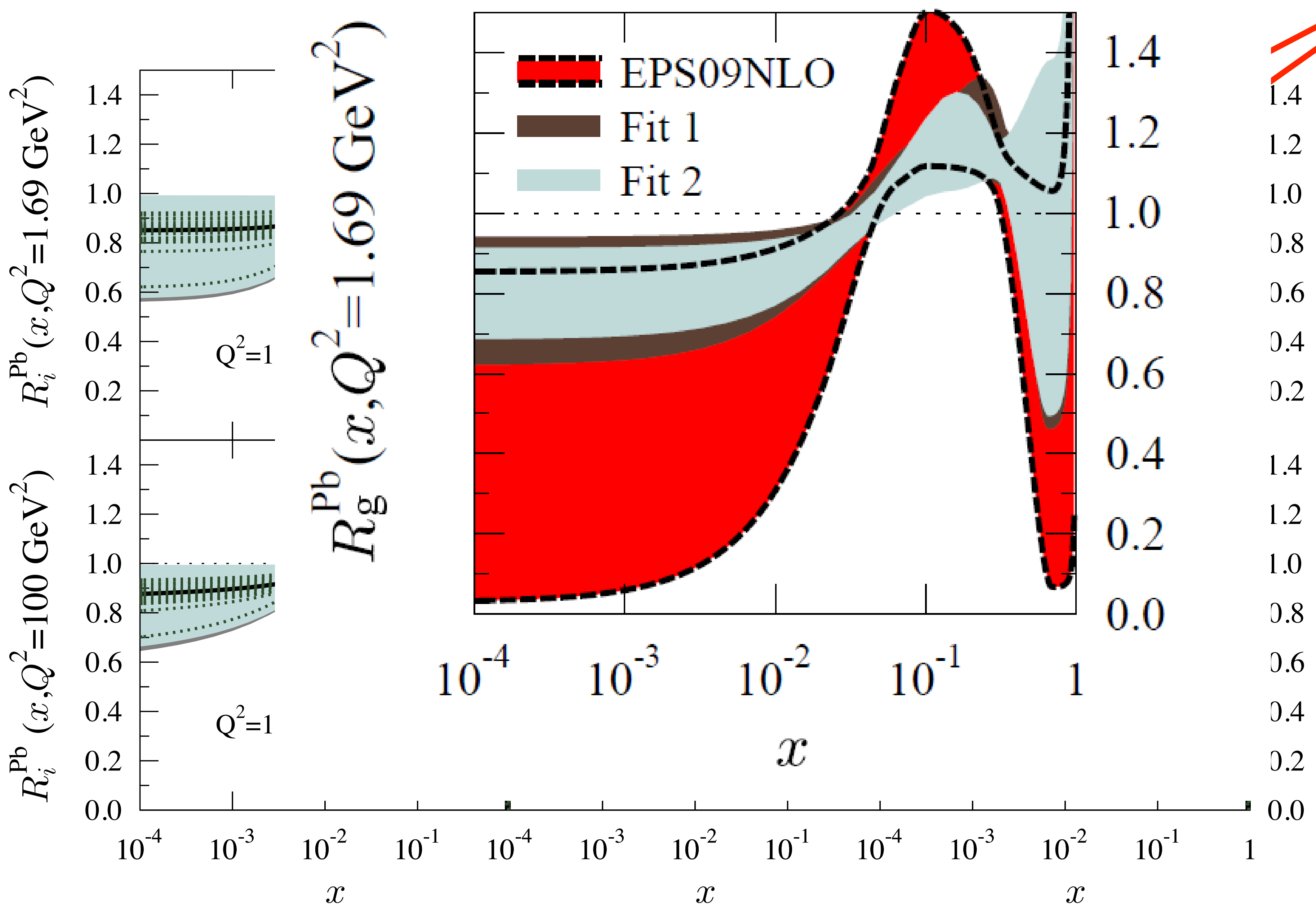

Much smaller uncertainties.

Very large constraint on the low x gluons and sea quarks with the LHeC pseudodata .

Also constraints at large x through sum rules and DGLAP evolution.

Measurements on F2 in eA up to x=0.6 for large $Q^2 = 1000\ \mathrm{GeV}^2$

Diffractive mass distribution

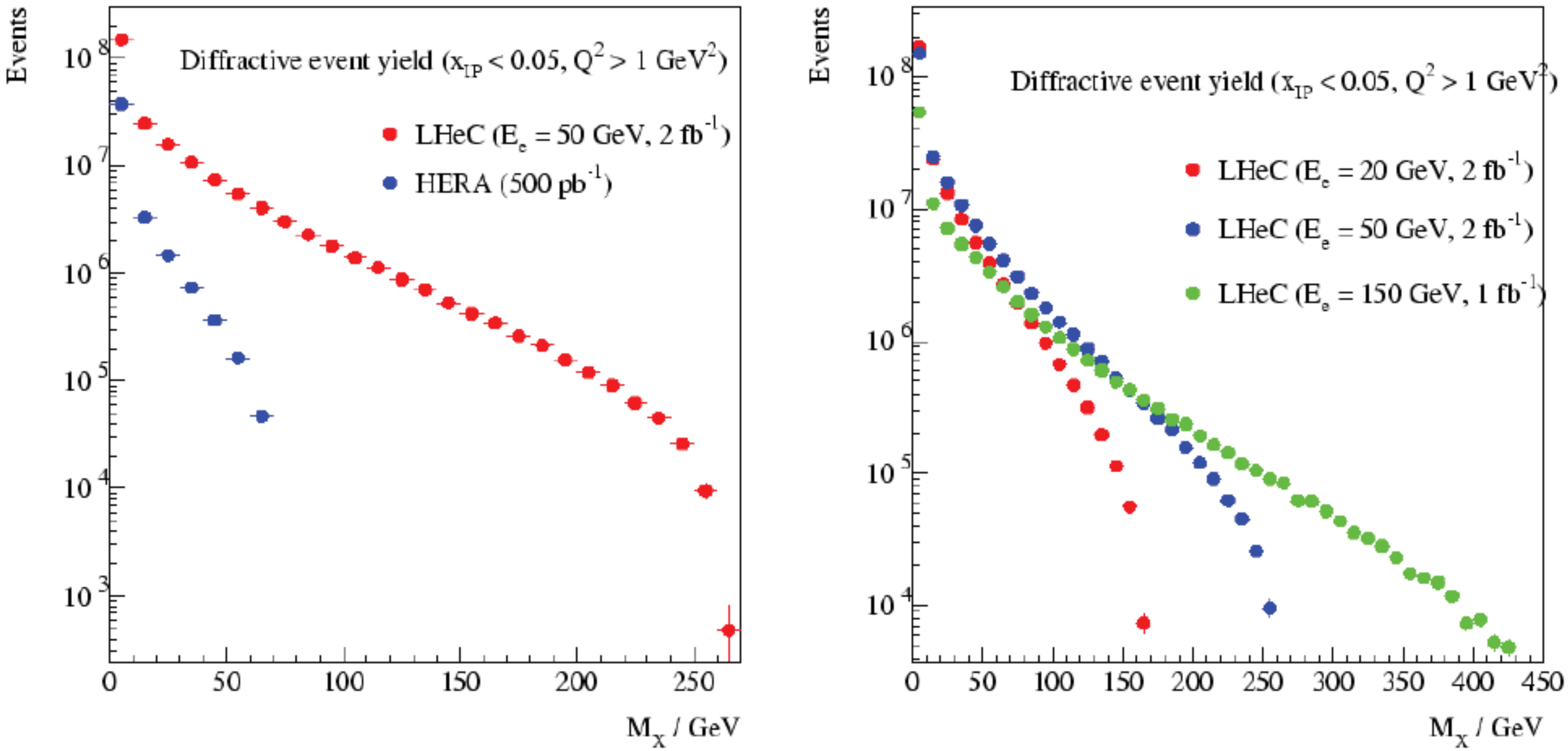

New domain of diffractive masses.
M_X can include W/Z/beauty

More in Pierre's talk

Inclusive diffraction in eA

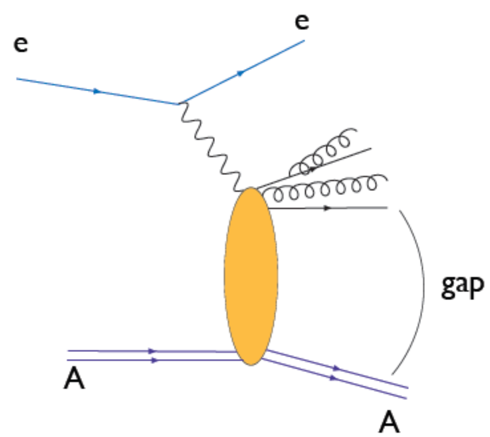

coherent

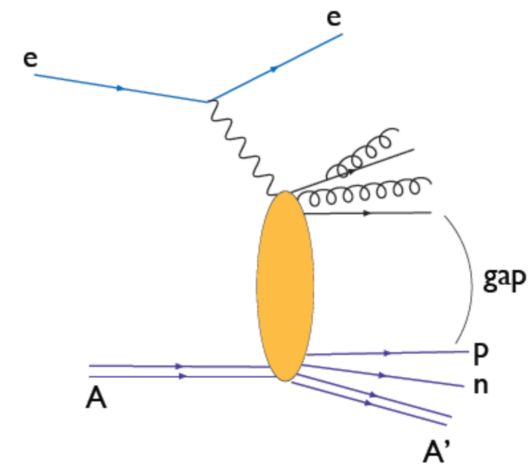

incoherent

Diffractive structure function for Pb

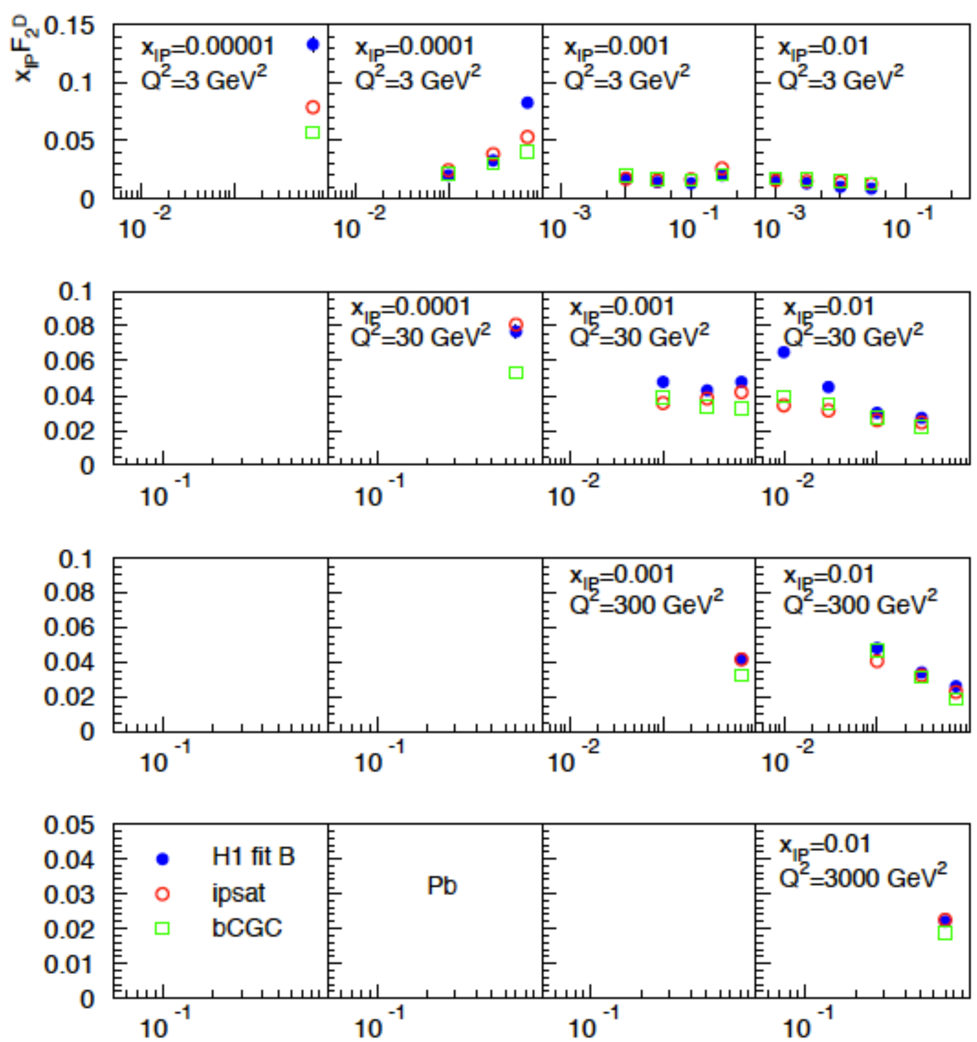

Diffractive to inclusive ratio for protons and Pb

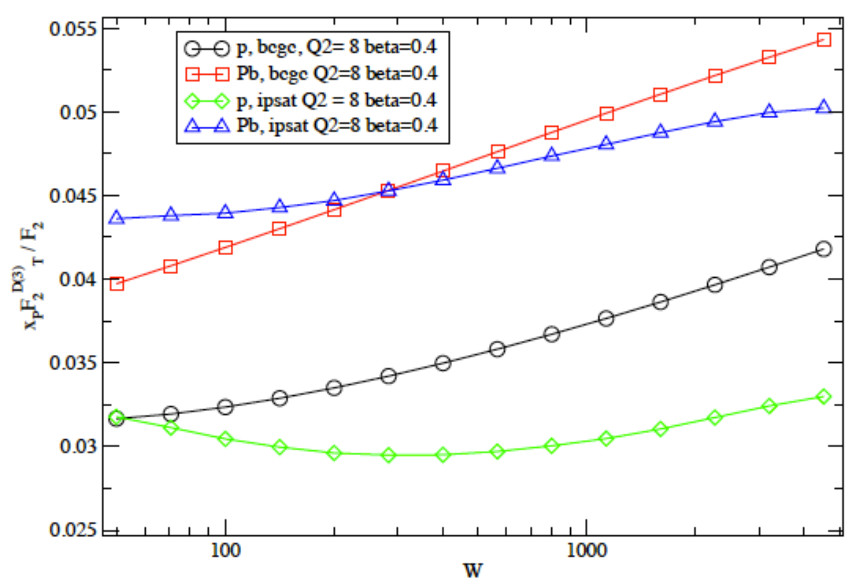

Enhanced diffraction in the nuclear case

Dihadron correlation

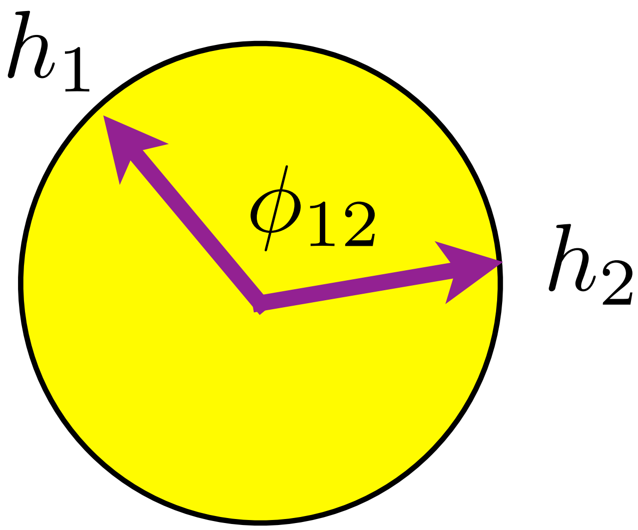

- Semi-inclusive production of two hadrons.
- (De)correlation provides a measure of the transverse momentum dependence of the parton density.
- Could be used as a test of saturation in nuclei at small x.

Correlation function:

$$C(\phi_{12}) = \frac{1}{\frac{d\sigma(\gamma^* N \to h_1 X)}{dz_{h1}}} \frac{d\sigma^{\gamma^* N \to h_1 h_2 + X}}{dz_{h1} dz_{h2} d\phi_{12}}$$

Single inclusive cross section:

$$\frac{d\sigma(\gamma^* N \to h_1 X)}{dz_{h1}}$$

ϕ_{12} azimuthal angle between the hadrons

z_{h1} and z_{h2} longitudinal momentum fractions of the hadrons

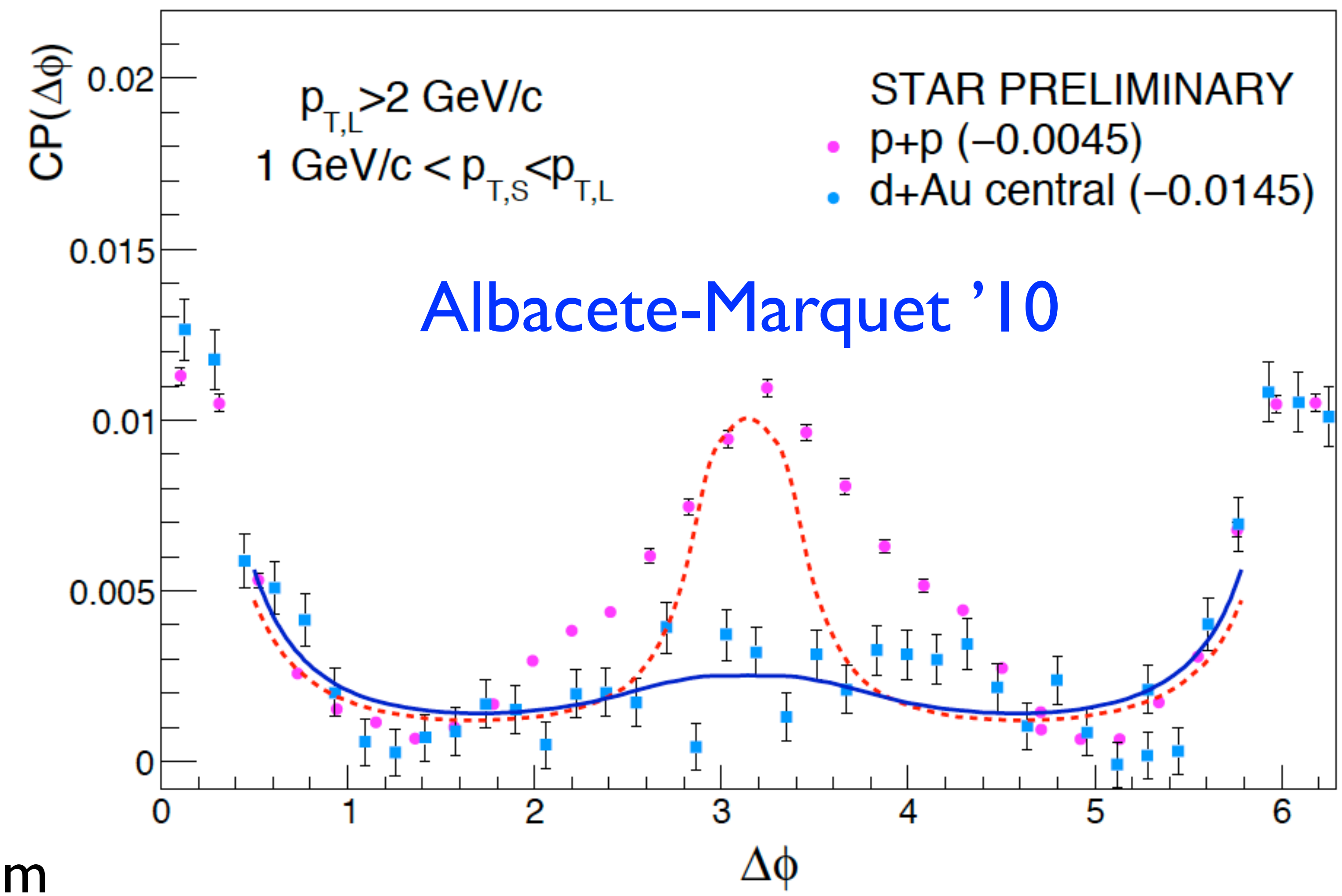

Nuclear parton distributions: uncertainty

Premilinary analysis

CTEQ nPDFs

$$Q^2 = 100 \text{ GeV}^2$$

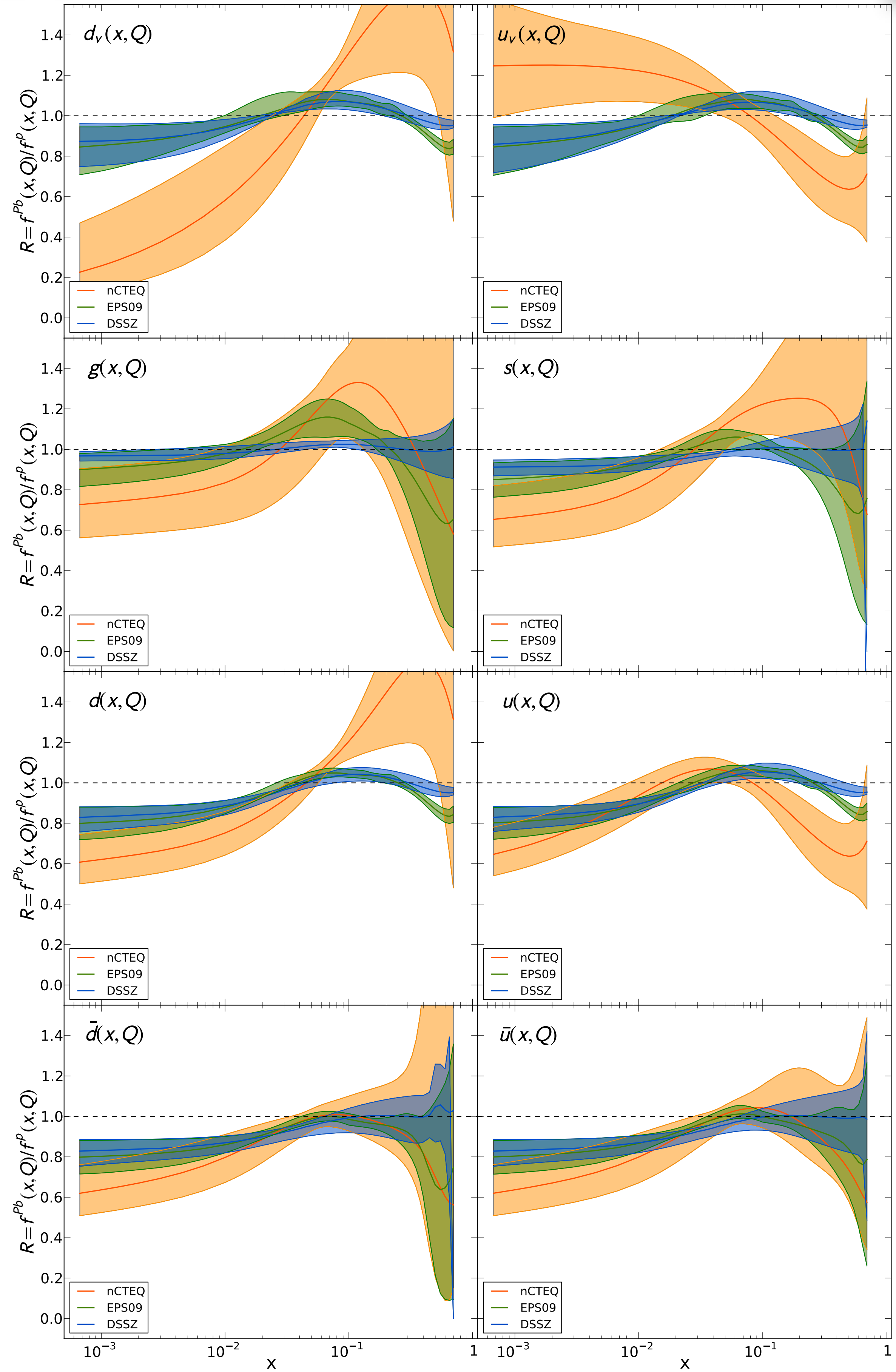

Dihadron correlation

Di-pion correlation function at LHeC:

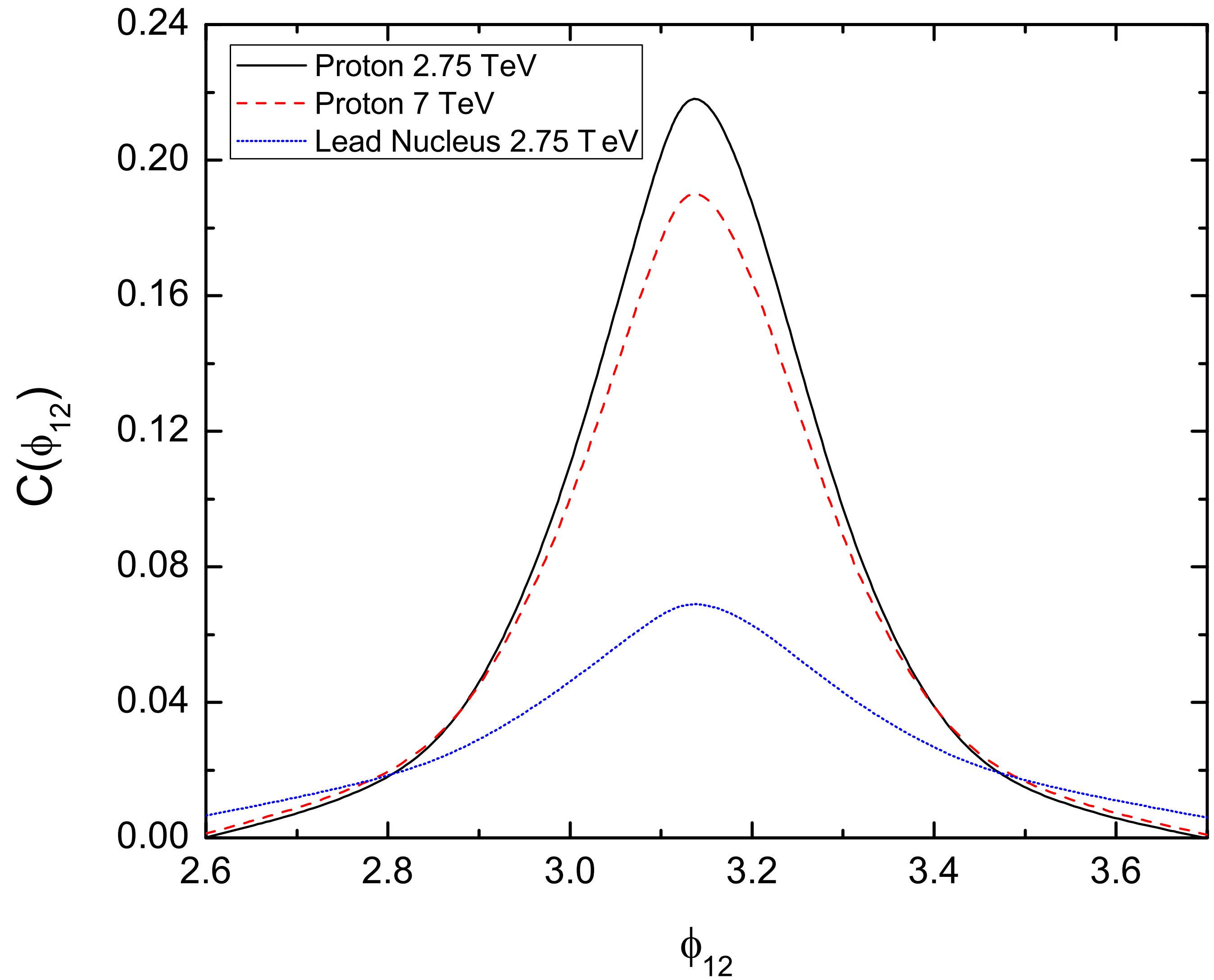

$$p_T^l > 3\ \mathrm{GeV}$$

$$p_T^a > 2\ \mathrm{GeV}$$

$$z_l = z_a = 0.3$$

$$y = 0.7$$

$$Q^2 = 4\ \mathrm{GeV}^2$$

- Correlation suppressed for a denser target (nucleus).
- Variation of the correlation with x indicates importance of ln(1/x) effects.
- In particular this observable provides a measure to small x Weizsacker-Williams unintegrated gluon distribution in the hadron/nucleus.

Diffraction and saturation

Dipole model at high energy: photon fluctuates into qqbar pair and undergoes an interaction with the target

$$\sigma_{T,L}(x,Q^2) = \int d^2\mathbf{r} \int_0^1 dz \sum_f |\Psi^f_{T,L}(\mathbf{r},z,Q^2)|^2 \, \hat{\sigma}(x,\mathbf{r}) \, .$$

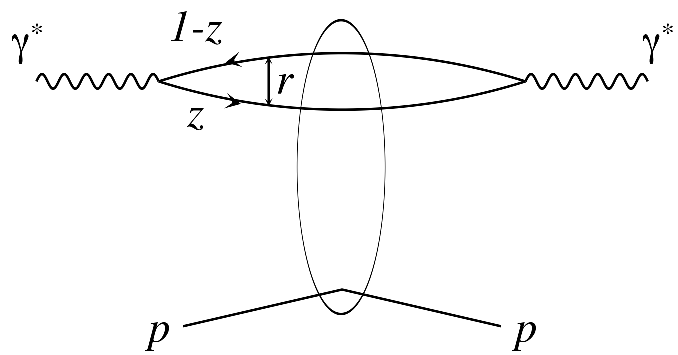

Inclusive: dominated by relatively hard component

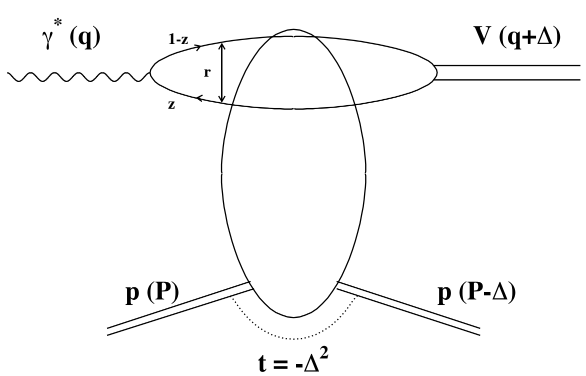

Diffractive: dominated by the semi-hard momenta

overlap function in the dipole model
typical dipole sizes involved in the process

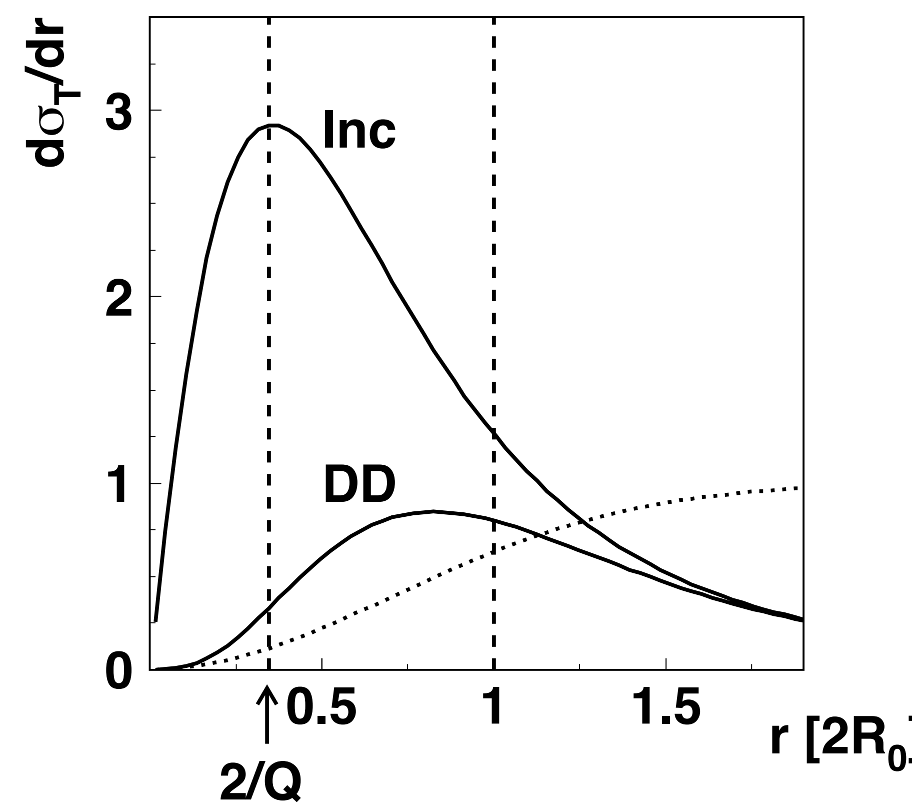

Diffraction is a collective phenomenon. Explore relation with saturation.

Exclusive diffraction

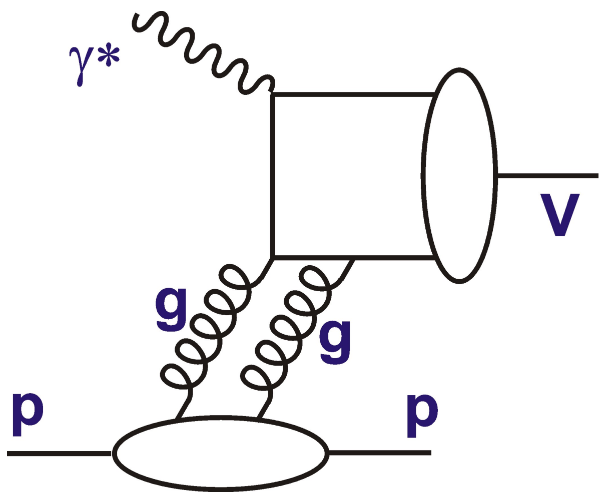

- Exclusive diffractive production of VM is an excellent process for extracting the dipole amplitude and GPDs
- Suitable process for estimating the ‘blackness’ of the interaction.
- t-dependence provides an information about the impact parameter profile of the amplitude.

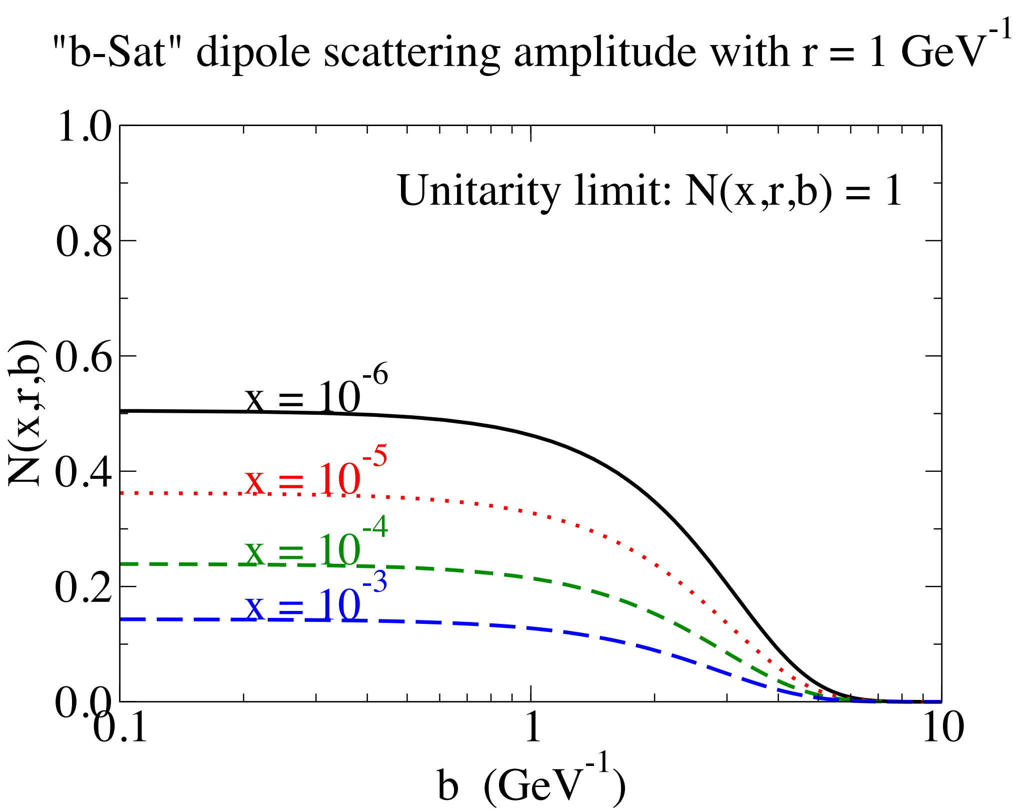

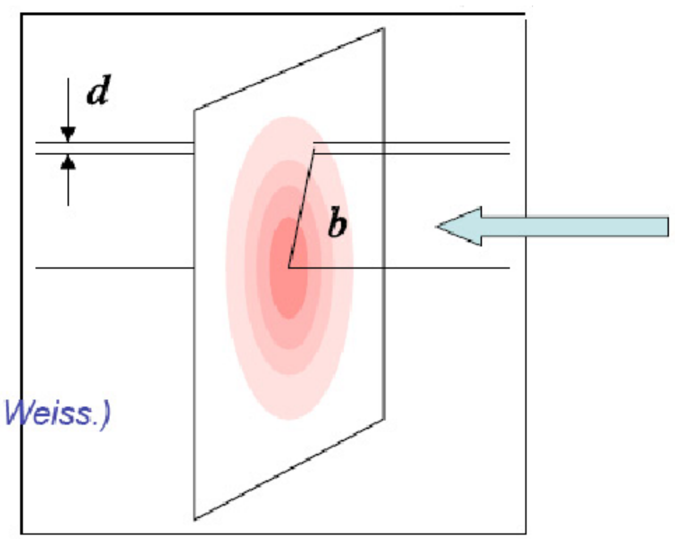

(figure from C. Weiss.)

Central black region growing with decrease of x.

Large momentum transfer t probes small impact parameter where the density of interaction region is most dense.

Exclusive processes: DVCS

MILOU generator using Frankfurt, Freund, Strikman model.

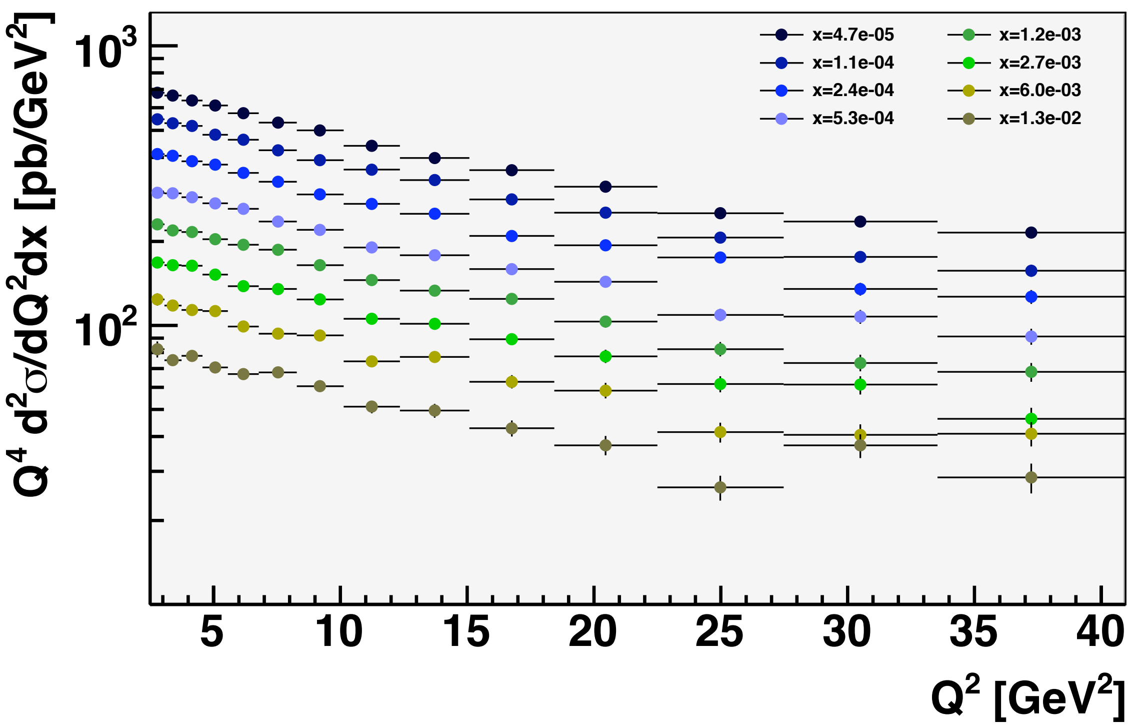

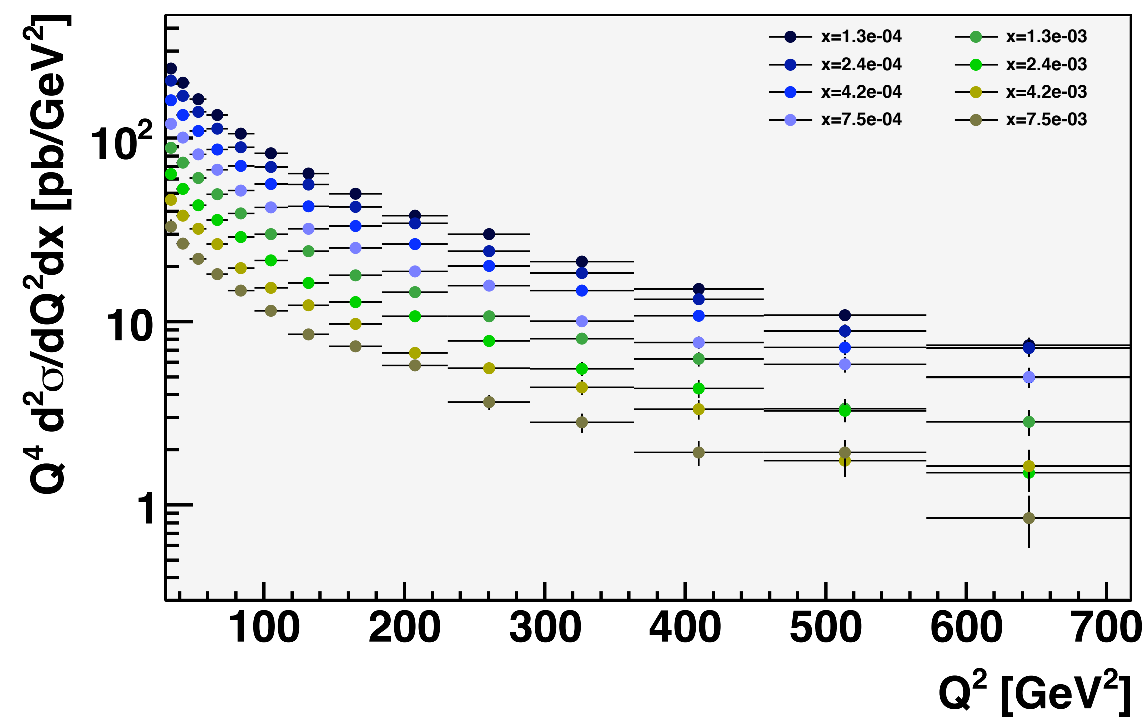

$$\mathcal{L} = 1\ \mathrm{fb}^{-1}$$

$$\theta = 1^o$$

$$p_T^\gamma = 2\ \mathrm{GeV}$$

$$2.5 < Q^2 < 40\ \mathrm{GeV}^2$$

low x

$$\mathcal{L} = 100\ \mathrm{fb}^{-1}$$

$$\theta = 10^o$$

$$p_T^\gamma = 5\ \mathrm{GeV}$$

$$50 < Q^2 \simeq 500\ \mathrm{GeV}^2$$

large scales

Exclusive diffraction: predictions

$$\sigma^{\gamma p \to J/\Psi + p}(W)$$

- b-Sat dipole model (Golec-Biernat, Wuesthoff, Bartels, Motyka, Kowalski, Watt)
- eikonalised: with saturation
- 1-Pomeron: no saturation

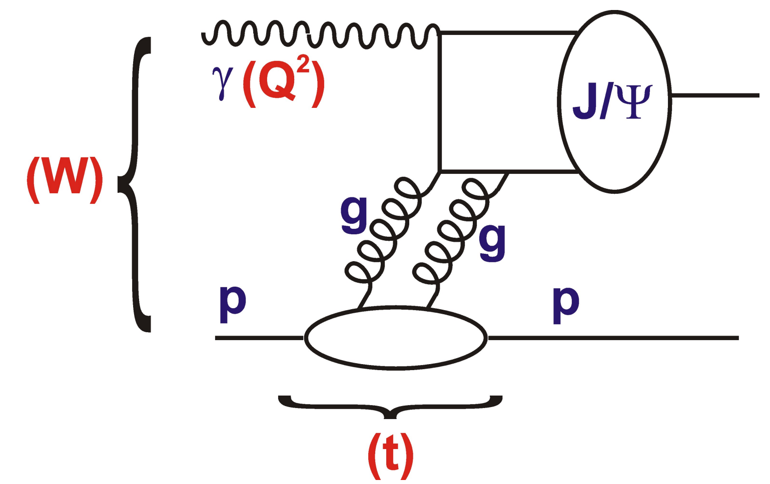

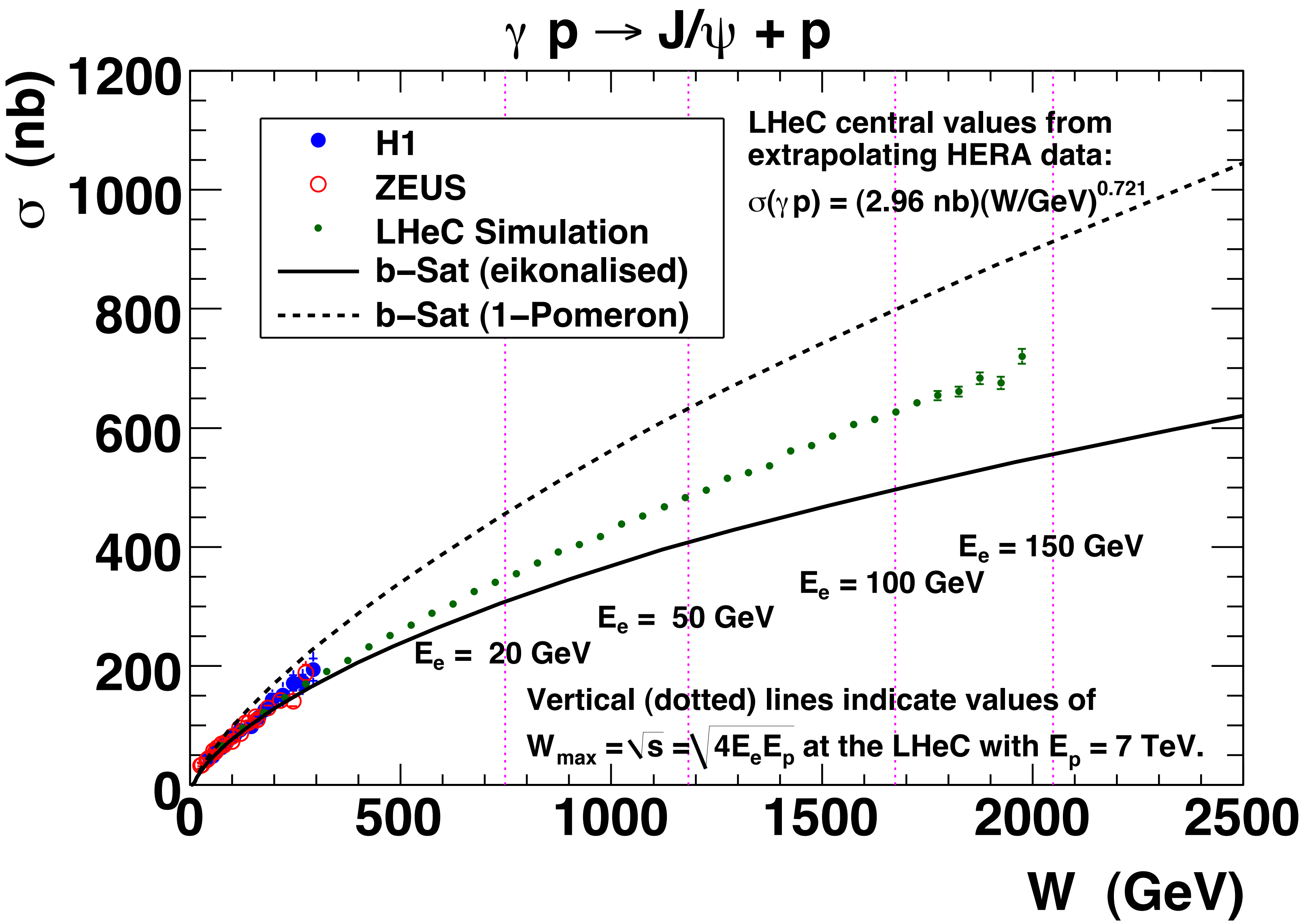

Large effects even for the t-integrated observable.

Different W behavior depending whether saturation is included or not.

Simulated data are from extrapolated fit to HERA data

LHeC can distinguish between the different scenarios.

Exclusive diffraction: t-dependence

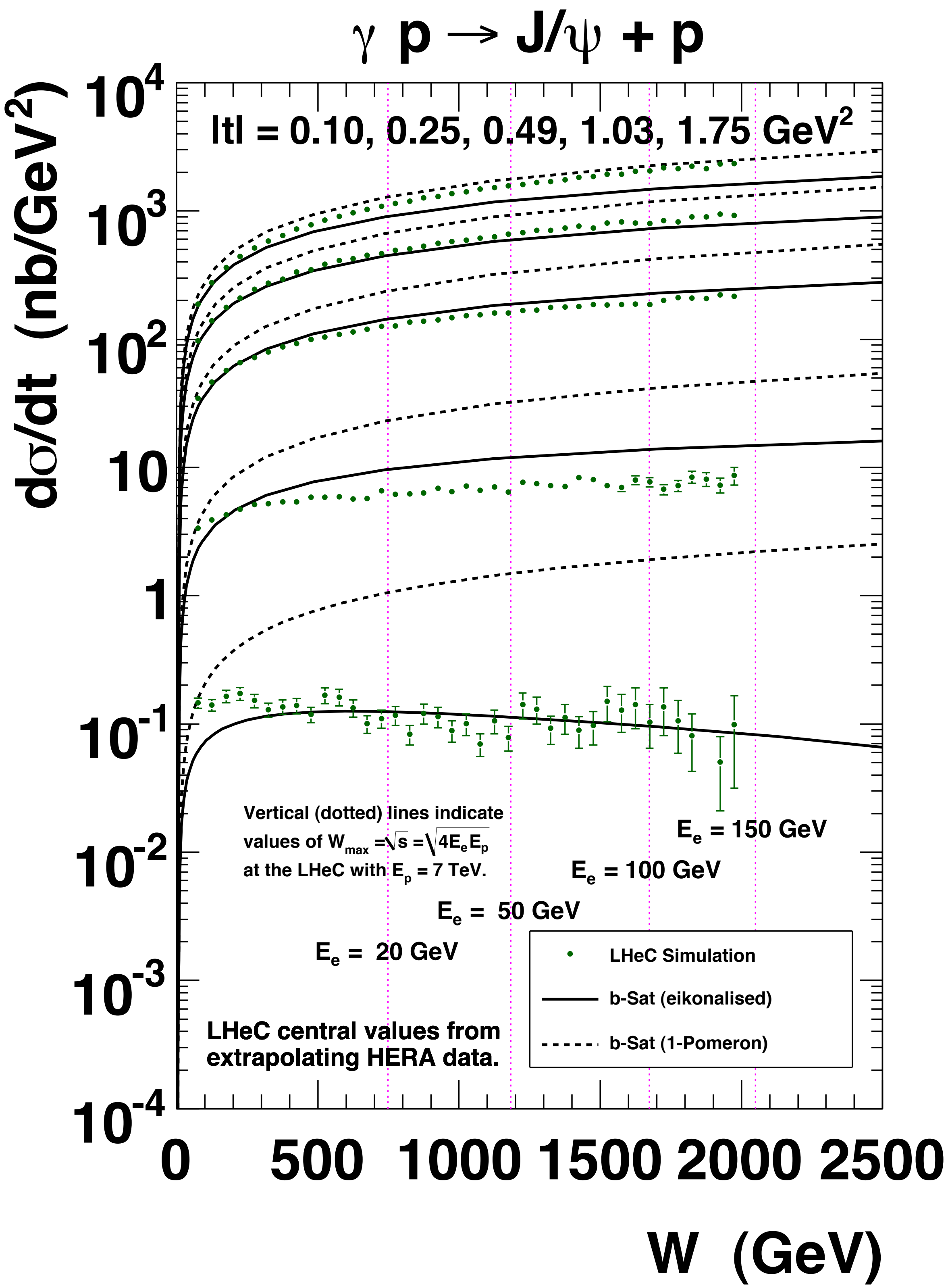

Photoproduction in bins of W and t.

Already for small values of t and smallest energies large discrepancies between the models. LHeC can discriminate.

Large values of t : increased sensitivity to small impact parameters.

Amplitude as a function of the impact parameter.

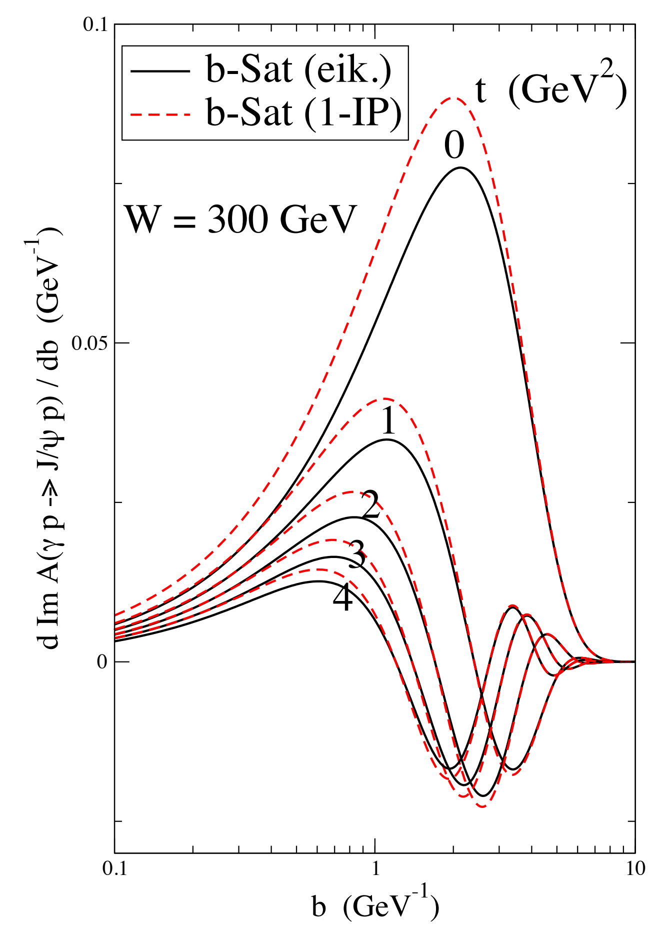

Exclusive diffraction on nuclei

Possibility of using the same principle to learn about the gluon distribution in the nucleus.
Possible nuclear resonances at small t?

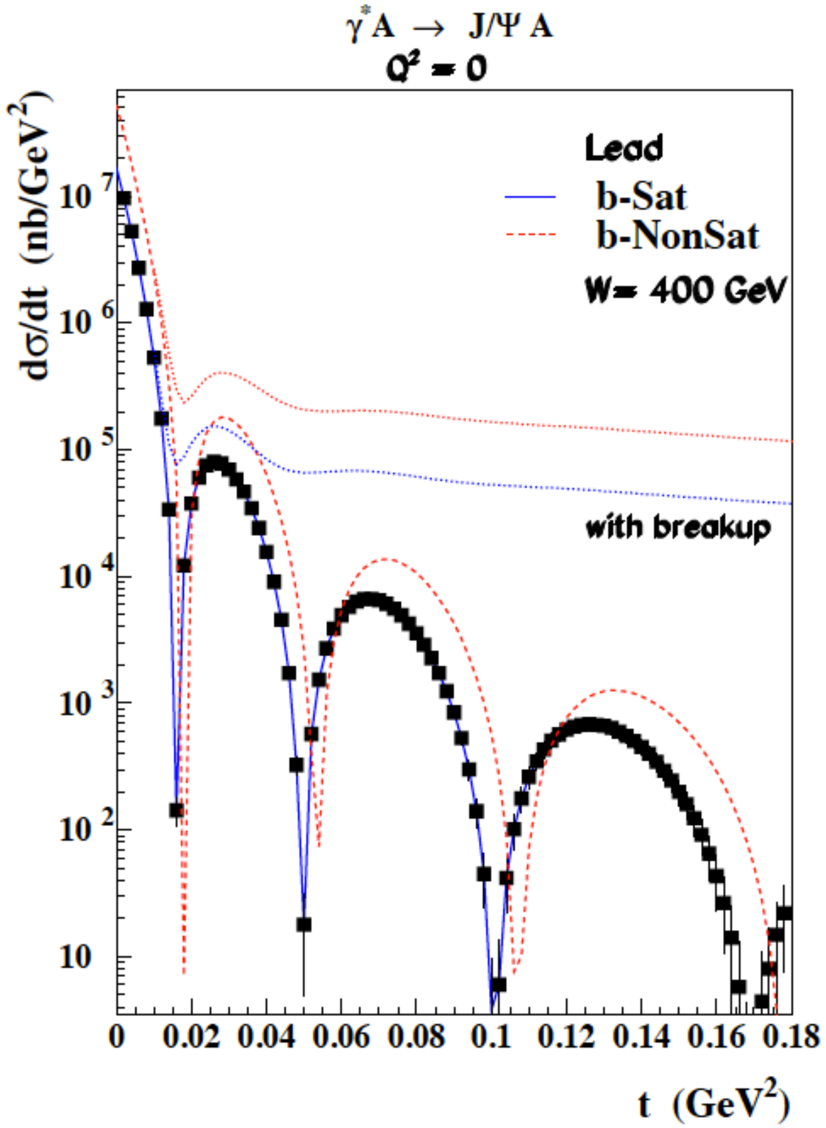

Energy dependence for different targets.

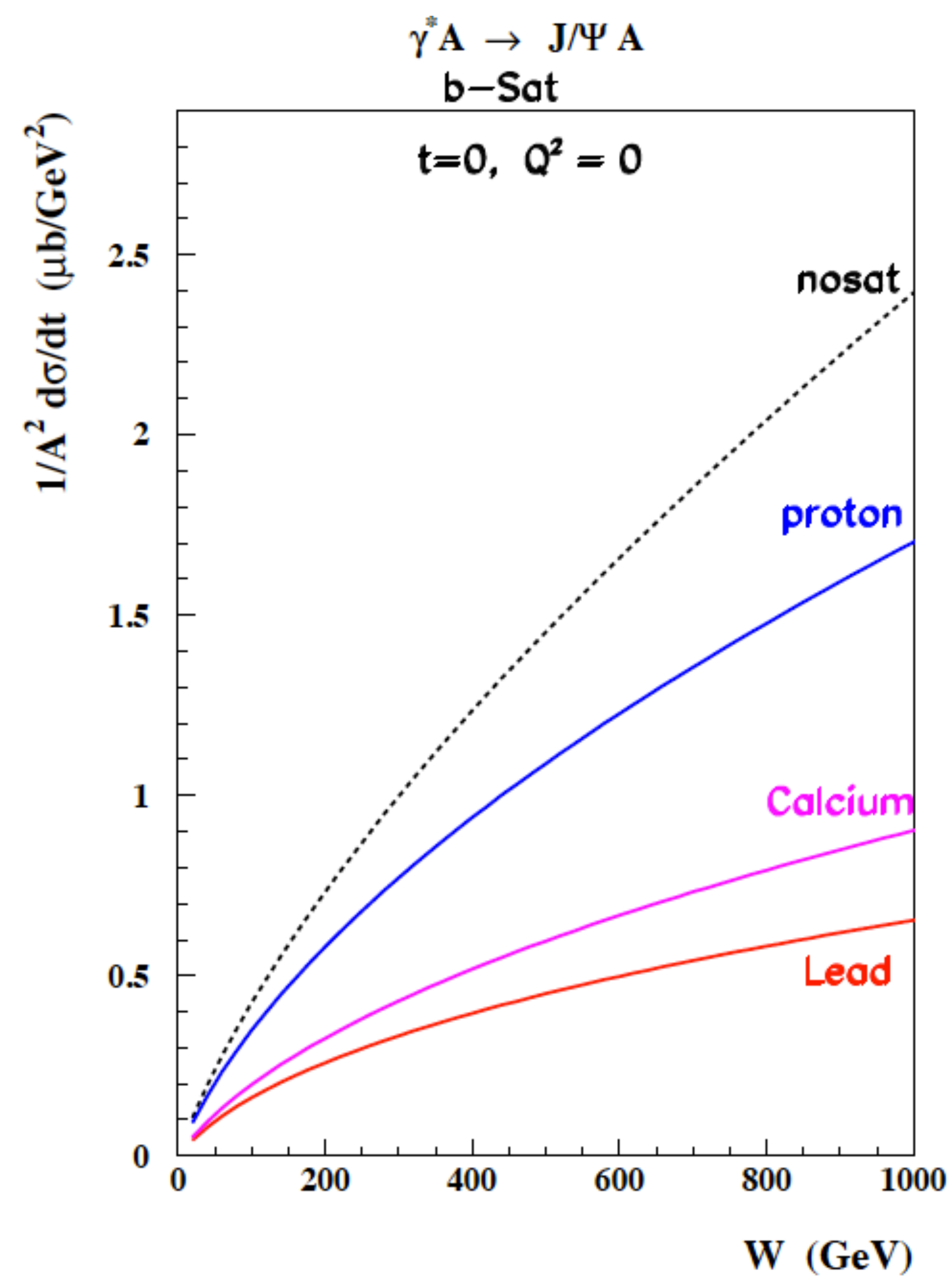

t-dependence: characteristic dips.
Challenges: need to distinguish between coherent and incoherent diffraction. Need dedicated instrumentation, zero degree calorimeter.

Importance of PDF

- If we see deviations from SM, will be important to characterize the physics underneath
- The case of strong production:

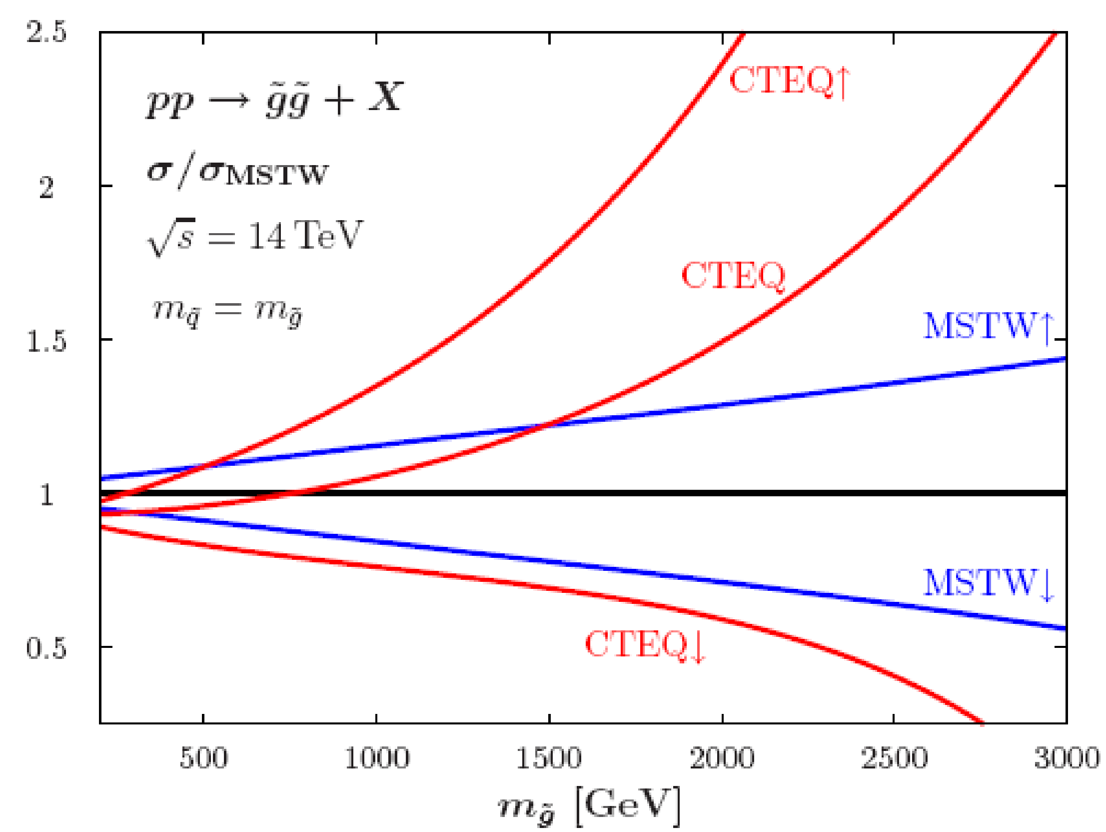

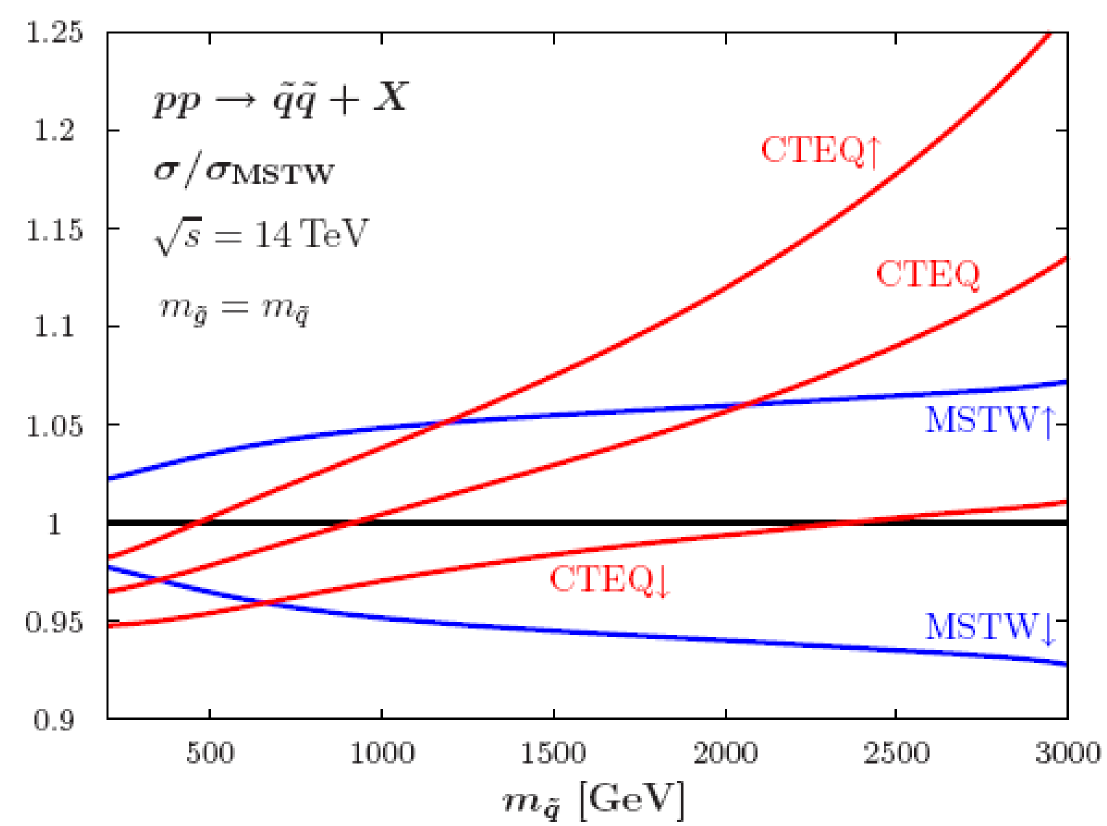

$\longrightarrow$ driven by gluon pdf at large x

$\longrightarrow$ sizeable uncertainty $\approx \pm 25\%$ for $m \approx 1$ TeV

$\longrightarrow$ driven by valence quark pdfs at large x

$\longrightarrow$ small uncertainty $\approx \pm 5\%$ for $m \approx 1$ TeV

Organisation for CDR

Scientific Advisory Committee

Guido Altarelli (Roma)
Sergio Bertolucci (CERN)
Stan Brodsky (SLAC)
Allen Caldwell (MPI Muenchen) - Chair
Swapan Chattopadhyay (Cockcroft Institute)
John Dainton (Liverpool)
John Ellis (CERN)
Jos Engelen (NWO)
Joel Feltesse (Saclay)
Roland Garoby (CERN)
Rolf Heuer (CERN)
Roland Horisberger (PSI)
Young-Kee Kim (Fermilab)
Aharon Levy (Tel Aviv)
Lev Lipatov (St. Petersburg)
Karlheinz Meier (Heidelberg)
Richard Milner (MIT)
Joachim Mnich (DESY)
Steve Myers (CERN)
Guenther Rosner (Glasgow)
Alexander N. Skrinsky (INP Novosibirsk)
Anthony Thomas (JLab)
Steve Vigdor (Brookhaven)
Ferdinand Willeke (Brookhaven)
Frank Wilczek (MIT)

LHeC

Steering Committee

Oliver Bruening(CERN)
John Dainton (Liverpool)
Albert De Roeck (CERN)
Stefano Forte (Milano)
Max Klein (Liverpool) - Chair
Paul Laycock (Liverpool)
Paul Newman (Birmingham)
Emmanuelle Perez (CERN)
Wesley Smith (Wisconsin)
Bernd Surrow (MIT)
Katsuo Tokushuku (KEK)
Urs Wiedemann (CERN)
Frank Zimmermann (CERN)

Working Group Convenors

Accelerator Design

Oliver Bruening (CERN)
John Dainton (Liverpool)

Interaction Region

Bernhard Holzer(CERN)
Uwe Schneekloth (DESY)
Pierre van Mechelen (Antwerpen)

Detector Design

Peter Kostka (DESY)
Alessandro Polini (Bologna)
Rainer Wallny (Zurich)

New Physics at Large Scales

Georges Azuelos (Montreal)
Emmanuelle Perez (CERN)
Georg Weiglein (Hamburg)

Precision QCD and Electroweak

Olaf Behnke (DESY)
Paolo Gambino (Torino)
Thomas Gehrmann (Zurich)
Claire Gwenlan (Oxford)

Physics at High Parton Densities

Néstor Armesto (Santiago de Compostela)
Brian A. Cole (Columbia)
Paul R. Newman (Birmingham)
Anna M. Stasto (PennState)

CERN Referees

Ring Ring Design
Kurt Huebner (CERN)
Alexander N. Skrinsky (INP Novosibirsk)
Ferdinand Willeke (BNL)
Linac Ring Design
Reinhard Brinkmann (DESY)
Andy Wolski (Cockcroft)
Kaoru Yokoya (KEK)
Energy Recovery
Georg Hoffstaetter (Cornell)
Ilan Ben Zvi (BNL)
Magnets
Neil Marks (Cockcroft)
Martin Wilson (CERN)
Interaction Region
Daniel Pitzl (DESY)
Mike Sullivan (SLAC)
Detector Design
Philippe Bloch (CERN)
Roland Horisberger (PSI)
Installation and Infrastructure
Sylvain Weisz (CERN)
New Physics at Large Scales
Cristinel Diaconu (IN2P3 Marseille)
Gian Giudice (CERN)
Michelangelo Mangano (CERN)
Precision QCD and Electroweak
Guido Altarelli (Roma)
Vladimir Chekelian (MPI Munich)
Alan Martin (Durham)
Physics at High Parton Densities
Alfred Mueller (Columbia)
Raju Venugopalan (BNL)
Michele Arneodo (INFN Torino)

LHeC kinematics: acceptance

Kinematics in ep

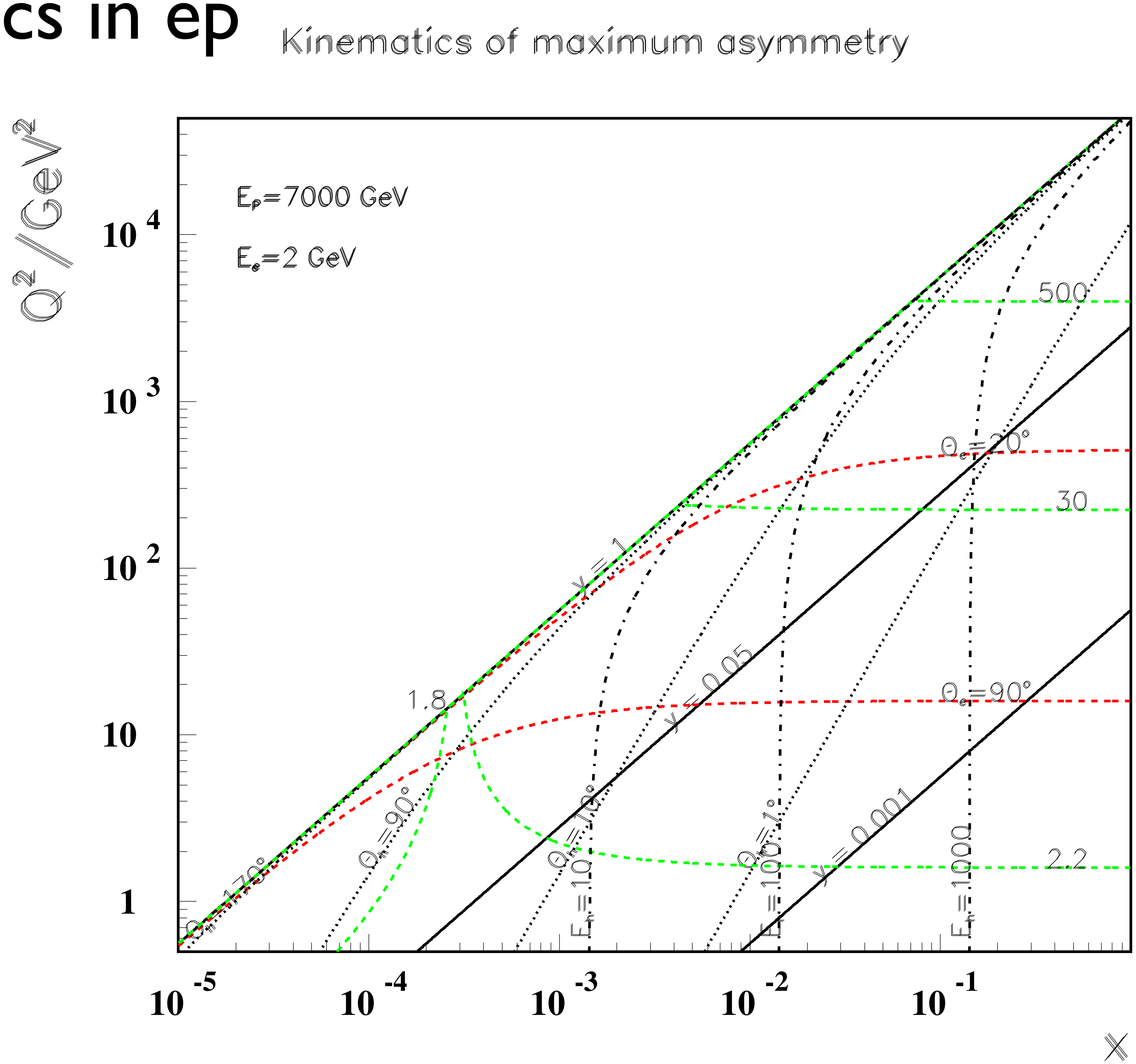

Lower electron energy does not help: extremely asymmetric kinematics. Large x becomes almost inaccessible.

LHeC kinematics: acceptance

Kinematics in ep

$$Q^2\ (x,\theta_{h,min}) \simeq [2E_p x \tan^2(\theta_{h,min}/2)]^2,$$

LHeC - hadronic final state kinematics

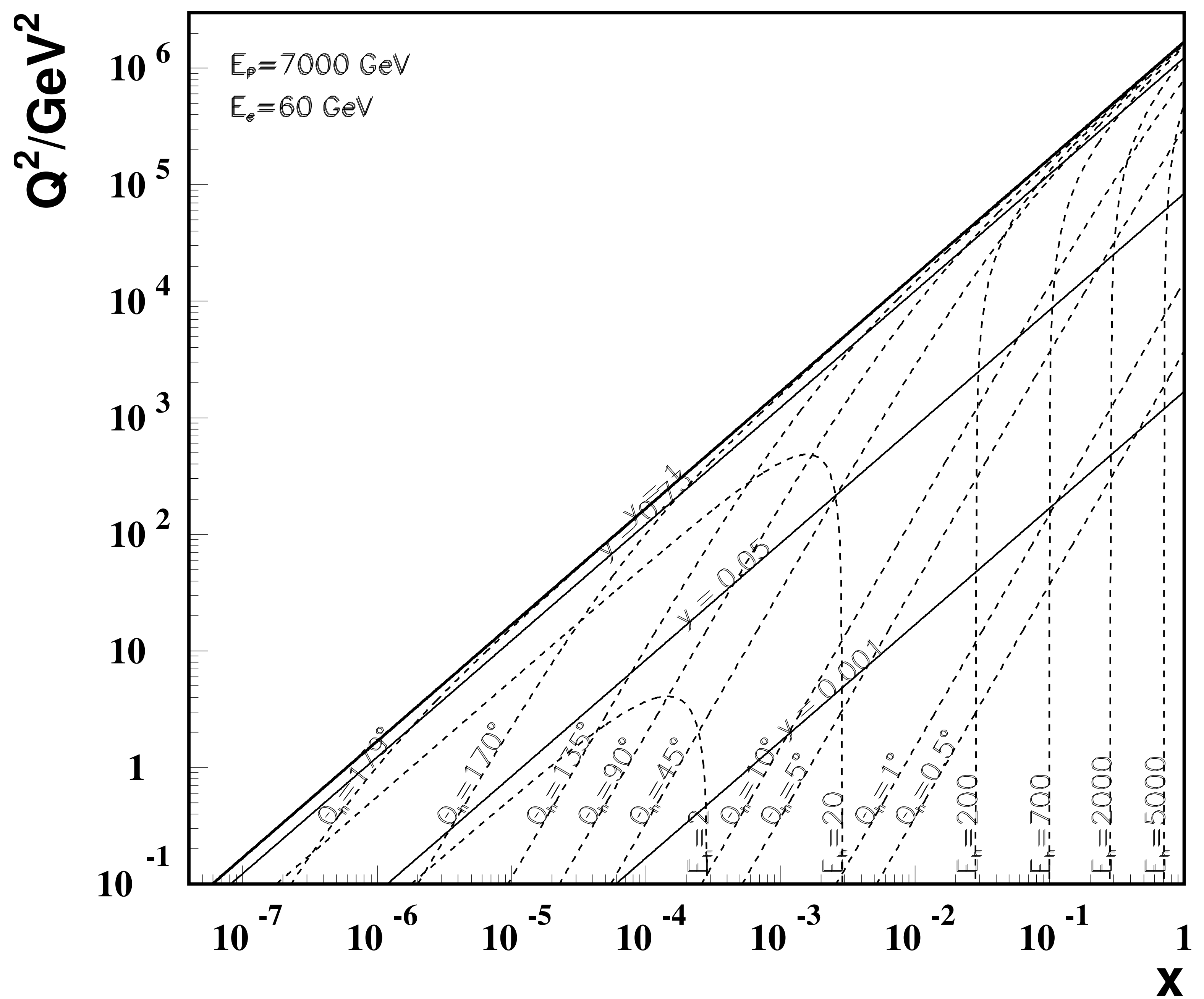

Similarly access to large x requires angle acceptance of hadrons down to 1 degree.

Photoproduction cross section

Explore dual nature of the photon: pointlike interactions or hadronic behavior.

Tests of universality of hadronic cross sections, unitarity, transition between perturbative and nonperturbative regimes.

Dedicated detectors for small angle scattered electrons at 62m from the interaction point.

Kinematics of events:

$$Q^2 \sim 0.01$$

$$y \sim 0.3$$

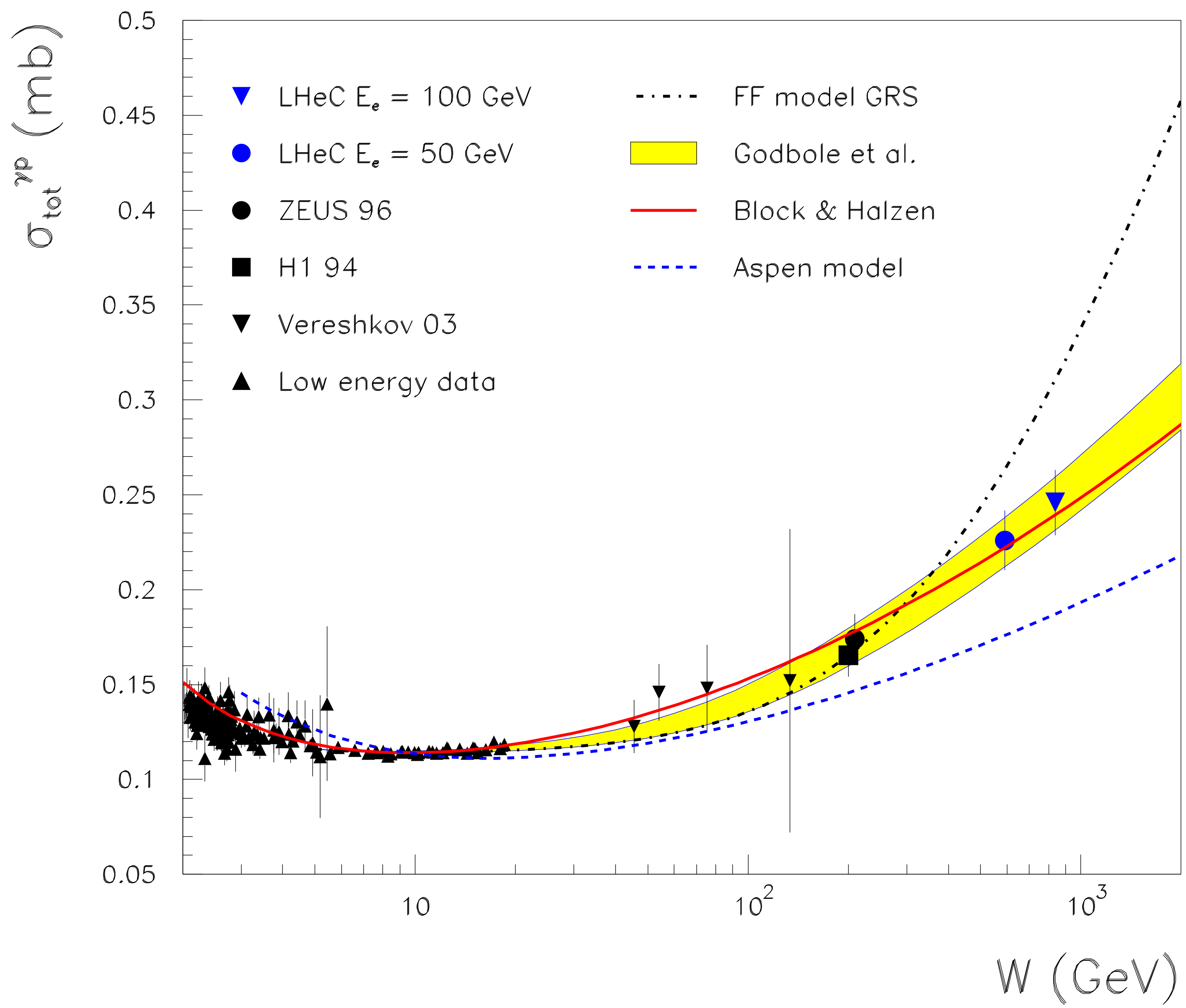

Systematics is the limiting factor here. Assumed 7% for the simulated data as in H1 and ZEUS.